CONTROLS ON ZOOPLANKTON ASSEMBLAGES IN THE NORTHEASTERN CHUKCHI SEA

By

Jennifer Marie Questel, B.S.

A Dissertation Submitted in Partial Fulfillment of the Requirements

For the Degree of

Doctor of Philosophy

in

Oceanography

University of Alaska Fairbanks

August 2016

APPROVED:

Russell R. Hopcroft, Committee Chair
Ann C. Bucklin, Committee Member
Jeremy T. Mathis, Committee Member
Thomas J. Weingartner, Committee Member
Kenneth O. Coyle, Committee Member
Jennifer R. Reynolds, Chair
Department of Oceanography
S. Bradley Moran, Dean
School of Fisheries and Ocean Sciences
Michael Castellini, *Dean of the Graduate School*

Abstract

The Chukchi Sea is a broad and shallow marginal sea of the western Arctic Ocean that lies between the Bering Sea and the deeper Amerasian basin. It plays a pivotal role as the only gateway for transporting heat, carbon, nutrients, and plankton from the North Pacific into the Arctic Ocean. I examined the seasonal and inter-annual variability of the zooplankton communities in the northeastern region of the Chukchi Sea as part of a high-resolution multidisciplinary ecosystem study. Specifically, I examined how the physical onset of each open water season influenced the composition, abundance, and biomass of zooplankton assemblages from the 2008 to 2010 field seasons. Copepods in the genus *Pseudocalanus* are key members of the Chukchi community, and may be undergoing species-level biogeographic shift in response to climate change. I determined the degree of gene flow and population connectivity in the Chukchi Sea through comparative phylogeographic analysis of the *Pseudocalanus* species complex to the northern Gulf of Alaska and Beaufort Sea. I then investigated the extent to which biogeochemical factors influence these zooplankton assemblages by relating a portion of the seasonal production to concurrent changes in herbivorous mesozooplankton biomass during 2010 and 2011. This work demonstrates just how complex and variable marine ecosystems of the western Arctic are, where multidisciplinary and analytical approaches will become essential in detecting change, especially with the rate of present-day climate perturbations.

Dedication

To Dr. Richard Back

For whom I am grateful to for nudging me into Lake Ontario on dark summer nights and providing me with my first ever zooplankton research experience.

I hope one day you will get that Boston Whaler back on the Lake to catch more *Hemimysis anomala*.

Table of Contents

Page

List of Figures

Page

List of Tables

Page

List of Appendices

Acknowledgments

The research presented in this dissertation was made possible by the Chukchi Sea Environmental Studies Program (CSESP), endorsed by ConocoPhillips Company, Anchorage, AK; Shell Exploration and Production Company, Anchorage, AK; and Statoil USA E&P, Inc., Anchorage, AK. I would also like to thank the Bureau of Ocean Energy Management for supporting the Transboundary Program as well as the North Pacific Research Board, Exxon Valdez Oil Spill, and Alaska Ocean Observing System for supporting the Seward Line cruises, both of which provided samples for Chapter 3. Additional support was provided by the University of Alaska Fairbanks through the Northern Gulf of Alaska Applied Research Award to aid in laboratory costs associated with Chapter 3.

I would especially like to thank Caryn Rea (ConocoPhillips) for conceptualizing CSESP, and to Mike Macrander (Shell) and Steinar Eldøy (Statoil) for believing in, and helping turn a two-year baseline study into a valuable unpresented seven-year time series for the Chukchi Sea. The extremely complicated logistics of CSESP were achieved by Olgoonik-Fairweather LLC. In particular, Sheyna Wisdom (Oloonik-Fairweather) provided personal and professional support, and displays characteristics as a woman in science that I aspire to match. The quality of research published from CSESP was critiqued by Chief Scientists Robert H. Day (ABR) and John Burns Sr. (Fairweather Science), who dauntlessly reviewed numerous publications and yearly reports over the entirety of the program. Thanks also to the amazingly talented captains and crew of the *R/V Westward Wind*, *M/V Tiglax*, and the *R/V Norseman II* whose efforts to ensure successful field seasons were always greatly appreciated.

I owe my degree and future life's work to my major advisor and mentor, Russ Hopcroft. To my committee members Ann Bucklin (University of Connecticut), Jeremy Mathis (National Oceanic and Atmospheric Administration; UAF), Thomas Weingartner (UAF), and Kenneth Coyle (UAF) for their advice and support throughout my doctoral program. To my co-author Cheryl Clarke-Hopcroft (UAF), for helping work up zooplankton and chlorophyll samples, as well as data analysis for Chapter 1. To my co-author Leocadio Blanco-Bercial (Bermuda Institute of Ocean Sciences; Chapter 3), who I cannot thank enough for his guidance with genetic

sequencing and help with gene flow model analysis which made for many successful presentations and a published manuscript.

I thank the lab support at UAF, especially Katherine Trahanovsky, Natalie Monacci, Daniel Naber, and T. Chris Stark for sample processing and analysis. Special thanks goes to Ian Herriott, director of UAF's Institute of Arctic Biology Core lab, for providing invaluable troubleshooting advice for Chapter 3. Equipment support used in Chapter 3 was made possible through an Institutional Development Award (IDeA) from the National Institute of General Medical Sciences of the National Institutes of Health to JMQ [grant number P20GM103395].

I thank my parents, Thomas and Judith Questel, Grandmother Evelyn Wells, and childhood best friend Casey DeBottis who unwillingly watched me move across the country to pursue my passions in the marine sciences. Thank you for all your love and support along the way.

To my extended Alaskan Family, for the amazing support, overwhelming love, and timeless friendships that have made my years in Alaska truly remarkable. Nothing can ever match the adventures and bonds we all share. Last but not least, I thank Odin, my Bernese Mountain Dog, who has kept me sane and my stress levels at bay during the final push.

General Introduction

The Chukchi Sea is a broad and shallow (<50 m) marginal sea of the western Arctic Ocean that lies between the Bering Sea and the deeper Amerasian basin. It is a gateway to the Arctic providing the only connection between the Pacific and Arctic Oceans. On a seasonal basis, a complex mixture of Pacific-derived water masses enter the Chukchi Sea through the Bering Strait with an estimated ~1–1.2 Sv average transport (Danielson et al., 2014), with most of the transport occurring during the open-water season (Coachman and Aagard, 1988; Woodgate et al., 2012; Danielson et al., 2014). Large quantities of Pacific-derived carbon, nutrients, phytoplankton, and an estimated 1.8×10^{12} g C of Bering Sea zooplankton (Springer et al., 1989) are transported into the region within three distinct water masses (i.e., Alaska Coastal Water, Bering Shelf Water, and Anadyr water), each with distinct assemblages and different quantities of zooplankton (Springer et al., 1989; Hopcroft et al., 2010; Ershova et al., 2015a). These zooplankton, along with the entrained phytoplankton communities, are responsible for the higher pelagic productivity of the Chukchi Sea than in adjoining regions of the Arctic Ocean (Grebmeier and Maslowski, 2014). This productivity is either: transferred through zooplankton to higher trophic levels such as planktivorous fishes, seabirds, and whales; exported to the sea floor (e.g., Carroll and Carroll, 2003; Grebmeier et al., 2006); or advected northward to the deep Arctic basins (e.g., Grebmeier et al., 2006).

During the open-water season, the Chukchi Sea's mesozooplankton fauna is primarily Pacific in character (Hopcroft et al., 2010; Ershova et al., 2015a). During the summer, nutrients and plankton of Pacific origin are diluted by waters from the Siberian Coastal Current and deeper regions of the Canada Basin or Chukchi Plateau (Grebmeier et al., 1995). Zooplankton assemblages are carried northward as far as the eastern side of Wrangel Island (Ershova et al., 2015a), as well as to the shelf break in the northeastern Chukchi Sea (Lane et al., 2008; Nelson et al., 2009, 2014). The pattern and intensity of advection of Pacific water masses then determines the reproductive success of both expatriate and resident zooplankton communities (Plourde et al., 2005; Hopcroft and Kosobokova, 2010).

The Chukchi Sea is heavily influenced by sea-ice that covers more than 90% of the region for most of the year and is an important driver of the regional climate. Sea-ice extent is highly influential on hydrographic processes such as circulation patterns, thermal structure, and

water column stratification (Wang et al., 2009). Patterns of sea-ice melt and retreat vary greatly on a yearly basis, but typically melt-pools and leads begin to open up by early-mid May (Weingartner et al., 2013). However, striking changes in the summer and winter sea-ice extent and concentrations have occurred over the past decade, with the Chukchi Sea experiencing the most rapid rate of change over the entire Arctic sector (www.nsidc.org). Changes in sea-ice cover have already been shown to have significant impacts on the Chukchi ecosystem (Dunton et al., 2005; Ershova et al., 2015b; Gall et al., 2016), stressing the ever-increasing need to understand the ecology of the region before it changes further.

Historically, studies on the ecology of Chukchi zooplankton assemblages date back nearly 100 years (see Ershova et al., 2015a). In the US, large-scale efforts began in the 1970s to better understand zooplankton distribution, composition, seasonal life cycles, and trophic interactions as part of the US Department of Commerce's Outer Continental Shelf Environmental Assessment Program (OCSEAP). In the 1980s the Inner Shelf Transfer and Recycling (ISHTAR) program focused on the cycling of carbon and nutrients (Springer et al., 1989; Walsh et al., 1989). A hiatus in sampling then occurred until the early 2000s when the Shelf-Basin Interactions (SBI) study sought to understand the physical and biogeochemical processes of the shelf, slope, and basin of the western Arctic (Codispoti et al., 2009; Grebmeier et al., 2009; Lane et al., 2008). In the southern region of the Chukchi Sea, zooplankton assemblages and their unique affinities to differing water masses entering the Chukchi Sea through the Bering Strait were studied during the Russian-American Long-term Census of the Arctic (RUSALCA) (Hopcroft et al., 2010; Ershova et al., 2015a).

From 2008 – 2014 the Chukchi Sea Environmental Studies Program (CSESP) was conducted to gather multi-level ecosystem baseline data, including physical, chemical, and biological oceanography, benthic and fisheries ecology, and marine seabirds and mammals, in preparation for wells for oil and gas exploration (Day et al., 2013). Three main study areas denoted Burger, Klondike, and Statoil were sampled in a standardized fixed oceanographic sampling scheme over multiple cruises in each field season. A strength of this program was that concurrent measurements of the full spectrum of trophic levels were made, strengthening our analyses for cross discipline comparisons. In 2011 and 2012 the study area was expanded to encompass the Greater Hanna Shoal study area to gain a broader context of the ecology of the region. The Chukchi Sea is also home to many native Alaskan communities whose cultures were

established on the subsistence hunting of marine mammals. The work and data collected through the CSESP study has helped inform them about the offshore communities and how ecosystem changes might impact the marine mammal communities.

The research presented in this dissertation examined the chemical and biological oceanography from CSESP, taking a three-pronged approach to understand the abiotic and biotic factors that affect the composition, abundance, biomass, and spatial distributions of zooplankton within the northeastern Chukchi Sea. The first chapter focused on the variability of the zooplankton communities in the Klondike, Burger, and Statoil study areas during the first three study years. I analysed seasonal and inter-annual changes in zooplankton composition, abundance, and biomass in relation to physical oceanographic characteristics during the open-water season. In particular, I looked at how variability in the patterns of sea-ice retreat and its effect on sea surface temperature propagated through and structured the biological communities.

The second chapter undertook a comparative phylogeographic and population connectivity analysis of the copepod genus, *Pseudocalanus* based on the mitochondrial cytochrome oxidase I (COI) gene. The genus is comprised of seven sibling species that co-occur at differing assemblages within their geographic ranges that span the Arctic and temperate-boreal marine ecosystems of the Northern Hemisphere. *Pseudocalanus* numerically dominate the shelf zooplankton communities of the North Pacific and the western Arctic Ocean, which allowed for the incorporation of populations outside of the Chukchi Sea for this study, including the northern Gulf of Alaska, Prince William Sound, and the adjacent Beaufort Sea. This study focused on two Arctic (*P. acuspes*, *P. minutus*) and two temperate species (*P. newmani*, *and P. mimus).* I utilized a model to test the likelihood of directional gene flow between populations.

The third chapter studied the biogeochemical controls on phytoplankton and herbivorous mesozooplankton assemblages in the Burger, Klondike, and Statoil study areas during the 2010 and 2011 CSESP field seasons. Net community production (NCP) was estimated from seasonal changes in dissolved inorganic carbon, total alkalinity, and nitrate during the summer period after the initial phytoplankton bloom had occurred. NCP rates were compared to concurrent changes in mesozooplankton biomass to understand the degree to which net production influenced the biological communities. Furthermore, I employed a simple box-model of carbon

production to determine if adequate amounts of carbon were produced from primary production to support growth and reproduction of mesozooplankton.

Together, these three chapters provide a better understanding of the complexities with regards to how Chukchi zooplankton assemblages are influenced by physical, historical, and biogeochemical interactions. This work thus provides a standard to which ongoing studies (i.e., Arctic Marine Biodiversity Observing Network, Distributed Biological Observatory) will be compared to elucidate inter-annual and long-term ecological and anthropogenic changes in the Chukchi Sea.

CHAPTER 1: SEASONAL AND INTERANNUAL VARIATION IN THE PLANKTONIC COMMUNITIES OF THE NORTHEASTERN CHUKCHI SEA DURING THE SUMMER AND EARLY FALL[1]

1.1 Abstract

We analyzed the seasonal and interannual variability of the planktonic communities in a densely sampled region of the northeastern Chukchi Sea as part of a multidisciplinary ecosystem study from 2008 to 2010. Observations of chlorophyll-a, inorganic macronutrients, and zooplankton (using both 150–μm and 505–μm mesh nets) were made within two 900–NM^2 grids (Klondike and Burger) at high spatial resolution three times each in 2008 and 2009, with a third grid (Statoil) sampled twice in 2010. Sea-ice conditions prior to sampling varied notably during the study: seasonal sea ice retreat was earlier and sea-surface temperatures (SSTs) were warmer in 2009 than in 2008, whereas SSTs for 2010 were intermediate between the 2008 and 2009 values. Eighty taxonomic categories of zooplankton, including 11 meroplanktonic categories, were recorded, with the greatest diversity found within the copepods (25 species), followed by the cnidarians (11 species). All species are typical for the region and most are seeded from the Bering Sea. A seasonal progression of the community structure was apparent over each survey area and was likely influenced by temperature. Cold oceanographic conditions in 2008 likely slowed growth and development of the zooplankton, such that holozooplankton abundance averaged 2389 and 106 individuals m^{-3} and biomass averaged 10.5 and 8.3 mg DW m^{-3} in the 150– and 505–μm nets, respectively. An early phytoplankton bloom in 2009 apparently supported a zooplankton community of greater abundance, but moderate biomass, averaging 6842 and 189 individuals m^{-3}, and 16.3 and 7.0 mg DW m^{-3} in the 150– and 505–μm nets, respectively. Highest zooplankton abundance and biomass values among the three years occurred in 2010: 7396 and 198 individuals m^{-3} and 102.9 and 33.5 mg DW m^{-3} in the 150– and 505–μm nets, respectively. Holozooplankton biomass changes were driven by increases in large-bodied, lipid-rich copepods. The contribution of meroplankton was substantial in this shallow-water ecosystem: numerically, they contributed 28% in 2008, 8% in 2009 and 56% in 2010 to the total

[1] Published as Questel, J.M., Clarke, C., and Hopcroft, R.R., 2013. Seasonal and interannual variation in the planktonic communities of the northeastern Chukchi Sea during the summer and early fall. Continental Shelf Research 67, 23–41.

zooplankton community and 43%, 27%, and 11%, respectively, terms of biomass for the 150–μm nets. Interannual differences in ice-melt timing, water temperatures, northward transport of water masses, and nutrients and chlorophyll concentrations resulted in highly variable pelagic productivity.

1.2 Introduction

The Chukchi Sea sustains a dynamic ecosystem at the Pacific Ocean's gateway into the Arctic Ocean where climate variability combines with the complex interplay of several distinct water masses of Pacific origin. Large quantities of Pacific-derived nutrients, phytoplankton, and zooplankton enter the region through the Bering Strait within three distinct water masses (i.e., Alaska Coastal Water, Bering Shelf Water, and Anadyr Water), each with unique assemblages and quantities of zooplankton (Springer et al., 1989; Coyle et al., 1996; Hopcroft et al., 2010). It is estimated that 1.8 million metric tonnes of Bering Sea zooplankton are carried into the Chukchi Sea annually (Springer et al., 1989) and that these zooplankton, along with the entrained phytoplankton communities, are responsible for the higher pelagic productivity of the Chukchi Sea than in adjoining regions of the Arctic Ocean (e.g., Plourde et al., 2005). The pelagic productivity is either transferred through zooplankton to higher trophic levels such as planktivorous fishes, seabirds, and whales, exported to the sea floor (e.g., Carroll and Carroll, 2003; Grebmeier et al., 2006), or advected northward to the deep Arctic basins (e.g., Grebmeier et al., 2006).

During ice-free periods, the southern Chukchi Sea's zooplankton fauna is primarily Pacific in character (Hopcroft et al., 2010). During the summer, nutrients and zooplankton of Pacific origin are diluted by waters from the Siberian Coastal Current and deeper regions of the Canada Basin and Chukchi Plateau (Grebmeier et al., 1995). Nonetheless, Pacific species are commonly carried northward as far as the eastern side of Wrangel Island (Hopcroft et al., 2010). The influx of these "rich" Pacific waters influences the reproductive success of both the imported and resident zooplankton communities (Plourde et al., 2005; Hopcroft and Kosobokova, 2010). Both interannual and long-term climate variation affect the relative transport of these various water masses and, hence, the composition, distribution, standing stock, and production of zooplankton and their predators within the Chukchi Sea.

Over the past decade, our understanding of the zooplankton communities of the Chukchi Sea has improved considerably due to synthetic activities (Hopcroft et al., 2008) and on-going research (Lane et al., 2008; Hopcroft et al., 2010; Matsuno et al., 2011). The regional community composition is now well documented and indicates moderate diversity, the most of which is

contributed by copepods (e.g., Sirenko, 2001; Sirenko et al., 2010). As with most oceanic regions, copepods dominate in abundance and biomass, but larvaceans and meroplankton contribute significantly to community abundance and biomass in the Chukchi Sea (Lane et al., 2008; Hopcroft et al., 2010). Similarly, a dozen species of jellyfish and two species of chaetognaths are important predatory components of the zooplankton community (Hopcroft et al., 2005; Lane et al., 2008; Hopcroft et al., 2010).

In this study we employed a fixed-station design sampled at high resolution repeatedly over the open-water period during three consecutive years to refine our understanding of the seasonal and interannual variability of the Chukchi Sea zooplankton community. Concurrent measurements of phytoplankton, nutrients, and physics provide the environmental context with which to interpret these patterns within the framework of a multidisciplinary effort that includes other ecosystem components (i.e., Day et al., 2013).

1.3 Material and methods

1.3.1 Study area description

Sampling in the northeastern Chukchi Sea was conducted from late-July to mid-October (i.e., the entire ice-free period) during 2008–2010 (Day et al., 2013). In 2008 and 2009, samples were collected in two 900–NM^2 (~3000–km^2) study-area boxes (named Klondike and Burger) three times each year at 25 fixed oceanographic stations spaced 7.5 NM (~13.8 km) apart (Fig. 1.1). In 2010, a third 900–NM^2 irregularly shaped study-area box (named Statoil) with 22 fixed oceanographic stations was added to the sampling regime that was surveyed twice along with Klondike and Burger; however, only Burger was sampled a third time in September/October. Bottom depths over both survey areas varied from 35 m to 45 m.

1.3.2 Sample collection

Phytoplankton biomass was assessed as chlorophyll-*a* concentrations from samples collected with 4–L Niskin bottles on a Seabird SBE25/SBE55 CTD rosette (Weingartner et al., 2013) during upcasts at 6 depths per station: surface, 5 m, 10 m, 20 m, 30 m, and 3 m above the sea floor. Samples were filtered under low pressure onto 47–mm Whatman GF/F filters, then frozen at –20 °C for post-cruise analysis (Parsons et al., 1984). Nutrient samples were taken from

the same Niskin bottles as chlorophyll, frozen immediately, then analyzed post-cruise for nitrate, phosphate, and silicate concentrations (Whitledge et al., 1981; Gordon et al., 1993).

Smaller zooplankton were collected at each station by paired 150–µm-mesh ring nets of 60–cm diameter hauled vertically from within 3 m of the bottom to the surface at 0.5 m s^{-1} while the ship remained stationary. The volume of water filtered by the ring nets was measured by Sea-Gear one-way flowmeters mounted in the mouth of each net. To target larger, more mobile zooplankton, a set of 60–cm-diameter 505–µm Bongo nets were deployed in a double oblique tow with the ship moving at an average speed of 2 kt (~1 m sec^{-1}). All nets were of MARMAP design. The volume of water filtered by the bongo nets was measured by General Oceanics flowmeters mounted in the mouth of each net. In 2008, oblique tows were done for 20 min; in 2009 and 2010, these tow durations were decreased to 10 min to improve sample quality. Zooplankton samples were preserved in 10% formalin buffered with sodium hexametaphosphate. Large cnidarians and ctenophores were removed, measured, photographed, identified, and then discarded prior to sample preservation.

1.3.3 Sample processing

Frozen filters from all oceanographic fixed stations were extracted in the dark at –20 °C for chlorophyll-a using 95% acetone for 24 h, with concentrations determined fluorometrically post-cruise (Parsons et al., 1984) using a Turner Trilogy Fluorometer. Integrated chlorophyll concentrations were calculated by assuming each depth represented the concentration to the midpoint depth between each sampling interval. Frozen nutrient samples were analyzed post-cruise using an Alpkem Rapid Flow Analyzer (Whitledge et al., 1981) with methodology that adhered to WOCE standards (Gordon et al., 1993).

Formalin-preserved samples from half the stations evenly spaced across the grid in each survey area were processed to determine species composition, abundance and biomass. Larger organisms (primarily shrimp and jellyfish) were removed, enumerated, measured, and weighed (to ±10 µg). The samples were then split with a Folsom splitter until the smallest fraction contained about 100 specimens of the more abundant taxa. Specimens were identified to the lowest taxonomic category possible, staged where appropriate, enumerated, and measured (Roff and Hopcroft, 1986). Increasingly larger fractions were examined to identify, measure, and

enumerate the larger, less abundant taxa, particularly in the 505–µm net, which typically captures the largest taxonomic diversity. A minimum of 300, and more typically 400–600, individual organisms were identified from each sample.

If earlier copepodites could not be distinguished, they were grouped with the sibling species; in contrast, all adults were identified to species. *Calanus glacialis* and *Calanus marshallae* copepodites and adults are often difficult to distinguish; for pragmatic reasons, they were aggregated as *C. glacialis*, the more prevalent species in the region (Nelson et al., 2009). The larger *Calanus hyperboreus* was distinguished by size (e.g., Unstad and Tande, 1991; Hirche et al., 1994). The dry weight (DW) of each specimen was predicted from species-specific length-weight relationships, or from relationships of a morphologically similar species of mero- or holozooplankton (Hopcroft et al., 2010).

1.3.4 Data analysis

A three-way analysis of variance (ANOVA) test was conducted with the statistical package R (V2.15.1). A 4th root transformation was performed on macronutrients, chlorophyll-a, and zooplankton abundance and biomass data to test for significant interactions among site (Klondike, Burger, and Statoil), year (2008–2010), and cruise (July/August, August/September, and September/October). P-values ≤ 0.05 were considered significantly different.

To examine the relationship between individual samples, statistical analysis was done using the PRIMER (V6) software package, which has become a useful tool in revealing patterns in zooplankton communities (e.g., Wishner et al., 2008; Clarke and Warwick, 2010). Data sets were power transformed (4^{th} root), and the Bray-Curtis similarity index was calculated among stations employing all taxonomic categories that contributed at least 3% to any sample in that dataset. Significant groups within the hierarchical clustering were established with the SIMPROF routine, and these clusters were superimposed on the 2D and 3D plots of the multi-dimensional scaled (MDS) datasets, as well as spatial plots of the data. Relationships linking observed zooplankton community patterns with normalized physical data (above and below the thermocline) and integral chlorophyll were explored using PRIMER's BEST routine. The BEST routine establishes the relationship between the multidimensional community matrix and the environmental variables using both forward-selection and backward-elimination techniques.

Seasonal shifts of the zooplankton communities in each study site for each cruise across years was depicted by plotting centroid markers calculated from averaged station positions given by the optimal projection in the 2D MDS plots. This approach enables both the direction and the magnitude of change in community evolution within and among years to be interpreted.

1.4 Results

1.4.1 Temperature

In 2008, water-column temperatures were the lowest recorded over the three study years' surveys, with the highest SSTs at Klondike reaching ~6 °C in September/October and those at Burger reaching ~2 °C in August/September (Fig. 1.2). In 2009, both Klondike and Burger had the highest SSTs in July/August, with temperatures reaching ~8 °C and ~6 °C, respectively, and representing the warmest temperatures observed over the entire study (Fig. 1.2); SSTs actually declined as the season progressed. In contrast, the system warmed up in 2010 later than in 2009, with the warmest SSTs (~7.5 °C) recorded in Klondike in August/September. Overall, all three years displayed similar temperature patterns in which the more southern study area, Klondike, maintained warmer SSTs than did Burger and Statoil.

1.4.2 Chlorophyll-a and nutrients

Chlorophyll-a concentrations in 2008 declined over all sites as the summer progressed, with highest integrated values found over Burger during July/August associated with the ice-edge, reflecting the initiation of the seasonal phytoplankton bloom. The lowest chlorophyll-a values were recorded over Klondike in September/October (Fig. 1.3, Table 1.1). On all cruises, a pronounced chlorophyll-a maximum occurred between 20 m and 30 m at most stations (Fig. 1.4a). Peak concentrations of inorganic nutrients (nitrate, phosphate, and silicate) also occurred in this subsurface chlorophyll maximum, but nutrient concentrations were generally irregular throughout the sampling region and depleted throughout surface waters. These patterns were more pronounced in Klondike than Burger (Fig. 1.4a). Maximal chlorophyll-a and nutrient concentrations typically occurred in subsurface waters, at and near the pycnocline.

In 2009, both chlorophyll-a and nutrients were depleted at all depths in the water-column on all cruises, indicating that sampling occurred post-bloom (Fig. 1.4b). There was no clear

seasonal or spatial pattern in nutrient profiles, but concentrations were slightly higher in Burger than in Klondike except for the September/October cruise, when overall concentrations were elevated, especially in Klondike (Fig. 1.4b).

In 2010, the latter part of the phytoplankton bloom was observed during the July/August cruise (Fig. 1.3); chlorophyll-a and nutrient concentrations were depleted from the surface layers but frequently had peaks between 20 m and 30 m at most stations (Fig. 1.4c). At Klondike, most subsurface chlorophyll and all subsurface nutrients were depleted at all depths on both surveys. In contrast, Burger and Statoil showed subsurface nutrients and chlorophyll in July/August that then declined at Statoil, but not Burger, in August/September. On all cruises Burger retained deep pools of nitrate and silicate. These observations suggest Klondike was sampled post-bloom in July/August, whereas the bloom was in its final stages at Burger and Statoil. It is unclear how the high subsurface chlorophyll and nutrients persisted throughout the summer at Burger, but they are clearly coupled. Different advection rates of phytoplankton and nutrients among the survey areas likely contribute to some of the observed differences.

Both nutrients and chlorophyll concentrations showed significantly different interactions when tested against site, year, and cruise (P-value ≤ 0.05, Table 1.2). This hierarchal grouping signifies that the magnitude of concentrations were different not only across all three years in the study sites but also between individual cruises, both seasonally and interannually.

1.4.3 Zooplankton abundance, biomass, and composition

A total of nearly 500 samples split equally between two net mesh-sizes were analyzed during this three-year study. We recorded 13 major taxonomic groups representing ~70 species, plus 11 meroplanktonic categories, over the study period. In 2008, holozooplankton abundances averaged 2381 and 106 individuals m^{-3} and biomass averaged 10.5 and 8.3 mg DW m^{-3} in the 150– and 505–µm nets, respectively (Table 1.3). In 2009, a higher abundance but moderate biomass was recorded for the holozooplankton community that averaged 6842 and 189 individuals m^{-3} and 16.3 and 7.0 mg DW m^{-3} in the 150– and 505–µm nets, respectively (Table 1.3). In 2010, overall holozooplankton abundances were similar to those in 2009, but their biomass was much higher than in 2009: 7396 and 198 individuals m^{-3} and 102.9 and 33.5 mg DW m^{-3} in the 150– and 505–µm nets, respectively (Table 1.3). These increases in the biomass

of holozooplankton in 2010 were driven by increases in the abundance of large-bodied, lipid-rich copepods. Although species-composition varied within and among years, samples were generally dominated numerically by the copepods *Pseudocalanus* spp., *Acartia* spp., *C. glacialis*, and *Oithona similis*; the larvaceans *Fritillaria borealis* and *Oikopleura vanhoeffeni*; and meroplanktonic stages of bivalves, barnacles, and polychaetes (Table 1.3). *Calanus glacialis* and the chaetognath *Parasagitta elegans* dominated the biomass, with *O. vanhoeffeni, Pseudocalanus* spp., and the jellyfish *Aglantha digitale* next in abundance (Table 1.3).

The contribution of meroplankton was substantial, but their patterns of abundance and biomass varied among years more than those of holozooplankton did, thereby blurring patterns for total zooplankton (Table 1.3). In 2008, meroplankton abundance averaged 948 and 84 individuals m^{-3} and biomass averaged 7.8 and 0.8 mg DW m^{-3} in the 150– and 505–µm nets, respectively (Table 1.3). Meroplankton numbers declined in the warm 2009 conditions, when we recorded 625 and 7 individuals m^{-3} as 6.0 and 0.2 mg DW m^{-3} in the 150– and 505–µm nets, respectively. In 2010, we recorded 9315 and 22 individuals m^{-3} and 12.1 and 0.2 mg DW m^{-3} in the 150– and 505–µm nets, respectively (Table 1.3); this intensification in 2010 resulted from increased abundances of small bivalve and, to a lesser extent, polychaete and ophiuroid, larvae. In all three years, barnacle larvae contributed the greatest biomass for all meroplanktonic categories, although they are not consistently captured by the 505–µm net. Decapod larvae appear to be the meroplankton captured most reliably by the 505–µm mesh nets. To place the contribution of meroplankton in perspective, they contributed 28% of numbers in 2008, 8% in 2009, and 56% in 2010 to the total zooplankton community in the 150–µm net and contributed 44%, 4%, and 10%, respectively, in the community caught by the 505–µm nets. In contrast, their contribution to biomass declined across years, from 43% to 11% in the 150–µm nets and from 9% to 0.6% in the 505–µm nets.

Overall, the patterns observed in the zooplankton communities can be attributed to a combination of interactions among site, year, and/or cruise for the major zooplankton categories (Table 1.2). Abundance, and to a lesser extent biomass, data from the 150–µm net showed significant differences influenced by the site, year, and cruise interaction. In contrast, this hierarchal three-way interaction was variable and had less of an impact for both abundance and biomass data from the 505–µm net. As anticipated, year provided to be the strongest variable for the significant differences observed among the zooplankton taxonomic categories collected by

the 505–µm nets. A comparison by sampling period across the three years does not show large differences in abundance during July/August (Figs. 1.5 & 1.6), although there is a suggestion of lower abundance of copepods in 2008 than in subsequent years. There was, however, significantly higher biomass of chaetognaths in July/August 2010 than in prior years and significantly higher biomass of large copepods in 2010 than in 2008 and 2009 (Figs. 1.7 & 1.8). In August/September, the abundance of copepods, meroplankton, and cnidarians was higher in 2010 than in previous years (Figs. 1.5 & 1.6), and the biomass of copepods, meroplankton, hydrozoans, chaetognaths, and the "other" category were also greater in 2010 than in previous years (Figs. 1.7 & 1.8). In September/October, larvacean abundance was significantly higher in 2009 than in 2008 and 2010, whereas copepod abundance was significantly higher in 2009 and 2010 than in 2008 (Figs. 1.5 & 1.6); biomass again showed a progressive increase in copepods and chaetognaths across years, along with a peak in hydrozoans in the Burger prospect for 2010 (Figs. 1.7 & 1.8).

In the 150–µm nets, abundance of the copepod genera *Oithona*, *Pseudocalanus*, *Acartia*, *Calanus*, and *Metridia* increased across all three years; the abundance of the cyclopoid copepod *Oncaea* and the larvacean *Fritillaria* were highest in 2009 and of both *Centropages* and *Oikopleura* were higher in 2008 and 2010 than in 2009 (Figs. 1.9a and b). Within the meroplankton, the abundance of barnacle larvae (nauplii plus cyprids) declined seasonally but showed no clear interannual pattern, whereas abundance of polychaete and bivalve larvae increased dramatically in 2010 (Fig. 1.9b). In the 505–µm nets, the abundance of the large copepod *C. glacialis* in 2010 was several-fold higher than that of previous years, whereas the abundance of *Neocalanus* and *Eucalanus* was extremely low in 2009 and higher in 2008 and 2010 (Fig. 1.10). The different abundance patterns observed between net types for *C. glacialis* arise because young, smaller stages of copepodites that are not retained well by the 505–µm net, were more abundant in 2009. The mucous-net feeding larvaceans *Oikopleura* and *Fritillaria* had reciprocal patterns of abundance, with the abundance of *Fritillaria* highest in 2009 and that of *Oikopleura* highest in 2008 and 2010 (Fig. 1.10). *Thysanoessa* spp. and their larval stages were variable in abundance, but were highest in 2009 and 2010 and lowest in 2008 (Fig. 1.10). Among the larger predators, the abundance of the cnidarian *A. digitale* was highest in 2010, the abundance of the ctenophore *Mertensia ovum* was highest in 2009 and 2010 (none were detected

in 2008), and the abundance of the chaetognath *P. elegans* was higher in 2010 than in prior years (Fig. 1.10).

Comparison of the copepod size spectra between nets and across seasons provides further resolution to the observed patterns. Based on the 150–µm collections (Fig. 1.11), far more copepods in all size categories occurred in 2010 than in 2008 and 2009, with 2008 being lowest in individuals >1500 µm in prosome length. These differences are more pronounced in biomass spectra than abundance spectra. The spectral peaks between 1500 µm and 4000 µm reflect the stages of *C. glacialis*, with still larger sizes contributed by *Neocalanus* species and *Eucalanus bungii*. The 505–µm collections (Fig. 1.12) typically provide much more robust data for copepods above ~1200–1500 µm (Hopcroft et al., 2001) and should progressively extrude copepods of decreasing size. Only the 2010 data shows the expected pattern, with 2009 showing a minor mode below 1000 µm and 2008 with an unexpectedly large peak below 1000 µm.

The peaks below 1000 µm in 2008, and to a lesser extent in 2009, arose due to an excess retention of smaller-bodied copepods (and other groups). This problem was most pronounced in 2008, when the larvacean *Oikopleura* and their mucus houses were prevalent. We believe this was accentuated by tows of nearly double the duration in 2008 than in subsequent years. This longer towing time in 2008 caused larvacean houses to decrease the effective mesh-size of the nets and the retention of smaller zooplankton that should have normally passed through the net. Based on knowledge of mesh-size retention and body-size spectra (Hopcroft et al., 2001), we suggest that over-retention increased the estimated abundance of copepods in the 505–µm net samples by 35–40 individuals m^{-3} (i.e., by ~80%) and is probably responsible for the higher abundance of *Acartia* spp., *Centropages*, and *Pseudocalanus* spp. observed in 2008 than in 2009 and 2010. The same postulations can be made for the meroplankton, especially the barnacles, in which numbers were uncharacteristically higher in 2008 than in subsequent years. The impacts of this bias on biomass are much less than those for abundance because small animals weigh little; they are estimated to be ~0.24 mg DW m^{-3} (11%) of the copepod biomass in 2008.

1.4.4 Zooplankton community patterns

Seasonally, the stations typically have 60–90% similarity, with slightly lower similarity among years. Consequently, the zooplankton communities appear to be distinctly different in all

three years, with little overlap in their clustering and distinct domains for multidimensional scaling of both 150–µm and 505–µm abundances (Fig. 1.13). Interestingly, the 2008 data show a tighter station clustering and higher within-year similarity than 2009 for the 505–µm samples, suggesting that one of the greatest differences between these years was changes in size composition.

When looking at each year individually, patterns of community dynamics become clearer. In 2008, ice covered much of the study region (see Weingartner et al., 2013) when sampling was initiated in mid-July. The July/August and August/September cruises for Klondike clustered together, but warmer water temperatures by late September shifted zooplankton communities in the 150–µm nets into a different spatial domain (Fig. 1.13). In Burger, however, changes in the zooplankton community from one month to the next were small, suggesting that the community's ability to grow and reproduce was slowed by the cold waters that persisted there. Stations in the 505–µm nets (Fig. 1.13) were much more tightly clustered than those in the 150–µm nets, having only a few outlier stations and little seasonal change.

In 2009, both Klondike and Burger showed almost identical patterns of spatial trajectory in the 150–µm nets (Fig. 1.13). As the season progressed from July/August to August/September, both areas showed a distinct transition in community composition; then, in September/October, the transition was again mirrored in a reversal towards the initial conditions due to the early onset of the fall cooling. The 505–µm nets (Fig. 1.13) at Klondike followed a pattern similar to that of the 150–µm nets but with a smaller transition from August/September to September/October. In contrast, Burger shifted much less than Klondike from July/August to August/September, then progressed equally in September/October. Interestingly, given the dissimilarity in magnitude of change between July/August and August/September, communities in both Klondike and Burger during September/October are similar.

In 2010, the Statoil study area was added to the sampling regime; in general, all three study areas showed similar seasonal transitions in community structure for both the 150– and 505–µm nets, with the most dramatic change observed in Klondike from July/August to August/September (Figs. 1.13). Very little seasonal change in community structure was seen in the 150–µm nets in Burger from August/September to September/October, although a larger

increase was seen in the 505–µm nets, consistent with the presence of much larger zooplankton species, especially the genera of larger copepods such as *Neocalanus* and *Calanus*.

For the entire dataset, correlations with environmental variables were fairly strong for the zooplankton communities from both net sizes (Table 1.4), with the strongest relationship associated with bottom temperature. The only exception was for 2009, where fluorescence, both above and below the mixed-layer depth, was the strongest relationship. In all cases, slight improvements to the models were made when additional variables were added, specifically surface temperature and fluorescence (2008), temperature and salinity (2009), and temperature, salinity, and fluorescence (2010). Although we have only presented the best explanatory 1–3–variable models, there was little improvement by adding additional parameters. Furthermore, our analysis does not allow us to determine when one model is significantly superior to another or the optimal number parameters to include. Nonetheless, the process gives us a greater appreciation for how these data are linked to the underlying physical and chemical processes. In 2008, correlations between environmental variables and the biological data were strengthened when the bycatch of smaller holozooplankton species and meroplankton in the 505–µm nets was eliminated.

1.5 Discussion

1.5.1 Chlorophyll-a and nutrients

As in other oceans, phytoplankton abundance in the Chukchi Sea is related to water-column irradiance and nutrient concentration (Hill et al., 2005; Lee et al., 2007). Nutrients in surface waters are depleted rapidly as the ice retreats from the shelf and the spring bloom occurs. Subsurface chlorophyll peaks of 2–12 mg m^{-3} have been observed during the spring bloom at the shelf break north of our study area, followed by low concentrations of chlorophyll and nutrients (Hill et al., 2005), consistent with our 2008 and 2010 observations. Farther to the south and west of our study area, chlorophyll-a concentrations in excess of 200 mg m^{-2} have been observed, although values below 50 mg m^{-2} also are common (Lee et al., 2007).

The differences in the nutrient and chlorophyll concentrations at the study sites among years reflect the time of the cruises relative to the seasonal bloom. Lower nutrient and

chlorophyll concentrations in surface and subsurface waters indicate that the observations were collected post bloom. Chlorophyll concentrations observed during the 2008–2010 cruises (Table 1.1) generally fall within the lower range of historical values from the 1974 to 1995 period (Dunton et al., 2005) except during the bloom captured in early 2008. Their study further suggests that large gradients of chlorophyll standing stocks can occur through the Chukchi Sea, with estimated values in the vicinity of the Klondike, Burger, and Statoil study areas being approximately 80–200 mg m^{-2}.

1.5.2 Regional zooplankton comparisons

The Chukchi Sea displays a level of diversity similar to, but a biomass higher than, the adjoining East Siberian (Jaschnov, 1940; Pavshtiks, 1994) and Beaufort (e.g., Horner, 1981; Lane et al., 2008) seas. In contrast, the Chukchi Sea has lower diversity than is present in the nearby vertically-structured Central Arctic Basin, where depths can exceed 3000 m (e.g., Kosobokova and Hirche, 2000; Kosobokova and Hopcroft, 2010). Most copepod species recorded in the current study are of subarctic Pacific Ocean and/or the Bering Sea affinity, rather than the Arctic (Brodsky, 1950, 1957), due to the generally northward advection of waters through Bering Strait (e.g., Weingartner et al., 2005 & 2013). Even the populations of the copepod *C. glacialis*, which is normally considered an arctic species, appear to originate in the northern Bering Sea (Nelson et al., 2009). In contrast to all other planktonic groups, the hydrozoan medusae are more arctic in character, presumably because many species are released only seasonally into the water-column by the benthic life-stage farther south in the Chukchi. Nonetheless, the planktonic community's species-composition is generally similar to that observed during the summer ice-free period in this region when similar fine-mesh (e.g., Springer et al., 1989; Kulikov, 1992; Hopcroft et al., 2010) or coarse-mesh nets (e.g., Wing, 1974; English and Horner, 1977) are used.

Our estimates of 2400–7400 holozooplankters m^{-3} (10.5–103 mg DW m^{-3}) captured by the 150–µm nets and 106–198 m^{-3} (7.0–33.5 mg DW m^{-3}) captured by the 505–µm net are similar to those from studies to the southwest of the Klondike and Burger survey areas where an average of 3500 holozooplankters m^{-3} (42 mg DW m^{-3}) recently were recorded with 150–µm vertical nets (Hopcroft et al., 2010). The number of meroplankton observed in that study (2300 m^{-3}) also overlaps our estimates. There is also a broad range of older biomass estimates for the

region, all of them lower than what we recorded: ~2 g DW m^{-2} for herbivorous zooplankton north and south of Bering Strait (Springer et al., 1989), 2.5–5.5 g DW m^{-2} on the US side of the Chukchi Sea (Turco, 1992a, 1992b), and 1.3 g DW m^{-2} spanning both sides of the Chukchi (Turco, 1992a, 1992b). Additional estimates of 14.8 g WW m^{-2} (Kulikov, 1992) and 356 mg WW m^{-3} (14.2 g WW m^{-2} (Pavshtiks, 1984) and 26.8–42.8 g WW m^{-2} (Matsuno et al., 2011) for all mesozooplankton spanning the Chukchi Sea are also somewhat lower, if we assume that DW is 10–15% of WW (Wiebe et al., 1975). Our 2010 estimates (33.7–115 mg DW m^{-3}) generally exceed the range of recent observations (3–58 mg DW m^{-3}) near the shelf break north of Klondike, Burger, and Statoil (Lane et al., 2008; Llinás et al., 2009) and estimates for the upper 50 m farther into the adjoining basin (Kosobokova and Hopcroft, 2010).

All of the species observed in this study previously have been reported for this region, but not within a single study. Our 505–μm data are directly comparable to data from the ISHTAR (Inner Shelf Transfer and Recycling) program (Springer et al., 1989; Turco, 1992a, 1992b), which also noted the predominance of the herbivorous *C. glacialis*, *Pseudocalanus* spp., *Acartia longiremis*, and *O. vanhoeffeni*. In addition to differences between plankton-net mesh-sizes, detailed comparison with many previous studies also requires an understanding of changes in taxonomic resolution (e.g., *Pseudocalanus* (Frost, 1989); *Neocalanus* (Miller, 1988); *Calanus* (Frost, 1974)). Even today, routine morphological separation of several of these species is difficult (Llinás, 2007; Lane et al., 2008), and molecular analyses are forcing us to reshape our views on ranges of even larger species such as *Calanus* (Nelson et al., 2009). Other holoplanktonic crustacean groups, such as euphausiids and cladocerans, present less of a taxonomic challenge, although they are not always reported to the species level. Non-crustacean groups have been recorded with variable resolution and proficiency in previous studies. This study is consistent with an emerging realization that considerable populations of larvaceans, specifically the large arctic *O. vanhoeffeni* and the much smaller polar/subpolar *F. borealis*, are present in both the northern Bering and Chukchi Seas (e.g., Kulikov, 1992; Lane et al., 2008; Hopcroft et al., 2010) and at times reach a biomass greater than that of crustaceans (Springer et al., 1989; Shiga et al., 1998; Hopcroft et al., 2010).

The dominant predators in terms of abundance and biomass were the chaetognaths, here exclusively *P. elegans*, consistent with other studies from the region (e.g., Cooney, 1977; Springer et al., 1989; Kulikov, 1992; Lane et al., 2008; Hopcroft et al., 2010). Consistent with

these studies, there also was considerable biomass of both small and large gelatinous organisms: *A. digitale, Aeginopsis laurentii, Catablema vesicarium,* and *Rathkea octopunctata* were most common, but larger species periodically were captured, although they were poorly quantified.

Suspension-feeding meroplanktonic larvae of benthic organisms were extremely common throughout the sampling region in all three years. High abundances of meroplankton are typical of the summer plankton community in this region (e.g., Cooney, 1977; Springer et al., 1989; Kulikov, 1992; Lane et al., 2008; Hopcroft et al., 2010), and knowledge of their distribution and abundance likely reflects variability in the reproduction and recruitment of these rich benthic communities (Bluhm et al., 2009; Blanchard et al., 2013–a, b). Although the abundance of some meroplanktonic groups such as barnacle larvae remained consistent across study years, the abundance of other groups such as bivalve, polychaete, and echinoderm larvae was highly variable, suggesting they are influenced by varying temperature and food conditions. Given their apparently large contribution to the zooplankton biomass in the survey areas, appropriate length-weight relationships for meroplanktonic groups need to be established to understand better their importance in ecosystem energetics.

1.5.3 Zooplankton community patterns

The spatial distribution of the zooplankton communities in the Chukchi Sea frequently has been tied to the different water masses in this region. Such patterns were first recognized by Russian researchers as early as the 1930s (Stepanova, 1937a, b), and were later refined by continued Russian efforts (e.g., Pavshtiks, 1984) that identified at least three water masses in the region. The observed community patterns in the Chukchi Sea are to a large extent a continuation of patterns observed in the northern Bering Sea (see review by Coyle et al., 1996). Although the first years of the ISHTAR program were restricted to sampling in US waters, oceanic Anadyr Water, neritic Bering Shelf Water, and low-salinity Alaska Coastal Water were recognized south of Bering Strait (Springer et al., 1989). Cross-basin studies by the international BERPAC (Bering-Pacific) program also identified three zooplankton clusters within the Chukchi Sea but failed to articulate their species assemblages or associate them with specific water masses (Kulikov, 1992). Recent sampling in the southern and western Chukchi Sea also confirms strong ties to water masses (Hopcroft et al., 2010).

Despite the proximity of the survey areas, we frequently were able to separate them based on community structure and were able to detect a seasonal evolution to the communities. Within years, temperature and, to a lesser degree, salinity and in situ chlorophyll fluorescence are variably correlated with community structure. Notably, the study area appears to have little direct influence from the Alaska Coastal Current (i.e., Hopcroft et al., 2010), although coastal species (e.g., *Podon leuckartii, Evadne nordmanni*, *Acartia hudsonica*, and *Eurytemora* spp.) were recorded in low numbers throughout our study areas.

1.5.4 Interannual patterns in zooplankton communities

Prior observations in the Chukchi Sea have shown large interannual variability in the abundance and biomass of plankton communities (Turco, 1992a, 1992b). The most striking feature of the zooplankton community from 2008 to 2010 was the large increase in the abundance of several ecologically important suspension-feeding copepod species (*Calanus* and *Pseudocalanus)*, microzooplanktonic predatory copepods (*Acartia* and *Oithona*), all categories of meroplankton, omnivorous euphausiids, and planktonic predators. It is particularly notable that overall increases in copepod abundance and biomass occurred in the large lipid-rich species that should be of greatest value to those vertebrates feeding on zooplankton. Large increases in the abundance of planktonic predators – most notably the ctenophore *M. ovum*, the cnidarian *A. digitale*, and the chaetognath *P. elegans* – are a likely result of the increased availability of their prey. The huge spikes in meroplankton abundance in August/September of 2010 also suggest that it was a productive year and that the benthos had received a considerable supply of food earlier in the season. The only notable species whose abundance did not increase in 2010 was the larvacean *F. borealis*.

We postulate that the interannual variability observed in the planktonic communities from 2008 to 2010 is related to a combination of both physical parameters observed at the study area and the intensity of physical advection from Bering Strait. Sea-surface temperatures (SSTs) in 2008 were low throughout the entire summer at Burger (i.e., generally <1 °C) but warmed over the summer at Klondike, reaching temperatures of up to 6 °C (Weingartner et al., 2013). These cold SSTs retarded zooplankton growth and development, resulting in lower abundances and smaller body sizes across all major taxa. In 2009, ice retreat was earlier than the previous year, and SSTs already were 5–7 °C in Klondike and only slightly cooler at Burger by the

July/August cruise. Temperatures declined slowly over subsequent 2009 cruises, but there was noticeably more "heat" in the system during 2009 and 2010, with the July/August 2009 average water-column temperatures in Klondike being the highest recorded across all years and all study areas (Weingartner et al., 2013). Warmer temperatures in 2009 should have favored the growth and reproduction of subarctic zooplankton (Liu and Hopcroft, 2008), contributing to the higher abundance of zooplankton in 2009 than in 2008 (i.e., a doubling in 150–μm net abundances). Such temperature increases appear to have supported more energy-rich, larger-bodied zooplankton earlier in the 2009 season, yet the chronically low concentrations of chlorophyll and nutrients over the entire summer suggest that grazing zooplankton would ingest little of their body carbon daily (Campbell et al., 2009) and that production rates would be low (Plourde et al., 2005) throughout most of the season. In 2010, ice retreat was slow at first but accelerated later, and SSTs warmed rapidly to as much as 8 °C. Similar to 2008, we captured some of the spring bloom signal in 2010; however, unlike 2009, nutrients persisted in the system at Burger and Statoil, maintaining intermediate concentrations of chlorophyll upon which zooplankton could feed, grow, and reproduce at higher rates. The extent and duration of ice-free zones during May-July also shows significant interannual variability (Weingartner et al., 2013) and may be important in priming the productivity of the zooplankton communities prior to our period of observation.

Changes in the abundance and relative contribution of crustacean and non-crustacean zooplankton, especially larger-bodied copepods and euphausiids, can help us to interpret the degree of dissimilarity in community structure from 2008 to 2010. We speculate that several larger species became progressively more abundant from 2008 to 2010 because the "productive" season started earlier in 2009 and 2010, yielding oceanographic conditions (especially temperatures) that were more optimal for their growth and/or reproduction throughout the study region and waters being advected in from the south. These factors placed populations of larger crustacean zooplankton in the survey areas sooner than in 2008 and at a time when they could be usefully exploited by fishes, planktivorous seabirds, and other higher trophic levels. These differences likely contributed to the contrasting seabird populations observed between 2008 and 2009 (Gall et al., 2013) but do not explain why seabirds failed to capitalize better on the dramatic 2010 increases in zooplankton abundance. Interestingly, when comparing the temporal evolution of the communities outlined by the centroids in the MDS plots (Fig. 1.13) with the heat budget

calculated (Weingartner et al., 2013), we see a striking resemblance in patterns, reinforcing our speculations about the importance of temperature in the seasonal evolution of zooplankton communities in high-latitude systems.

1.6 Conclusions

We believe that the variations in water temperature and timing of the phytoplankton bloom in 2008–2010 resulted in large differences in both seasonally and spatially averaged zooplankton abundance and biomass. It is likely that both the intensity of zooplankton transport from more southern waters and downstream productivity are also important. Sampling during three consecutive years has allowed us to recognize the level of inter- and interannual variability of a plankton community that primarily is Pacific in faunal character. Future surveys will help to further refine the scales of spatial and interannual variability.

Compounding the large degree of seasonality and interannual variations that occur within the region, sampling location also influences the biological community observed. Thus, a spatially consistent sampling design is essential for separating ecological patterns driven by site-specific conditions from longer-term climatological shifts. The use of a consistent sampling protocol allowed us to detect differences in both the timing and magnitude of the planktonic communities and other interconnected ecosystem components (Blanchard et al., 2013–a, b; Gall et al., 2013) and place them in a larger ecosystem perspective (Day et al., 2013). Alterations to water-column productivity due to interannual variability, long-term climate change, or human activity could have direct impacts on this ecosystem. The data collected through this program, combined with historical and regional data, provide us with direct observations of community composition and biomass; these are the fundamental elements for comparing temporal variation in biological communities with environmental change.

1.7 Acknowledgments

We thank ConocoPhillips, Shell Exploration and Production, and Statoil USA E & P for supporting this study. We thank Olgoonik-Fairweather LLC for their logistical support. We thank the captains and crew members of the M/V *Bluefin* (2008) and R/V *Westward Wind* (2009 and 2010), the marine technicians, and Aldrich Offshore Services. Chris Stark, Daniel Naber, Katherine Trahanovsky, and Elizabeth Stockmar assisted with the processing of samples.

Finally, Robert H. Day, Kenneth O. Coyle, and comments from three anonymous reviewers improved this manuscript.

1.8 Appendix A. Supporting information

Supplementary data associated with this article can be found in the online version at http://dx.doi.org/10.1016/j.csr.2012.11.003.

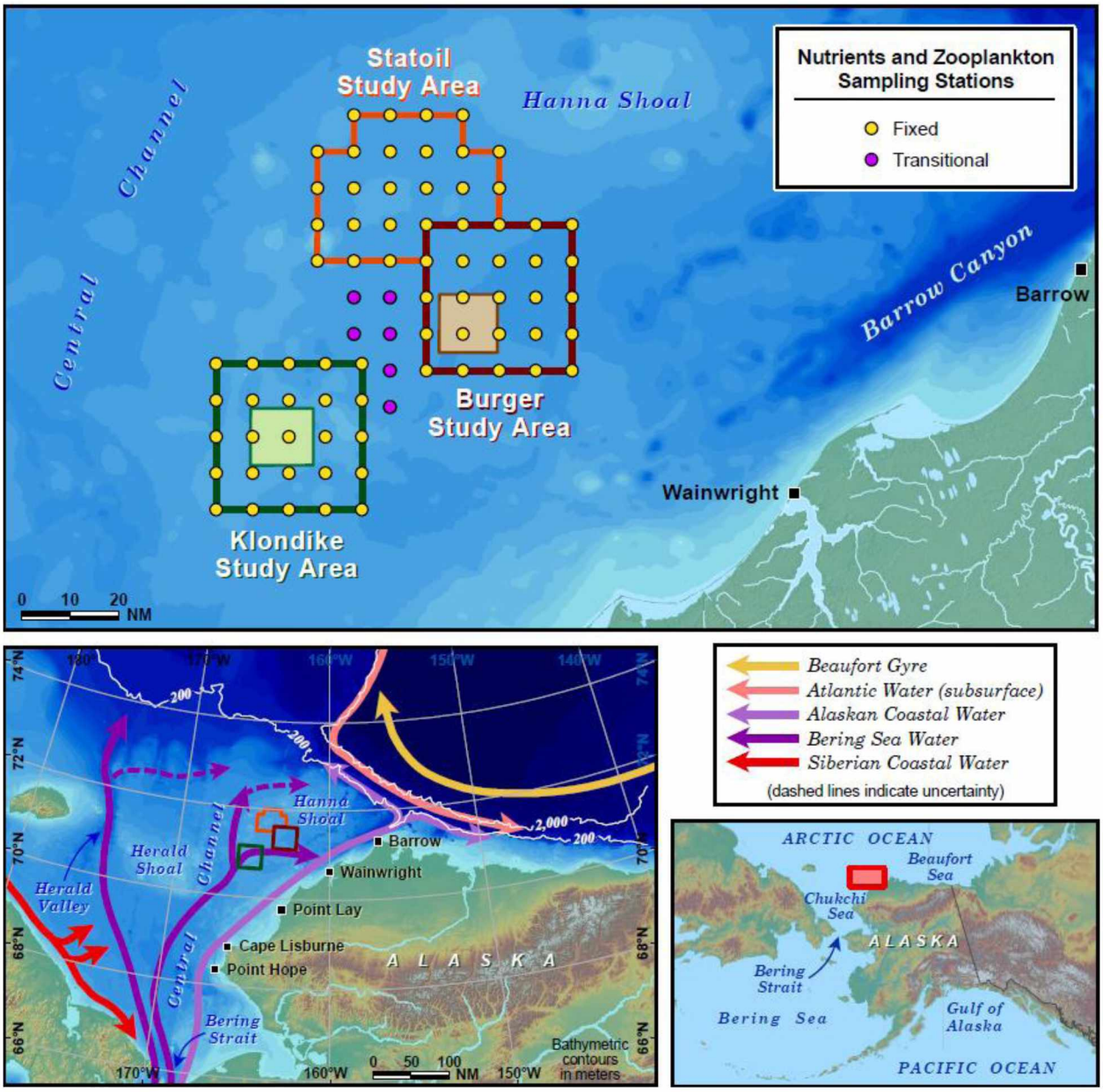

Figure 1.1 Locations of the Klondike, Burger, and Statoil survey grids in the northeastern Chukchi Sea. Station layout for each survey grid (upper panel) with generalized currents for the region (lower left panel).

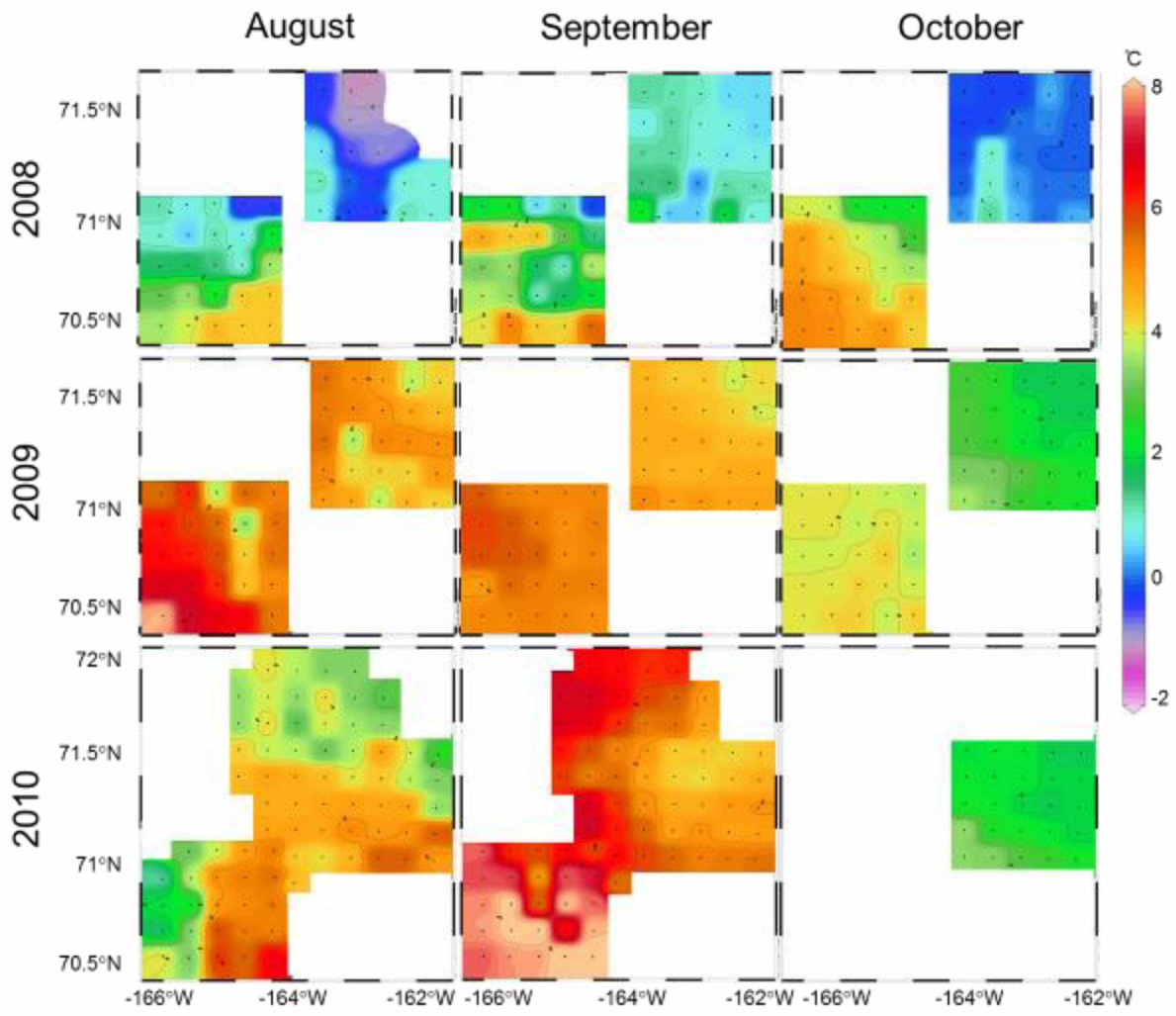

Figure 1.2 Temperature (°C) averaged over the upper 10 m of the water column for the Klondike, Burger, and Statoil grids in the Chukchi Sea from 2008 to 2010.

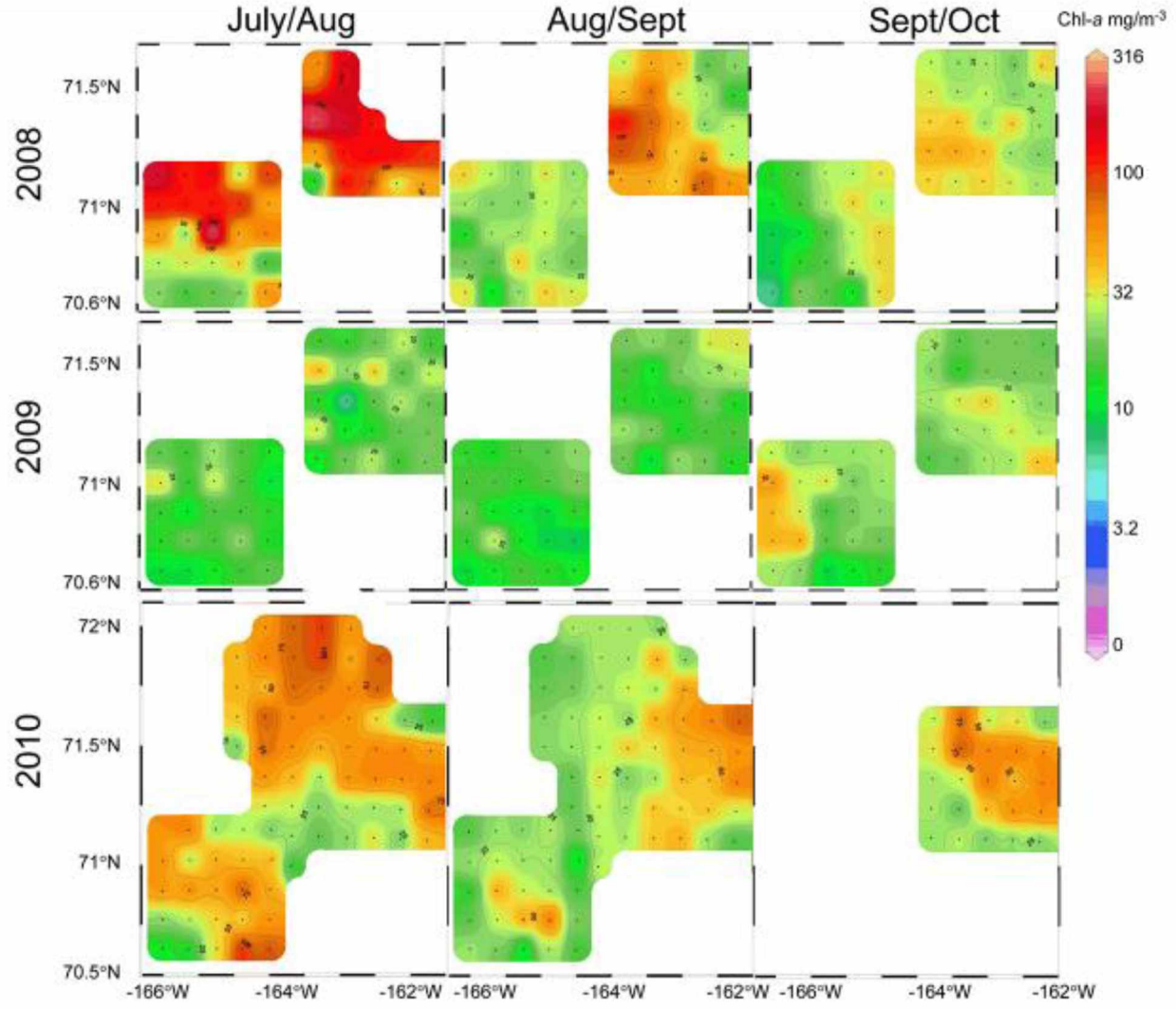

Figure 1.3 Integrated chlorophyll-a plotted over a log scale in the Klondike, Burger, and Statoil grids in the Chukchi Sea from 2008 to 2010.

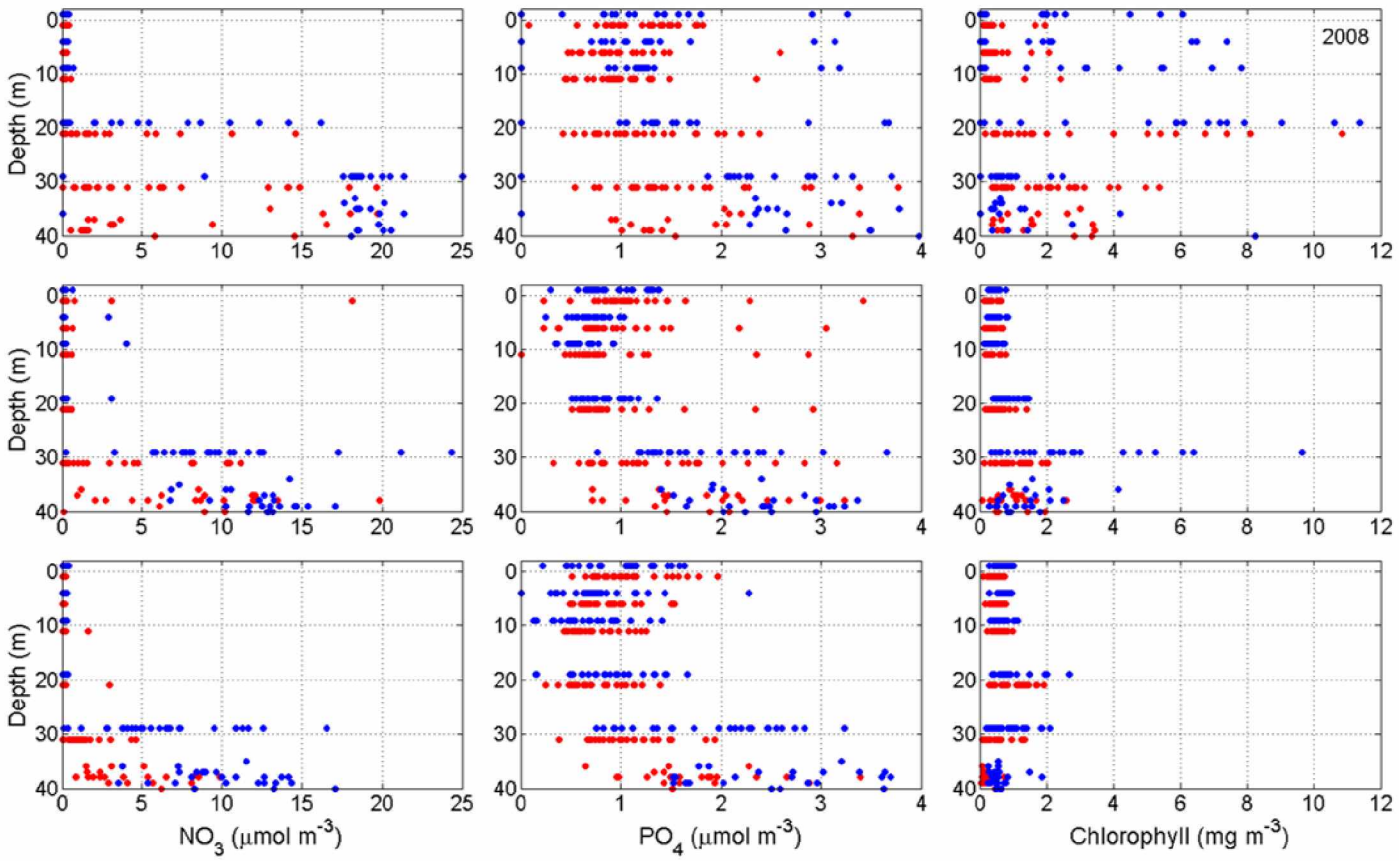

Figure 1.4a Depth distributions of nitrate, phosphate, and chlorophyll-a concentrations in the Chukchi Sea for all stations in Klondike, Burger, and Statoil per cruise for 2008. Silicate data not shown. Data points offset by ±1 m for Klondike and Burger, respectively. Klondike (red circles); Burger (blue circles); and Statoil (green circles).

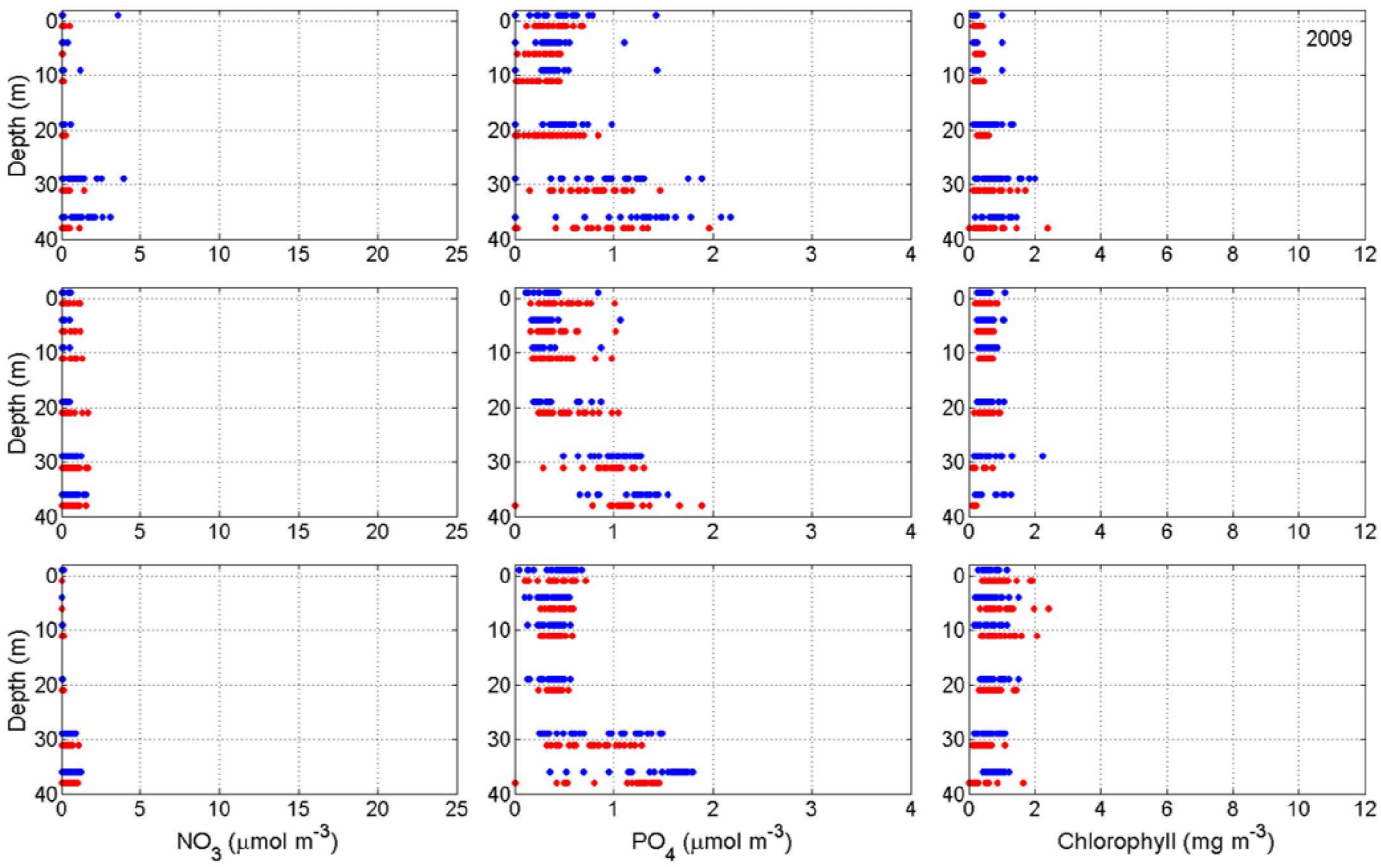

Figure 1.4b Depth distributions of nitrate, phosphate, and chlorophyll-a concentrations in the Chukchi Sea for all stations in Klondike, Burger, and Statoil per cruise for 2009.

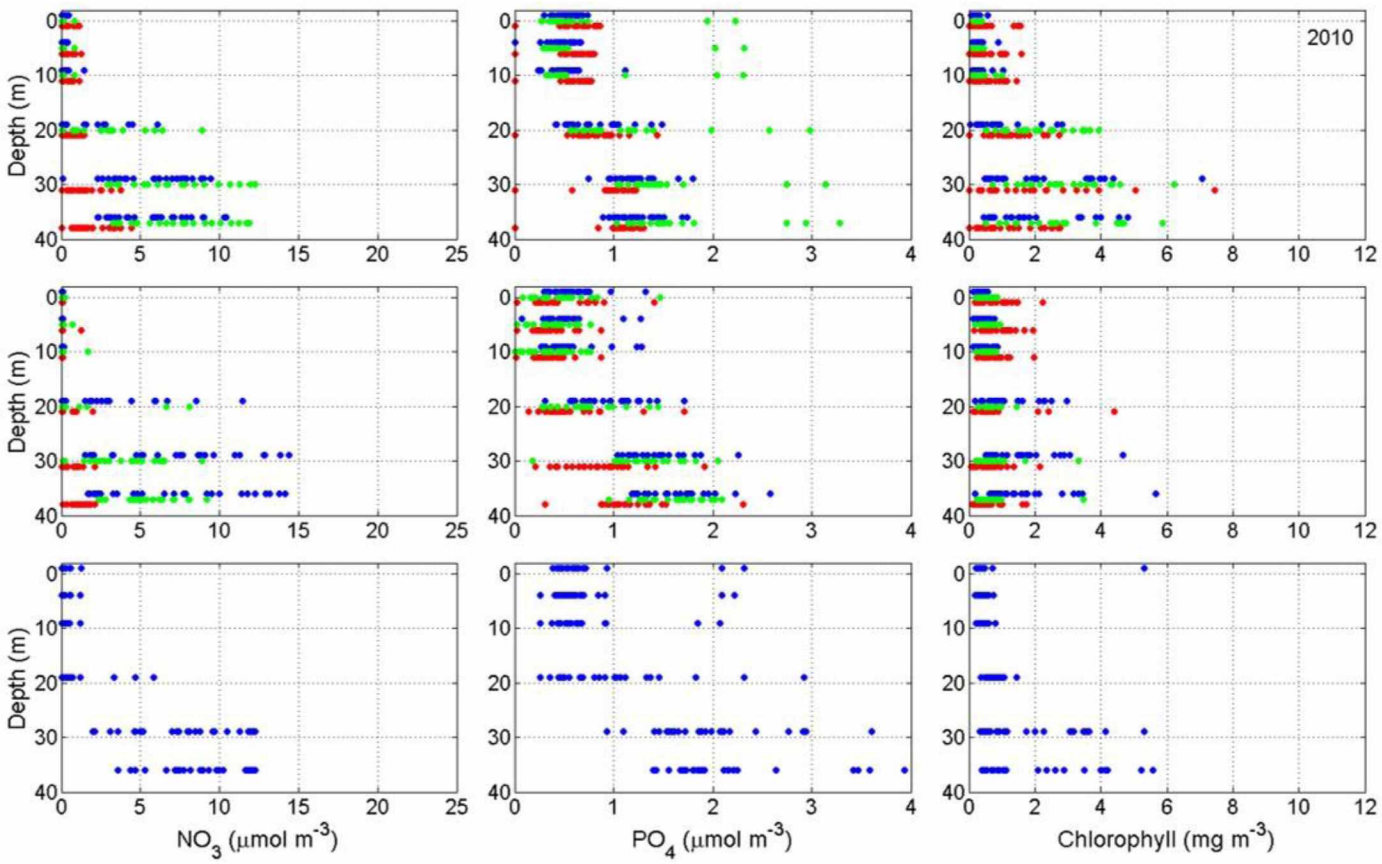

Figure 1.4c Depth distributions of nitrate, phosphate, and chlorophyll-a concentrations in the Chukchi Sea for all stations in Klondike, Burger, and Statoil per cruise for 2010.

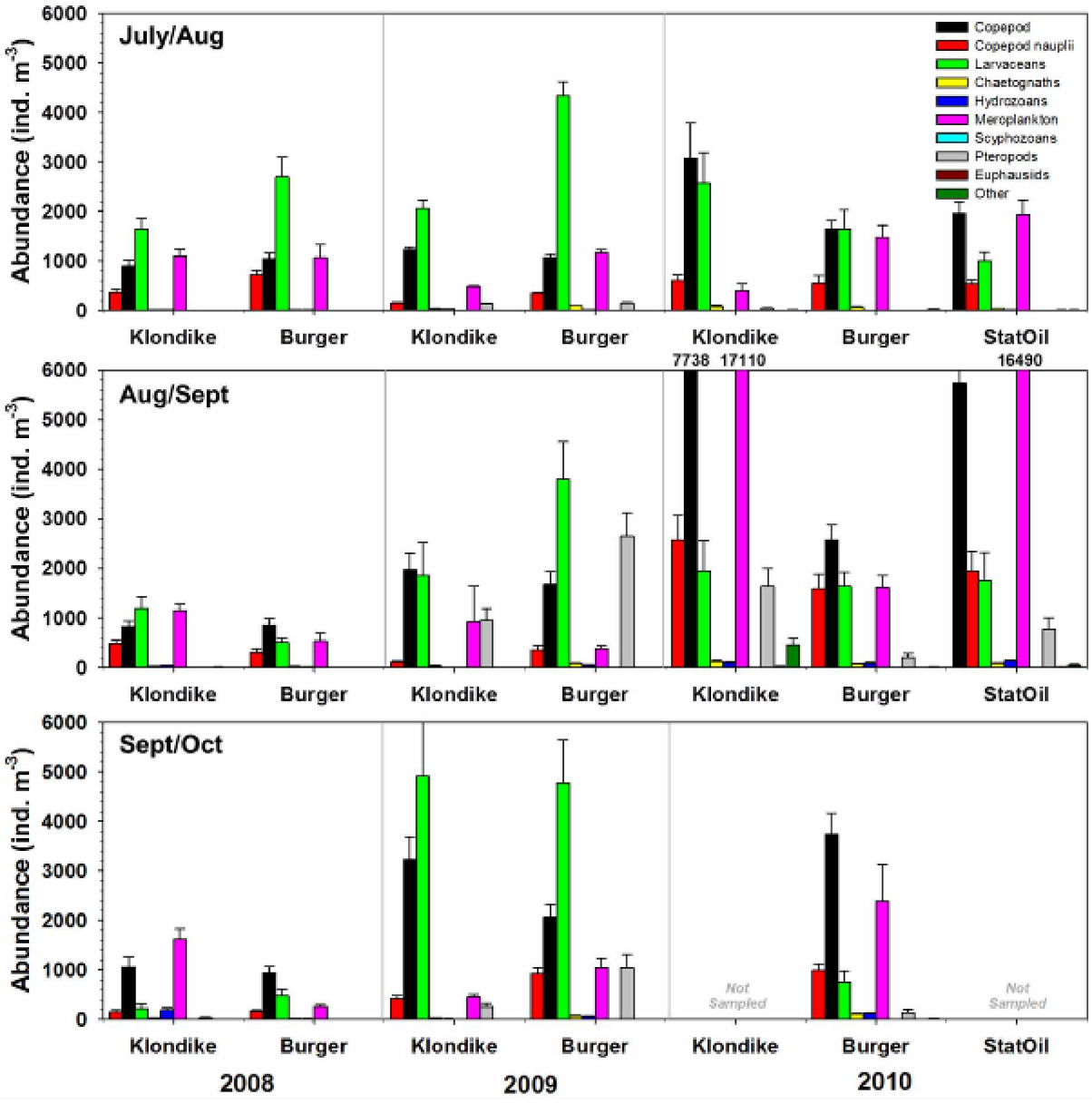

Figure 1.5 Abundance of the major zooplankton taxonomic groups for the 150–µm nets at each survey grid in the Chukchi Sea spanning the 2008–2010 seasons. T-Bars are standard errors of the means.

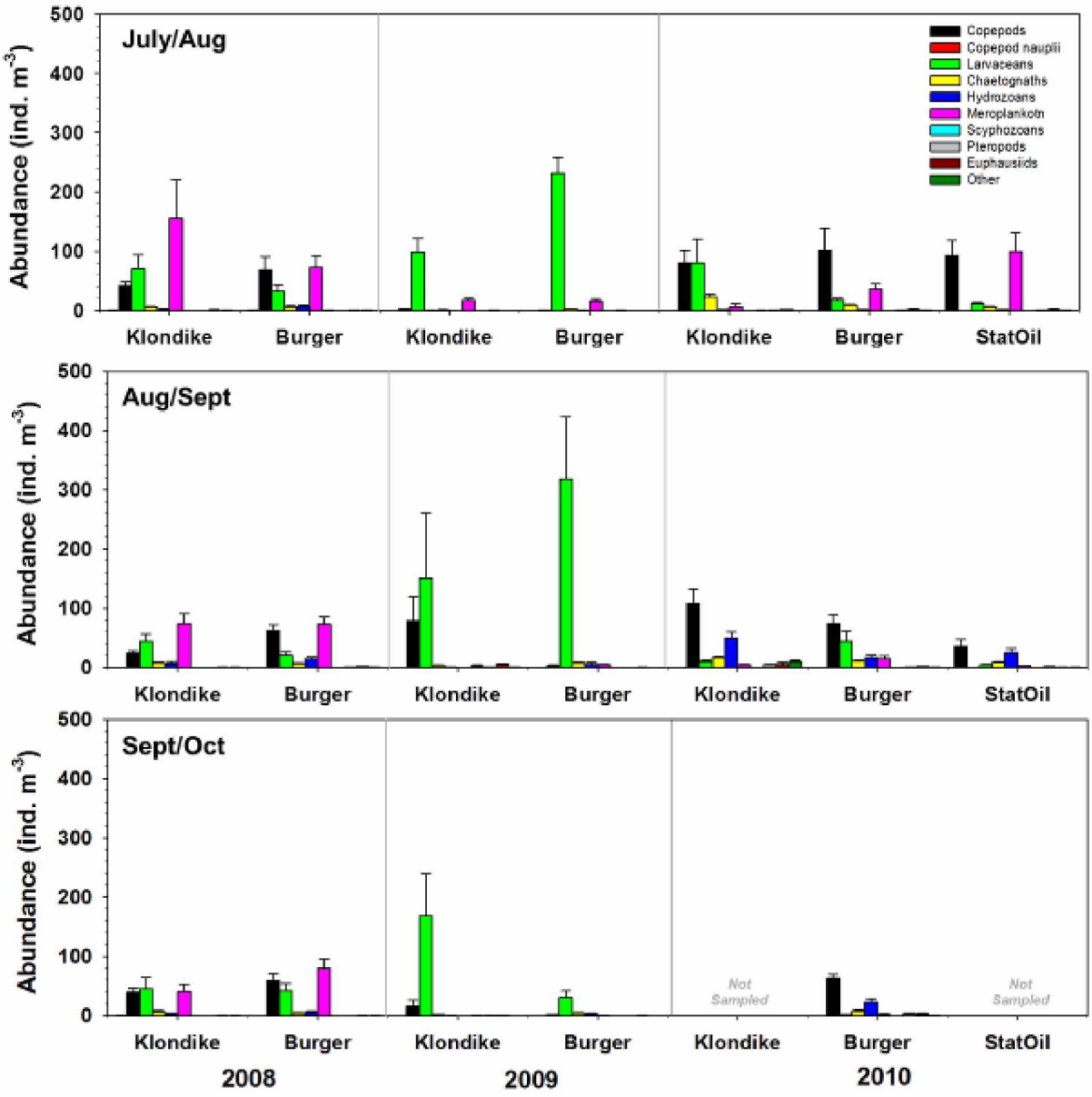

Figure 1.6 Abundance of the major zooplankton taxonomic groups for the 505–µm nets at each survey grid in the Chukchi Sea spanning the 2008–2010 seasons. T-Bars are standard errors of the means.

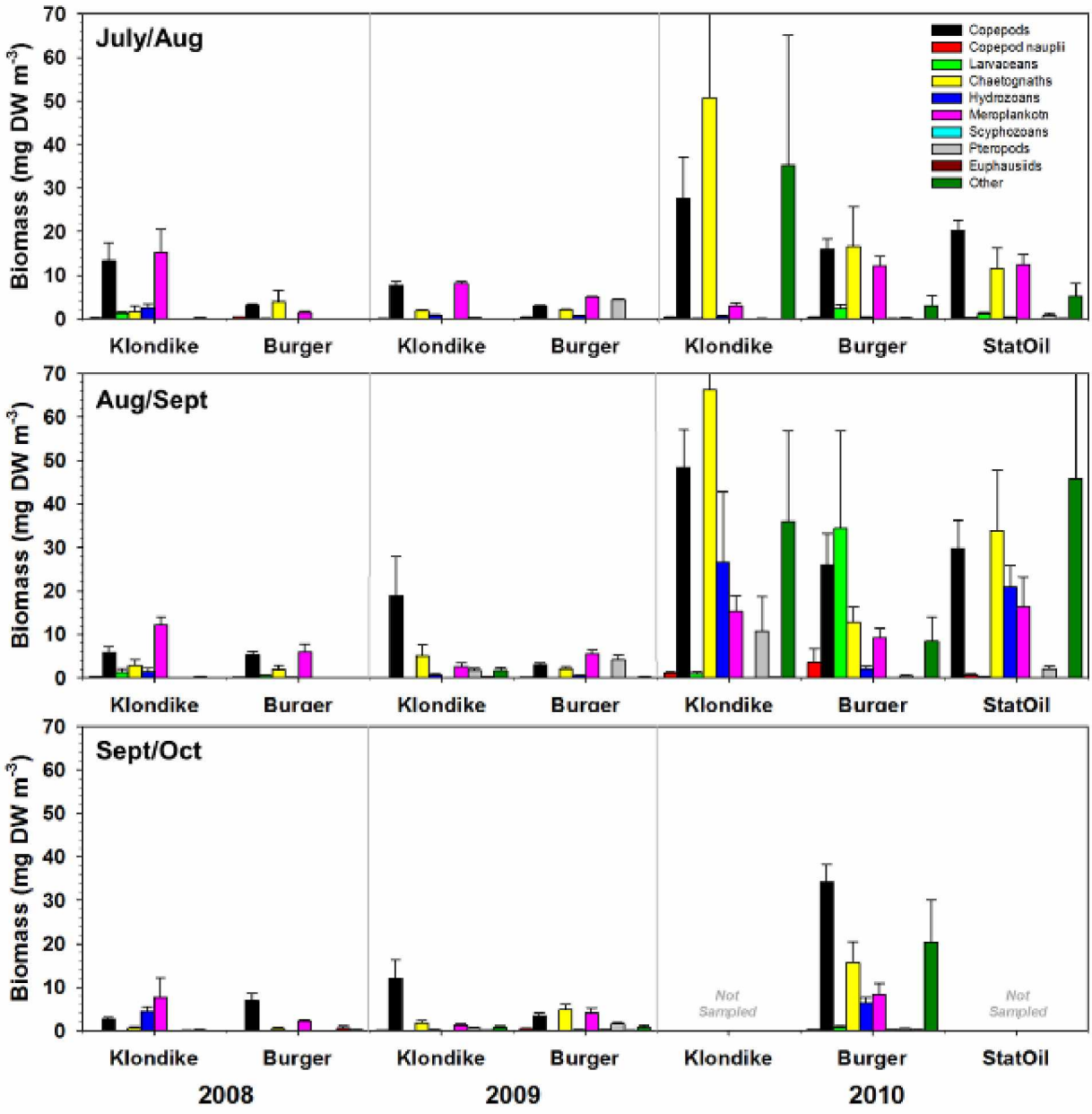

Figure 1.7 Biomass of the major zooplankton taxonomic groups for the 150–µm nets at each survey grid in the Chukchi Sea spanning the 2008–2010 seasons. T-Bars are standard errors of the means.

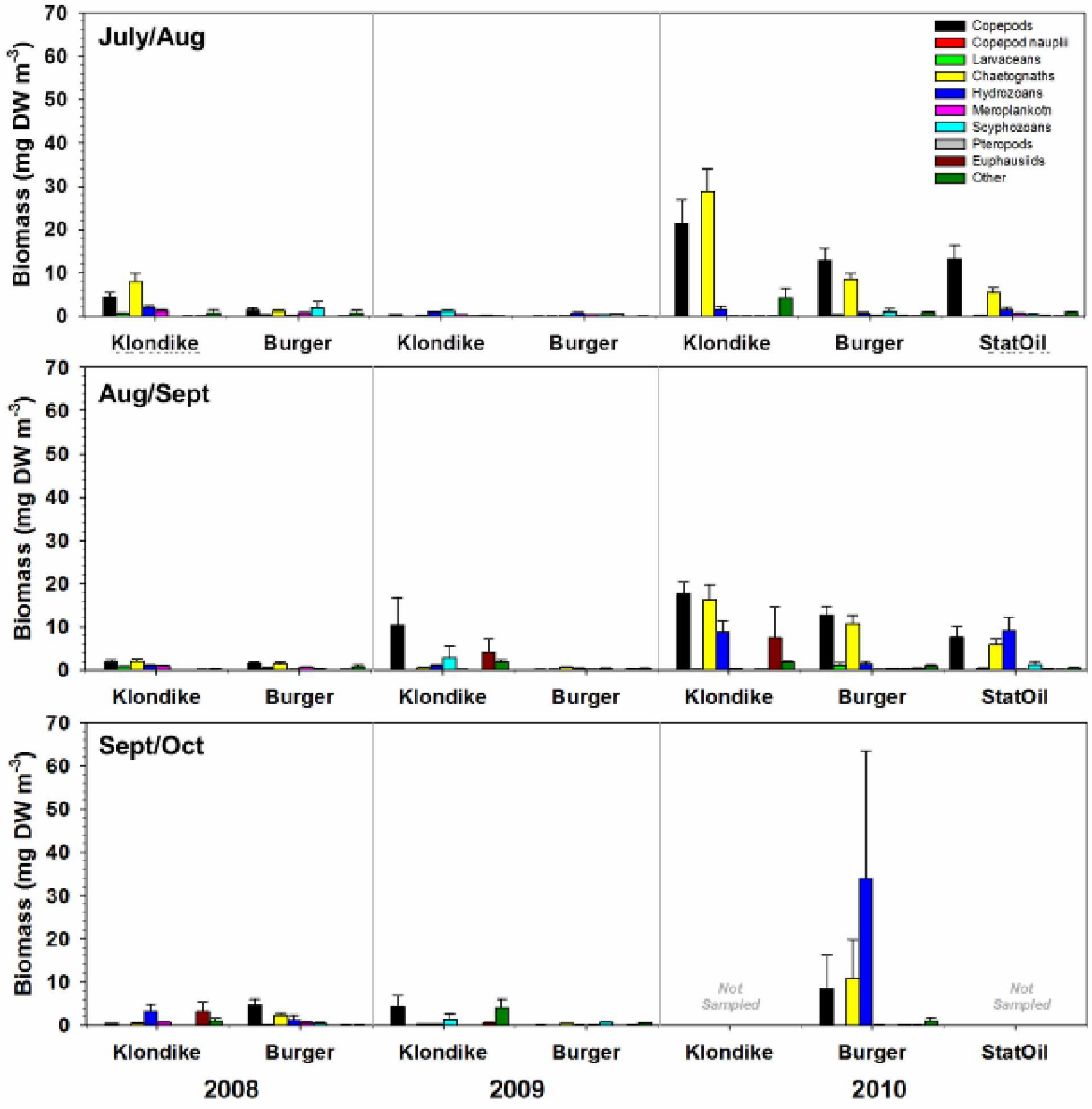

Figure 1.8 Biomass of the major zooplankton taxonomic groups for the 505–µm nets at each survey grid in the Chukchi Sea spanning the 2008–2010 seasons. T-Bars are standard errors of the means.

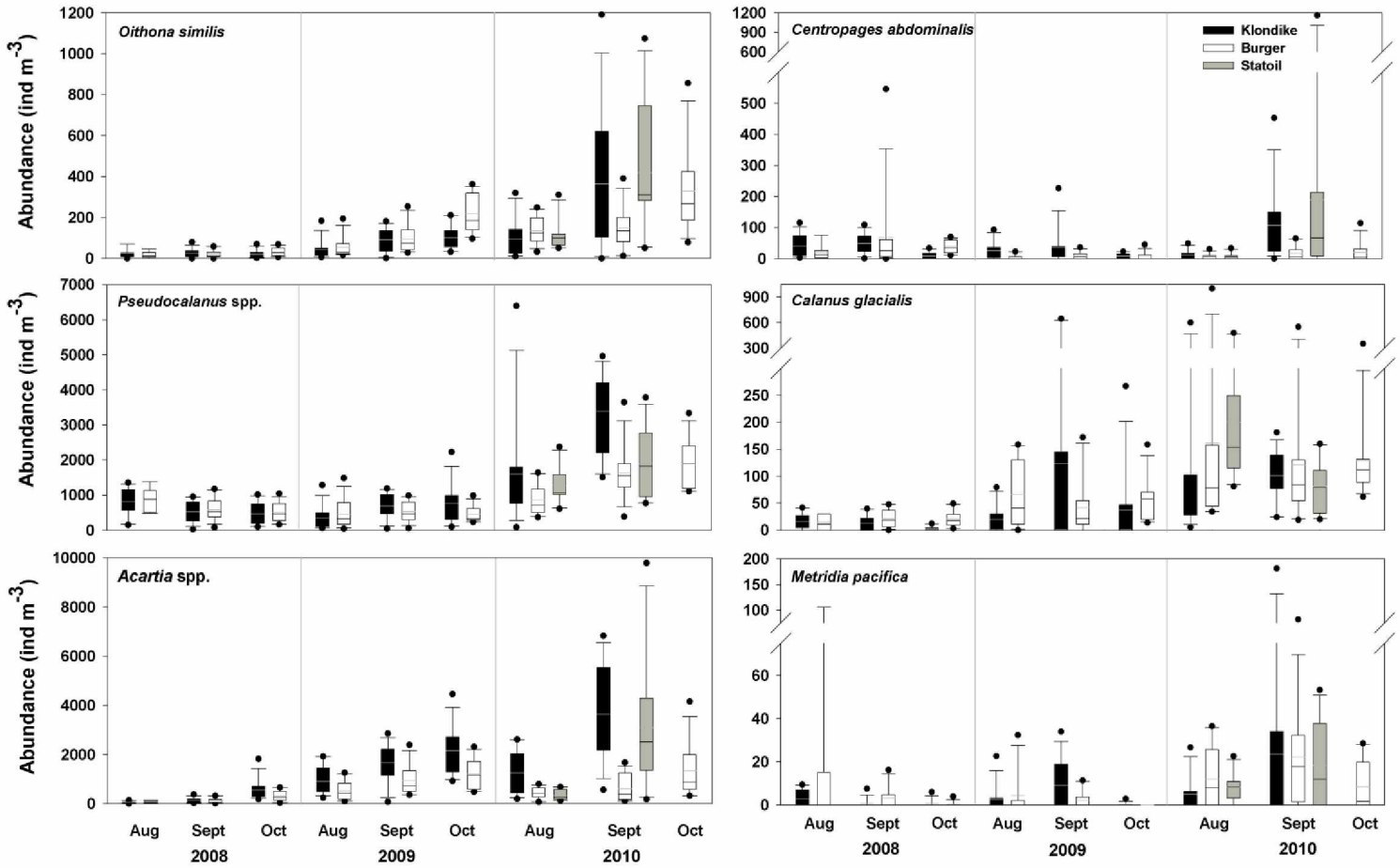

Figure 1.9a Abundance of the dominant copepod species during each survey grid in the Chukchi Sea spanning the 2008–2010 seasons as captured by the 150–µm net. The black or white line through the box is the sample median; gray line is the mean, limits of the box are the 25th and 75th percentile. Whiskers are the 10th and 90th percentiles and the single points are the 5th and 95th percentiles. Features may be absent where number of samples with occurrence is low. Month reflects timeframe when majority of samples were collected.

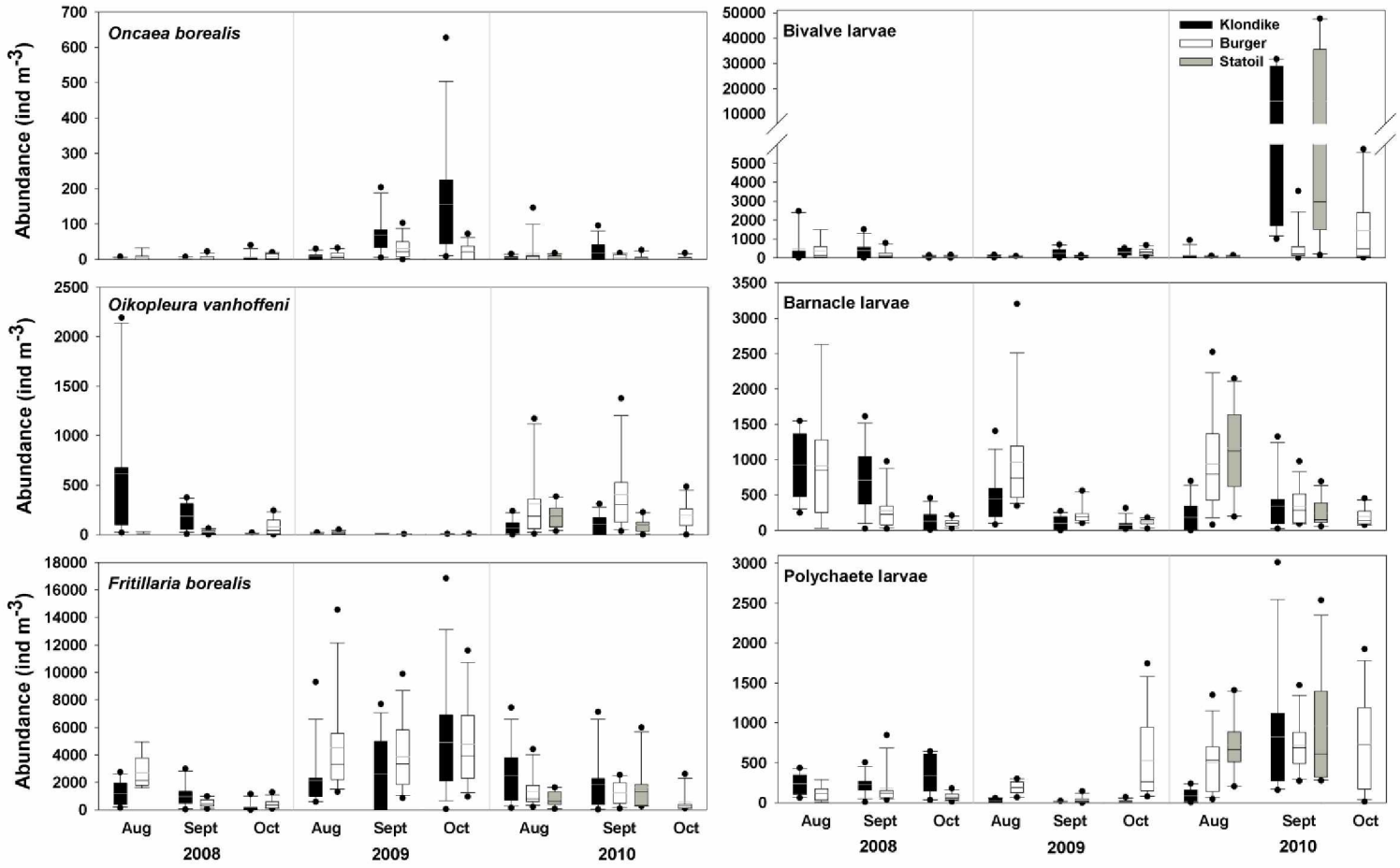

Figure 1.9b Abundance of the small copepod *Oncaea*, and the dominant larvacean species and meroplankton groups during each survey grid in the Chukchi Sea spanning the 2008–2010 seasons as captured by the 150–µm net.

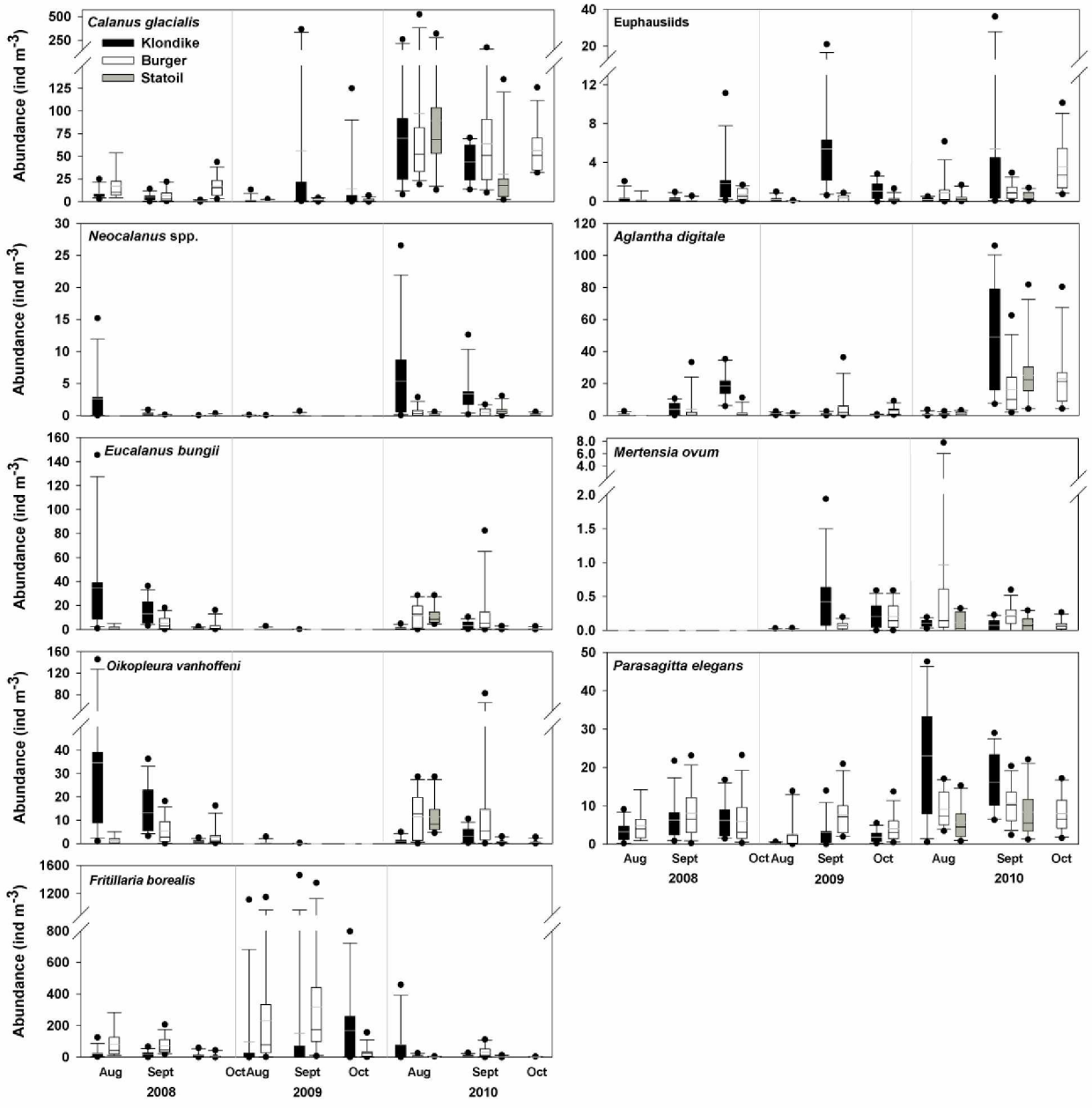

Figure 1.10 Abundance of the dominant zooplankton species during each survey grid in the Chukchi Sea spanning the 2008–2010 seasons as captured by the 505–µm net.

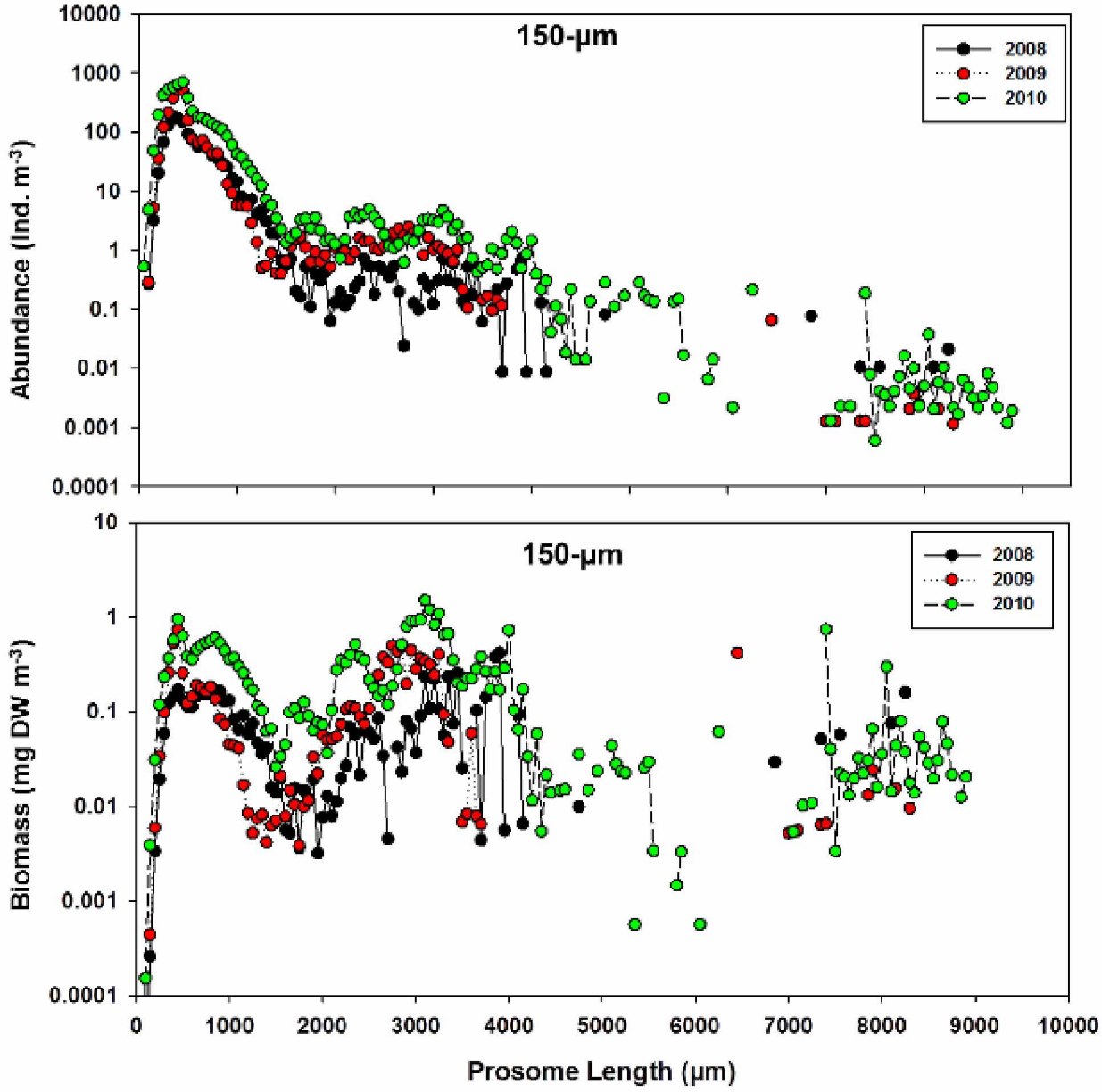

Figure 1.11 Average size-spectra of the copepod community captured by the 150–µm net for each survey year in the Chukchi Sea across all collections. Data are sorted into 50–µm wide bins and gaps reflect an absence of data in that bin within the portion of samples examined.

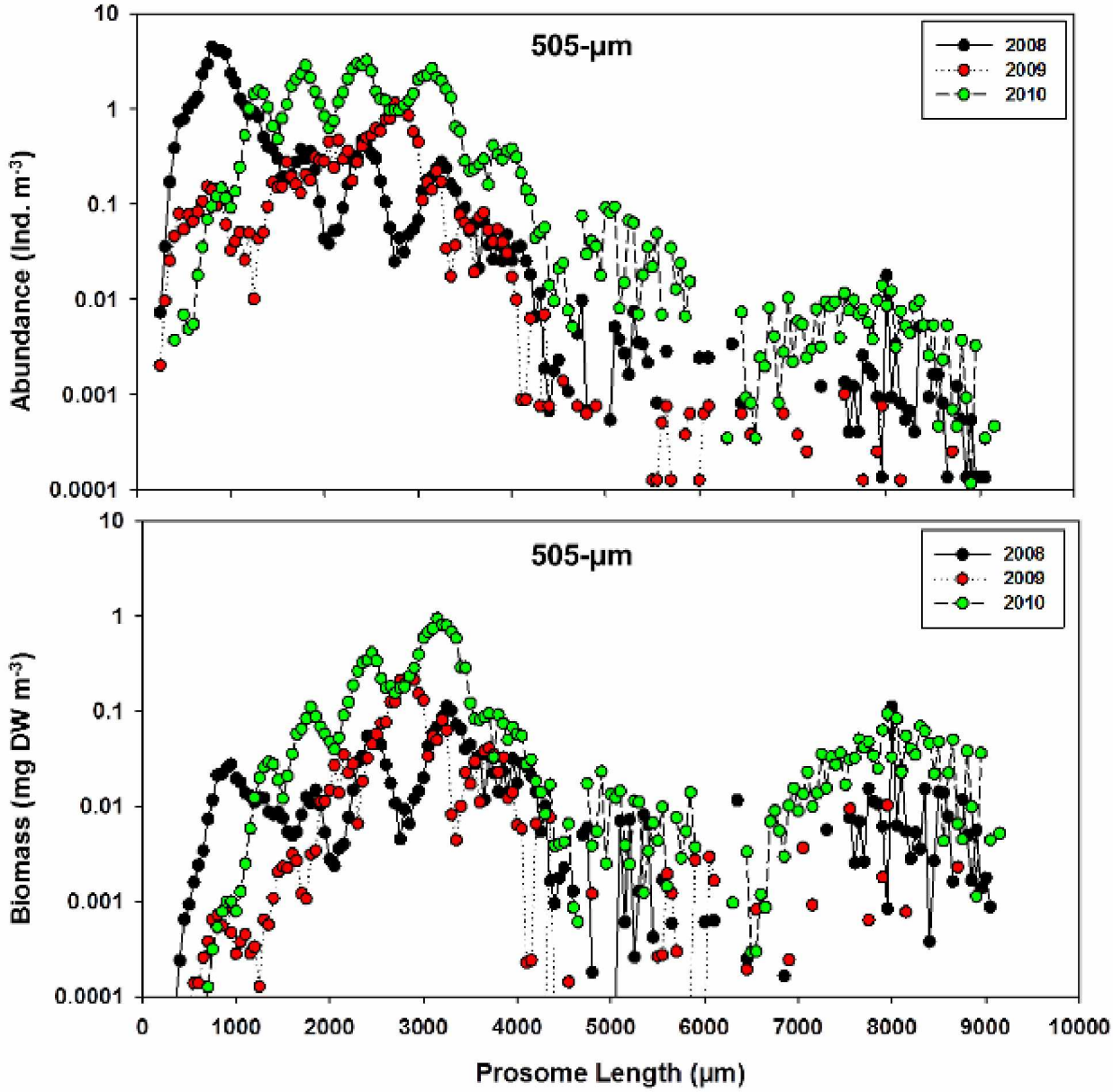

Figure 1.12 Average size-spectra of the copepod community captured by the 505–µm net for each survey year in the Chukchi Sea across all collections.

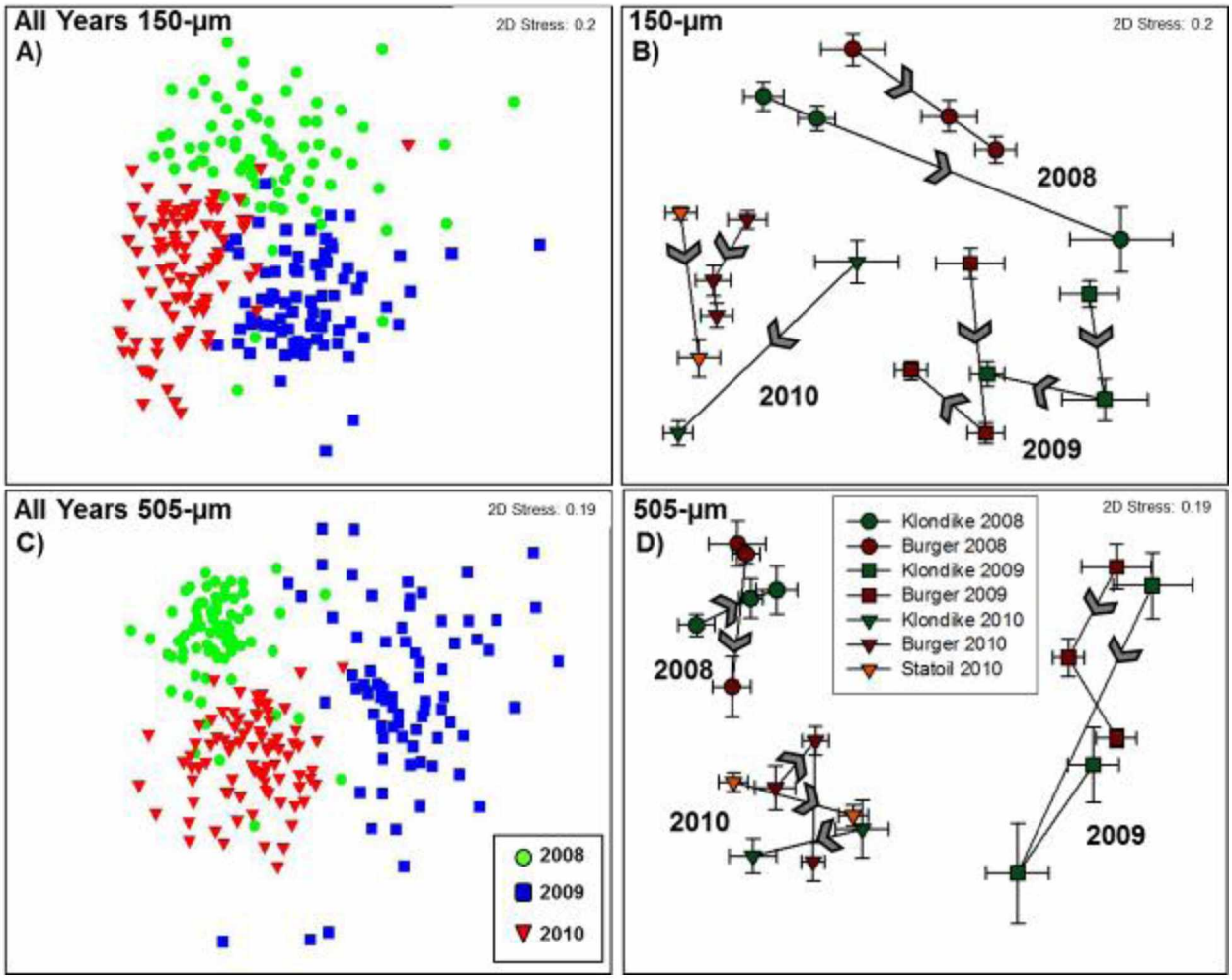

Figure 1.13 Spatial distribution of the Bray-Curtis similarity clusters for the zooplankton communities in the northeastern Chukchi Sea collected by the 150–µm and 505–µm nets from 2008 to 2010 (A & C) with centroids displaying spatial movement within seasons for each study site (B and D). Symbols and colors are consistent for each grid/station/month combination.

Table 1.1 Average integral chlorophyll concentrations (mg m^{-2}) in the Klondike, Burger and Statoil survey grids in the Chukchi Sea from 2008 to 2010.

Cruise	2008		2009		2010		
	Klondike	**Burger**	**Klondike**	**Burger**	**Klondike**	**Burger**	**Statoil**
August	62.5	104.8	17.6	21.4	46.1	42.7	66.3
September	25.1	47.1	16	20.1	26.2	40.2	26.3
October	21.8	30.9	27.2	25.1	*Not sampled*	42.2	*Not sampled*

Table 1.2 Three-way analysis of variance (ANOVA) of macronutrients, chlorophyll-a, and the major taxonomic groups by site (Klondike, Burger, and Statoil), year (2008, 2009, and 2010), and cruise (July/August, August/September, and September/October) in the northeastern Chukchi Sea. Bold values are significantly different ($P \leq 0.05$).

		SITE	YEAR	CRUISE	SITE: YEAR	SITE: CRUISE	YEAR: CRUISE	SITE:YEAR: CRUISE
Nuts & Chl	**PO_4**	**0.00**	**0.00**	**0.00**	**0.00**	0.12	**0.00**	**0.00**
	NO_3	**0.00**	**0.00**	**0.00**	**0.00**	0.15	**0.00**	**0.00**
	SiO_4	**0.00**	**0.00**	**0.00**	**0.00**	**0.00**	**0.00**	**0.00**
	Chlorophyll-a	**0.00**	**0.00**	**0.00**	**0.00**	**0.01**	**0.00**	**0.01**
150–µm Abundance	**Copepods**	**0.00**	**0.00**	**0.00**	**0.00**	**0.00**	**0.00**	**0.01**
	Copepod nauplii	**0.00**	**0.00**	**0.00**	**0.00**	**0.01**	**0.00**	0.24
	Larvaceans	0.17	**0.00**	0.25	0.27	0.85	**0.00**	0.73
	Chaetognaths	0.73	**0.00**	**0.00**	**0.03**	0.70	0.35	**0.00**
	Hydrozoans	**0.04**	0.22	**0.00**	**0.00**	**0.01**	**0.01**	**0.00**
	Meroplankton	**0.00**	**0.00**	**0.00**	**0.00**	**0.00**	**0.00**	**0.00**
	Scyphozoans	0.54	0.34	0.37	0.41	0.54	0.38	0.29
	Pteropods	0.14	**0.00**	**0.00**	**0.00**	**0.00**	**0.00**	**0.00**
	Euphausiids	**0.04**	0.10	0.91	0.43	0.19	0.84	0.51
	Other	**0.00**	**0.00**	**0.00**	**0.00**	**0.00**	**0.00**	**0.00**
505–µm Abundance	**Copepods**	0.44	**0.00**	0.08	**0.00**	0.28	**0.04**	0.06
	Copepod nauplii	0.66	**0.02**	0.26	0.56	0.61	0.11	0.57
	Larvaceans	0.21	**0.00**	0.29	0.43	0.46	0.15	0.08
	Chaetognaths	0.79	**0.05**	0.43	0.39	0.71	0.81	0.43
	Hydrozoans	0.61	0.11	**0.02**	**0.00**	0.59	0.34	0.07
	Meroplankton	0.09	**0.00**	**0.03**	0.62	0.09	0.31	**0.05**
	Scyphozoans	0.23	0.85	0.95	0.30	0.90	0.31	0.36
	Pteropods	0.09	**0.00**	0.82	**0.00**	0.28	0.92	0.88
	Euphausiids	**0.00**	**0.00**	**0.00**	**0.00**	**0.00**	**0.00**	**0.00**
	Other	**0.01**	**0.01**	0.52	0.41	**0.02**	0.86	0.93
150–µm Biomass	**Copepods**	**0.00**	**0.00**	0.25	0.70	0.13	0.16	0.38
	Copepod nauplii	**0.00**	**0.00**	**0.01**	**0.00**	0.17	**0.00**	**0.03**
	Larvaceans	**0.02**	**0.00**	0.31	**0.00**	0.86	0.51	0.66
	Chaetognaths	0.13	**0.00**	**0.00**	**0.00**	0.74	**0.00**	0.49

Table 1.2 continued…

	Hydrozoans	**0.00**	**0.00**	0.34	**0.00**
	Meroplankton	**0.00**	0.74	0.09	0.37
	Scyphozoans	0.92	0.16	0.59	0.06
	Pteropods	**0.01**	**0.00**	0.06	0.00
	Euphausiids	**0.00**	**0.00**	0.58	**0.04**
	Other	**0.00**	**0.00**	**0.00**	**0.04**
505–µm Biomass	**Copepods**	**0.00**	**0.00**	0.42	0.14
	Copepod nauplii	0.25	**0.00**	0.10	0.23
	Larvaceans	0.94	**0.01**	0.07	0.41
	Chaetognaths	**0.00**	**0.00**	**0.00**	**0.01**
	Hydrozoans	0.10	**0.03**	0.12	0.48
	Meroplankton	0.23	**0.00**	0.07	0.22
	Scyphozoans	0.84	0.08	0.95	0.06
	Pteropods	0.09	**0.04**	**0.00**	0.13
	Euphausiids	0.84	0.64	0.90	0.18
	Other	0.17	**0.00**	**0.00**	0.33

0.00	0.11	**0.00**
0.01	0.62	0.24
0.96	0.50	0.79
0.00	**0.03**	**0.02**
0.03	0.09	0.06
0.00	**0.00**	**0.01**
0.40	**0.00**	0.16
0.03	0.23	**0.02**
0.50	0.12	0.72
0.00	**0.00**	**0.00**
0.38	0.50	0.45
0.63	0.28	0.89
0.51	0.55	0.65
0.19	**0.01**	**0.03**
0.26	0.15	0.39
0.29	**0.00**	0.69

Table 1.3 Average abundance and biomass across all samples examined of zooplankton species observed from 2008 to 2010 in the Chukchi Sea's Klondike, Burger and Statoil surveys. Data are presented for both vertical 150–µm ring net collections and the 505–µm oblique tows. "Trace" refers to taxa found only once or twice during analysis and of insignificant biomass.

	Abundance (Ind. m^{-3})						Biomass (mg DW m^{-3})					
	150–µm mesh			505–µm mesh			150–µm mesh			505–µm mesh		
	2008	2009	2010	2008	2009	2010	2008	2009	2010	2008	2009	2010
Copepods[a]												
Acartia spp.	8.6	66.6	150.5	1.1	0.2	—	Trace	0.01	0.02	Trace	Trace	—
A. longiremis	6.2	27.7	82.7	2.7	0.3	0.5	0.04	0.11	0.38	0.02	Trace	Trace
A. hudsonica	7.6	6.2	2.1	0.3	—	—	0.03	0.02	0.01	Trace	—	—
Eurytemora pacifica	4.1	1.1	0.4	0.5	Trace	Trace	0.04	0.01	Trace	0.01	Trace	0.01
Calanus glacialis	14.6	57.7	123.6	9.4	12.6	62.4	2.62	6.83	16.54	1.46	2.48	10.99
Centropages abdominalis	38.0	15.3	54.1	4.4	0.1	1.4	0.09	0.04	0.15	0.02	Trace	0.03
Epilabidocera amphitrites	0.1	—	—	—	Trace	Trace	Trace	—	—	—	Trace	Trace
Eucalanus bungii	0.4	13.6	14.1	0.1	3.3	5.4	0.04	0.14	0.89	0.01	0.05	0.38
Heterorhabdus sp. (juvenile)	—	—	Trace	—	—	—	—	—	Trace	—	—	—
Metridia pacifica	3.2	3.1	13.5	0.1	0.1	2.0	0.02	0.01	0.17	Trace	Trace	0.11
Neocalanus flemingeri	0.8	—	2.2	0.3	—	1.3	0.45	—	1.58	0.20	—	0.63
Neocalanus plumchrus	1.5	—	0.4	0.1	Trace	Trace	0.41	—	0.14	0.09	0.01	0.01
Neocalanus cristatus	0.1	Trace	0.2	0.1	Trace	0.2	0.35	0.10	0.97	0.36	0.01	1.41
Pseudocalanus male	6.7	6.5	42.2	1.7	Trace	Trace	0.07	0.04	0.30	0.01	Trace	Trace
Pseudocalanus spp.	555.6	494.9	1555.3	19.7	0.3	0.3	1.32	0.99	3.80	0.11	Trace	0.01
Pseudocalanus minutus	7.7	0.7	25.5	1.8	Trace	2.2	0.11	0.01	0.38	0.04	Trace	0.05
Pseudocalanus acuspes	18.0	6.3	51.1	2.8	Trace	1.2	0.23	0.06	0.54	0.03	Trace	0.02
Pseudocalanus newmani	14.6	33.8	127.2	2.9	0.2	0.1	0.10	0.17	0.71	0.02	Trace	Trace
Pseudocalanus mimus	5.4	—	0.6	0.1	Trace	Trace	0.07	—	0.01	Trace	Trace	Trace
Tortanus discaudata	—	—	0.1	Trace	Trace	Trace	—	—	Trace	Trace	Trace	Trace
Oithona similis	223.1	1235.5	1552.6	—	—	—	0.31	1.46	1.98	—	—	—

Table 1.3 continued…

Triconia (Oncaea) borealis	3.9	49.4	8.6	—	—	—
Harpacticoida	8.3	3.4	14.3	—	—	—
calanoid nauplius	295.0	324.6	1138.8	—	—	—
cyclopoid nauplius	46.1	90.1	140.5	—	—	—
Larvaceans						
Oikopleura vanhoeffeni	139.1	2.1	198.4	10.3	0.1	5.9
Fritillaria borealis	897.6	3808.5	1424.8	33.1	166.0	17.6
Pteropods						
Limacina helicina	5.1	525.1	426.9	0.3	0.2	1.4
Clione limacine	Trace	Trace	0.1	Trace	Trace	0.1
Cladocerans						
Evadne nordmanni	—	—	1.7	0.1	—	1.2
Podon leuckartii	0.3	0.5	67.8	0.1	—	0.2
Euphausiids[b]						
Euphausiid calyptopis	—	0.3	4.8	0.3	Trace	0.6
Euphausiid furcillia\juvenile	2.6	0.3	1.3	0.4	1.0	1.4
Thysanoessa inermis	—	—	—	0.1	Trace	Trace
Thysanoessa raschii	—	—	4.8	Trace	0.2	0.3
Thysanoessa spinifera	—	—	1.3	—	Trace	Trace
Shrimps and mysids[c]						
Hippollytidae (juveniles)	—	—	8.3	0.1	Trace	0.2
Eualus gaimardii	—	—	0.2	0.1	—	Trace
Pandalidae	—	—	—	—	Trace	—
Amphipods[d]						
Themisto abyssorum/pacifica	—	—	—	Trace	Trace	Trace
Themisto libellula	Trace	—	0.9	Trace	Trace	Trace
Hyperoche medusarum	—	—	—	—	Trace	Trace
Gammaridae	0.1	—	—	—	Trace	—

Trace	0.07	0.01	—	—	—
0.07	0.02	0.09	—	—	—
Trace	0.28	0.97	—	—	—
0.02	0.03	0.04	—	—	—
0.54	Trace	5.69	0.34	Trace	0.26
0.02	0.04	0.05	0.01	0.03	Trace
0.01	0.90	2.16	Trace	0.05	0.14
0.01	0.01	0.05	0.02	0.02	0.03
—	—	0.02	Trace	—	0.04
Trace	Trace	0.62	0.12	—	Trace
—	0.10	0.01	0.01	Trace	0.01
0.22	0.04	0.12	0.22	0.11	0.13
—	—	—	0.38	Trace	0.01
—	—	0.01	0.05	0.74	1.02
—	—	0.12	—	Trace	Trace
—	—	9.10	0.18	0.01	0.15
—	—	1.24	0.04	—	0.03
—	—	—	—	0.019	—
—	—	—	0.08	Trace	0.01
0.03	—	5.73	0.03	0.55	0.22
—	—	0.01	—	Trace	0.01
Trace	—	—	—	Trace	—

Table 1.3 continued…

Hyperidae	—	Trace	—	Trace
Amphipod (misc.)	—	—	—	Trace
Ctenophores				
Beröe cucumis	0.5	—	Trace	Trace
Mertensia ovum	—	1.0	1.2	—
Cnidarians[e]				
Aeginopsis laurentii	—	—	13.0	—
A. digitale	35.1	12.7	51.9	5.3
Catablema vesicarium	—	0.0	2.2	—
Obelia spp.	1.9	1.6	0.9	0.4
Rathkea octopunctata	0.9	0.4	1.1	0.5
Miscellaneous hydrozoans	7.8	—	—	Trace
Aurelia aurita	—	—	—	—
Cyanea capillata	—	Trace	Trace	Trace
Chaetognaths				
Parasagitta elegans	20.6	53.5	80.8	6.2
Ostracoda	—	—	—	Trace
Cumacea	—	—	—	Trace
Total Holozooplankton	**2381**	**6842**	**7396**	**106**
Bivalve larvae	235.5	153.2	8011.9	5.5
Barnacle cyprius	291.4	274.5	339.5	34.3
Barnacle nauplius	185.9	22.7	139.9	36.1
Decapod zoea	0.7	1.7	2.0	0.3
Megalops	—	0.1	0.1	—
Polychaete larvae	197.3	132.0	663.2	7.2
Ophiuroid larvae	6.2	34.6	94.8	—
Asteroid bipinnaria	5.8	0.4	3.5	Trace
Echinoid larvae	24.9	6.2	60.4	0.1
Total Meroplankton	**948**	**625**	**9315**	**84**

Trace	—	—	0.01	—	Trace	0.01	—
Trace	—	—	—	—	0.01	Trace	—
—	—	0.01	—	0.05	0.13	—	—
0.1	0.2	—	0.58	3.82	—	0.56	0.87
Trace	0.1	—	—	0.29	—	Trace	Trace
0.9	17.3	0.63	0.22	6.06	0.81	0.68	4.18
Trace	Trace	—	0.02	8.71	—	0.01	0.03
Trace	Trace	0.35	0.02	0.14	0.34	Trace	Trace
Trace	Trace	0.01	Trace	0.01	0.11	0.11	Trace
—	Trace	0.50	—	—	0.06	—	0.11
Trace	Trace	—	—	—	—	0.68	0.06
Trace	Trace	—	0.03	0.05	—	0.52	0.40
3.2	11.6	1.81	3.93	29.08	2.63	0.33	11.94
Trace	—	—	—	—	Trace	Trace	—
Trace	—	—	—	—	Trace	Trace	—
189	**198**	**10.5**	**16.3**	**102.9**	**8.3**	**7.0**	**33.5**
Trace	—	0.75	0.04	2.50	Trace	Trace	—
5.1	1.0	5.23	5.25	5.37	0.67	0.12	0.02
0.6	19.5	0.78	0.02	0.27	0.04	Trace	0.075
1.0	1.2	0.10	0.14	0.01	Trace	0.01	0.04
0.2	0.1	—	0.03	0.01	—	0.03	0.02
Trace	0.8	0.88	0.55	3.86	0.10	Trace	0.03
—	—	0.01	Trace	0.01	—	—	—
—	—	0.01	Trace	0.01	Trace	—	—
—	—	0.01	Trace	0.04	Trace	—	—
7	**22**	**7.8**	**6.0**	**12.1**	**0.8**	**0.2**	**0.2**

Table 1.3 continued…

Total Zooplankton	**3329**	**7468**	**16711**	**189**	**196**	**220**	**18.3**	**22.3**	**115.0**	**9.1**	**7.1**	**33.7**

[a] Trace amounts of the copepods *Acartia tumida*, *Calanus hyperboreus*, *Clausocalanus* spp., *Microcalanus* spp., *Scaphocalanus* spp., and *Scolecithricella minor* were found but not reported in the table.
[b] Trace amounts of the euphausiids specie *Thysanoessa longipes* was found but not reported in the table.
[c] Trace amount of the mysid *Neomysis awatschens* was found nut not reported in the table.
[d] Trace amounts of the amphipod specie *Hyperia galba/medusarum* was found but not reported in the table.
[e] Trace amounts of the cnidarian species *Bougainvillia supercilliaris, Euphysa flammea, Sarsia tubulosa, Melicertum octocostatum, Chrysaora melanaster, Halitholus cirratus,* and *Ptychogena* spp. were found but not reported in the table.

Table 1.4 Relationships between environmental variables and abundance of zooplankton communities in the northeastern Chukchi Sea, observed by the 150– and 505–µm nets. The most explanatory variables for an increasing number of factors are presented, along with their Spearman's Rank correlation. T–temperature, S–salinity, F–fluorescence, MLD–mixed layer depth, bMLD–below mixed layer depth, #V–number of variables.

	ALL years (2008–2010)		**2008**	
#V	**150–µm net**	**505–µm net**	**150–µm net**	**505–µm net**
1	T-bottom (0.353)	T-bottom (0.300)	T-bottom (0.451)	F-MLD (0.217)
	T-bMLD (0.321)	T-bMLD (0.284)	T-bMLD (0.444)	Integral Chlorophyll (0.193)
2	T-bottom, S-bottom (0.375)	T-bottom, T-bMLD (0.333)	T-bottom, T-bMLD (0.460)	T-top, F-MLD (0.282)
	T-top, T-bottom (0.375)	S-bottom, T-bMLD (0.311)	T-bottom, S-bottom (0.445)	T-bMLD, F-MLD (0.275)
	T-bottom, F-mean (0.371)	T-bottom, S-bottom (0.301)	T-bottom, F-MLD (0.428)	T-bottom, F-MLD (0.274)
3	T-top, T-bottom, F-bMLD (0.397)	T-bottom, S-bottom, T-bMLD, (0.330)	T-bottom, T-bMLB, F-MLD (0.477)	S-top, T-bottom, F-MLD (0.289)
	T-top, T-bottom, F-MLD (0.384)	T-bottom, T-bMLD, F-bMLD (0.322)	T-bottom, T-bMLB, F-bMLD (0.477)	S-top, T-bMLD, F-MLD (0.288)
		T-bottom, T-bMLD, MLD (0.317)	T-bottom, S-bottom, T-bMLD (0.457)	T-top, F-MLD, F-bMLD (0.286)
	2009		**2010**	
	150–µm net	**505–µm net**	**150–µm net**	**505–µm net**
1	F-MLD (0.290)	F-bMLD (0.253)	T-bottom (0.478)	T-top (0.439)
	F-bMLD (0.282)	F-MLD (0.240)	S-top (0.476)	T-bottom (0.421)
2	F-MLD, F-bMLD (0.358)	F-MLD, F-bMLD (0.311)	S-top, T-bMLD (0.577)	T-top, S-bottom (0.511)
	S-top, F-MLD (0.346)	T-top, F-bMLD (0.292)	S-top, T-bottom (0.572)	S-top, T-bottom (0.498)
	T-top, S-top (0.330)	T-bottom, F-bMLD (0.292)	T-bottom, F-MLD (0.540)	T-top, T-bottom (0.488)
3	T-top, F-MLD, F-bMLD (0.388)	T-top, F-MLD, F-bMLD (0.350)	S-top, S-bottom, T-bMLD (0.595)	S-top, S-bottom, F-bMLD (0.531)
	T-bMLD, F-MLD, F-bMLD (0.378)	T-bMLD, F-MLD, F-bMLD (0.339)	S-top, T-bMLD, F-MLD (0.593)	T-top, S-bottom, F-MLD (0.530)
	T-top, S-top, F-MLD (0.373)	T-bottom, F-MLD, F-bMLD (0.329)	S-top, T-bMLD, F-mean (0.578)	T-top, S-top, S-bottom (0.524)

1.9 References

Blanchard, A.L., Parris, C.L., Knowlton, A.L., Wade, N.R., 2013a. Benthic ecology of the northeastern Chukchi Sea Part I: Environmental characteristics and macrofaunal community structure. Continental Shelf Research 67, 52–66.

Blanchard, A.L., Parris, C.L., Knowlton, A.L., Wade, N.R., 2013b. Benthic ecology of the northeastern Chukchi Sea Part II: Spatial variation of megafaunal community structure, 2009–2010. Continental Shelf Research67, 67–76.

Bluhm, B.A., Iken, K., Mincks-Hardy, S., Sirenko, B.I., Holladay, B.A., 2009. Community structure of epibenthic megafauna in the Chukchi Sea. Aquatic Biology 7, 269–293.

Brodsky, K.A., 1950. Copepods (Calanoida) of the Far-Eastern Seas of the USSR and the Polar Basin. Zoological Institute of the Academy of Sciences of the USSR, Leningrad, in Russian.

Brodsky, K.A., 1957. The Copepod Fauna (Calanoida) and Zoogeographic Zonation of the North Pacific and Adjacent Waters. Izvestiya Akademii USSR, Leningrad, in Russian.

Campbell, R.G., Sherr, E.B., Ashjian, C.J., Plourde, S., Sherr, B.F., Hill, V., Stockwell, D.A., 2009. Mesozooplankton prey preference and grazing impact in the western Arctic Ocean. Deep Sea Research Part II: Topical Studies in Oceanography 56, 1274–1289.

Carroll, M.J., Carroll, J., 2003. The Arctic Seas. In: Black, K.D., Shimmield, G.B. (Eds.), Biogeochemistry of Marine Systems. CRC Press, Boca Raton, Florida.

Clarke, K.R., Warwick, R.M., 2010. Change in Marine Communities: An Approach to Statistical Analysis and Interpretation, second ed. PRIMER-E, Plymouth, United Kingdom.

Cooney, R.T., 1977. Zooplankton and Micronekton Studies in the Bering-Chukchi/Beaufort Seas, NOAA OCSEP Annual Report 10, pp. 275–363.

Coyle, K.O., Chavtur, V.G., Pinchuk, A.I., 1996. Zooplankton of the Bering Sea: a review of Russian-language literature. In: Mathisen, A.O., Coyle, K.O. (Eds.), Ecology of the Bering Sea: A review of the Russian Literature. Alaska SeaGrant College Program, Fairbanks, Alaska, pp. 97–133.

Day, R.H., Weingartner, T.J., Hopcroft, R.R., Aerts, L.A.M., Blanchard, A.L., Gall, A.E., Gallaway, B.J., Hannay, D.E., Holladay, B.A., Mathis, J.T., Norcross, B.L., Questel, J.M., Wisdom, S.S., 2013. The offshore northeastern Chukchi Sea, Alaska: a complex high-latitude ecosystem. Continental Shelf Research 67, 147–165.

Dunton, K.H., Goodall, J.L., Schonberg, S.V., Grebmeier, J.M., Maidment, D.R., 2005. Multi-decadal synthesis of benthic-pelagic coupling in the western Arctic: role of cross-shelf advective processes. Deep Sea Research Part II: Topical Studies in Oceanography 52, 3462–3477.

English, T.S., Horner, R., 1977. Beaufort Sea Plankton Studies, NOAA OCSEAP Annual Report 9, pp. 275–627.

Frost, B.W., 1974. *Calanus marshallae*, a new species of calanoid copepod closely allied to the sibling species *C. finmarchicus* and *C. glacialis*. Marine Biology 26, 77–99.

Frost, B.W., 1989. A taxonomy of the marine calanoid genus *Pseudocalanus*. Canadian Journal of Zoology 67, 525–551.

Gall, A.E., Day, R.H., Weingartner, T.J., 2013. Structure and variability of the marine-bird community in the northeastern Chukchi Sea. Continental Shelf Research 67, 96–115.

Gordon, C., Jennings, A.A., Krest, J.M., 1993. A suggested protocol for continuous flow automated analysis of seawater nutrients (phosphate, nitrate, nitrite, and silicic acid) in the WOCE Hydrographic Program and the Joint Global Ocean Fluxes Study. Oregon State University, Corvallis, Oregon, p. 51.

Grebmeier, J.M., Cooper, L.W., Feder, H.M., Sirenko, B.I., 2006. Ecosystem dynamics of the Pacific-influenced northern Bering and Chukchi Seas in the Amerasian Arctic. Progress in Oceanography 71, 331–361.

Grebmeier, J.M., Smith, W.O., Jr., Conover, R.J., 1995. Biological processes on Arctic continental shelves: ice-ocean-biotic interactions. In: Smith, W.O., Jr., Grebmeier, J.M. (Eds.), Arctic Oceanography: Marginal Ice zones and Continental Shelves. American Geophysical Union, Washington, DC, pp. 231–261.

Hill, V., Cota, G., Stockwell, D., 2005. Spring and summer phytoplankton communities in the Chukchi and Eastern Beaufort Seas. Deep Sea Research Part II: Topical Studies in Oceanography 52, 3369–3385.

Hirche, H.-J., Hagen, W., Mumm, N., Richter, C., 1994. The northeast water Polyna, Greenland Sea. III. Meso- and macrozooplankton distribution and production of dominant herbivorous copepods during spring. Polar Biology 14, 491–503.

Hopcroft, R.R., Bluhm, B.A., Gradinger, R.R., 2008. In: Board, N.P.R. (Ed.), Arctic Ocean Synthesis: Analysis of Climate Change Impacts in the Chukchi and Beaufort Seas with Strategies for Future Research, second ed. Anchorage, Alaska, p. 153.

Hopcroft, R.R., Clarke, C., Nelson, R.J., Raskoff, K.A., 2005. Zooplankton communities of the Arctic's Canada basin: the contribution by smaller taxa. Polar Biology 28, 197–206.

Hopcroft, R.R., Kosobokova, K.N., 2010. Distribution and egg production of *Pseudocalanus* species in the Chukchi Sea. Deep Sea Research Part II: Topical Studies in Oceanography 57, 49–56.

Hopcroft, R.R., Kosobokova, K.N., Pinchuk, A.I., 2010. Zooplankton community patterns in the Chukchi Sea during summer 2004. Deep Sea Research Part II: Topical Studies in Oceanography 57, 27–39.

Hopcroft, R.R., Roff, J.C., Chavez, F.P., 2001. Size paradigms in copepod communities: a re-examination. Hydrobiologia 453/454, 133–141.

Horner, R., 1981. Beaufort Sea Plankton Studies, NOAA OCSEP Final Report 13, pp. 65–314.

Jaschnov, V., 1940. Plankton productivity of the northern seas of the USSR. Moscovskoe Obshestvo Ispytatelei Prirody Press, Moscow, in Russian.

Kosobokova, K., Hirche, H.-J., 2000. Zooplankton distribution across the Lomonosov Ridge, Arctic Ocean: species inventory, biomass and vertical structure. Deep Sea Research Part II: Topical Studies in Oceanography 47, 2029–2060.

Kosobokova, K.N., Hopcroft, R.R., 2010. Diversity and vertical distribution of mesozooplankton in the Arctic's Canada basin. Deep Sea Research Part II: Topical Studies in Oceanography 57, 96–110.

Kulikov, A.S., 1992. Characteristics of zooplankton communities. In: Nagel, P.A. (Ed.), Results of the Third Joint US-USSR Bering and Chukchi Seas expedition (BERPAC), Summer 1988. US Fish and Wildlife Service, Washington, pp. 161.

Lane, P.V.Z., Llinás, L., Smith, S.L., Pilz, D., 2008. Zooplankton distribution in the western Arctic during summer 2002: hydrographic habitats and implications for food chain dynamics. Journal of Marine Research 70, 97–133.

Lee, S.H., Whitledge, T.E., Kang, S.-H., 2007. Recent carbon and nitrogen uptake rates of phytoplankton in Bering Strait and the Chukchi Sea. Continental Shelf Research 27, 2231–2249.

Liu, H., Hopcroft, R.R., 2008. Growth and development of *Pseudocalanus* spp. in the northern Gulf of Alaska. Journal of Plankton Research 30, 923–935.

Llinás, L., 2007. Distribution, Reproduction, and Transport of Zooplankton in the Western Arctic, Ph.D. Dissertation. University of Miami, Coral Gables, Florida p. 185.

Llinás, L., Pickart, R.S., Mathis, J.T., Smith, S.L., 2009. Zooplankton inside an Arctic Ocean cold-core eddy: Probable origin and fate. Deep Sea Research Part II: Topical Studies in Oceanography 56, 1290–1304.

Matsuno, K., Yamaguchi, A., Hirawake, T., Imai, I., 2011. Year-to-year changes of the mesozooplankton community in the Chukchi Sea during summers of 1991, 1992 and 2007, 2008. Polar Biology 34, 1349–1360.

Miller, C.B., 1988. *Neocalanus flemingeri*, a new species of Calanidae (Copepoda: Calanoida) from the subarctic Pacific Ocean, with comparative redescription of *Neocalanus plumchrus* (Marukawa) 1921. Progress in Oceanography 20, 223–273.

Nelson, R.J., Carmack, E.C., McLaughlin, F.A., Cooper, G.A., 2009. Penetration of pacific zooplankton into the western Arctic Ocean tracked with molecular population genetics. Marine Ecology Progress Series 381, 129–138.

Parsons, T.R., Maita, Y., Lalli, C.M., 1984. A Manual for Chemical and Biological Methods in Seawater Analysis. Pergamon Press, Toronto, Canada.

Pavshtiks, E.A., 1984. Zooplankton of the Chukchi Sea as indices of water origins. Trudy Arkticheskogo i Antarkicheskogo Nauchno-Issledovatel'skogo Institute 368, 140–153, in Russian.

Pavshtiks, E.A., 1994. Composition and Quantitative Distribution of the Zooplankton on the East Siberian Sea, Ekosistemy, Flora i Fauna Chaunskoi Guby Vostochno-Sibirskogo Morya. Zoological Institute RAS, St. Petersburg, pp. 17-47 (in Russian).

Plourde, S., Campbell, R.G., Ashjian, C.J., Stockwell, D.A., 2005. Seasonal and regional patterns in egg production of *Calanus glacialis/marshallae* in the Chukchi and Beaufort Seas during spring and summer, 2002. Deep Sea Research Part II: Topical Studies in Oceanography 52, 3411–3426.

Roff, J.C., Hopcroft, R.R., 1986. High precision microcomputer based measuring system for ecological research. Canadian Journal of Fisheries and Aquatic Sciences 43, 2044–2048.

Shiga, N., Takagi, S., Nishiuchi, K., 1998. Interannual variation and vertical distribution of appendicularians in the south of St. Lawrence Island, northern Bering Sea shelf, in summer. Memoirs of the Faculty of Fisheries, Hokkaido University 45, 48–51.

Sirenko, B.I., 2001. List of species of free-living invertebrates of Eurasian Arctic Seas and adjacent deep waters. Russian Academy of Sciences, Exploration of the Fauna of the Sea 51, 1–129.

Sirenko, B.I., Clarke, C., Hopcroft, R.R., Huettmann, F., Bluhm, B.A., Gradinger, R.R., eds., 2010. The Arctic Register of Marine Species (ARMS) Compiled by the Arctic Ocean Diversity (ArcOD) Project.

Springer, A.M., McRoy, C.P., Turco, K.R., 1989. The paradox of pelagic food webs in the northern Bering Sea - II. Zooplankton communities. Continental Shelf Research 9, 359–386.

Stepanova, V.S., 1937a. Biological indicators of currents in the northern Bering and southern Chukchi Seas. Issledovanija Morei SSSR 25, 175–216, in Russian.

Stepanova, V.S., 1937b. Distribution of Bering Sea water in the Chukchi Sea (from data of the analysis of zooplankton from a cruise on the icebreaker Krasin in 1935). Trudy Arkticheskogo Nauchno-Issledovatel'skogo Institute 82, 113–143, in Russian.

Turco, K., 1992a. Zooplankton Taxa, Abundance and Biomass Data. ISHTAR Data Report no. 6, Part 1 (1985–1987). Institute of Marine Science, University of Alaska Fairbanks, Fairbanks, Alaska, 620 pp.

Turco, K., 1992b. Zooplankton Taxa, Abundance and Biomass Data. ISHTAR Data Report No. 6, Part 1 (1988-1989). Institute of Marine Science, University of Alaska Fairbanks, Fairbanks, Alaska, 620 pp.

Unstad, K.H., Tande, K.S., 1991. Depth distribution of *Calanus finmarchicus* and *C. glacialis* in relation to environmental conditions in the Barents Sea. Polar Research 10, 409–420.

Weingartner, T.J., Aagaard, K., Woodgate, R.A., Danielson, S.L., Sasaki, Y., Cavalieri, D., 2005. Circulation on the north central Chukchi Sea shelf. Deep Sea Research Part II: Topical Studies in Oceanography 52, 3150–3174.

Weingartner, T.J., Dobbins, E., Danielson, S.L., Potter, R., Statscewich, H., Winsor, P., 2013. On the hydrographic variability of the northeast Chukchi Sea Shelf in summer– fall 2008–2010. Continental Shelf Research 67, 5-22.

Whitledge, T.E., Malloy, S.C., Patton, C.J., Wirick, C.D., 1981. Automated Nutrient Analyses in Seawater. Brookhaven National Laboratory, Upton, New York p. 216.

Wiebe, P.H., Boyd, S., Cox, J.L., 1975. Relationships between zooplankton displacement volume, wet weight, dry weight, and carbon. Fisheries Bulletin 73, 777–786.

Wing, B.L., 1974. Kinds and Abundances of Zooplankton Collected by the USCG Icebreaker Glacier in the Eastern Chukchi Sea, September–October 1970. Technical Report SSRF-679. National Marine Fisheries Services, Seattle, p 18.

Wishner, K.F., Gelfman, C., Gowing, M.M., Outram, D.M., Rapien, M., Williams, R.L., 2008. Vertical zonation and distributions of calanoid copepods through the lower oxycline of the Arabian Sea oxygen minimum zone. Progress in Oceanography 78, 163–191.

Appendix 1.1 Percentages of averaged abundance and biomass across all samples examined of zooplankton species observed from 2008–2010 in the Chukchi Sea's Klondike, Burger, and Statoil surveys. Data are presented for both vertical 150–µm ring net collections and the 505–µm oblique tows. 'Trace" refers to taxa found only once or twice during analysis and of insignificant biomass.

	Abundance (Ind. m^{-3})						Biomass (mg DW m^{-3})					
	150–µm mesh			505–µm mesh			150–µm mesh			505–µm mesh		
	2008	2009	2010	2008	2009	2010	2008	2009	2010	2008	2009	2010
Copepods[a]												
Acartia spp.	0.26	0.89	0.9	0.57	0.09	—	Trace	0.04	0.02	Trace	Trace	—
A. longiremis	0.19	0.37	0.49	1.4	0.16	0.23	0.19	0.48	0.33	0.19	Trace	Trace
A. hudsonica	0.23	0.08	0.01	0.14	—	—	0.19	0.08	0.01	Trace	—	—
Eurytemora pacifica	0.12	0.01	Trace	0.27	Trace	Trace	0.2	0.05	Trace	0.07	Trace	0.02
Calanus glacialis	0.44	0.77	0.74	4.98	6.44	28.34	14.28	30.62	14.39	16.02	34.82	32.66
Centropages abdominalis	1.14	0.2	0.32	2.33	0.07	0.61	0.51	0.16	0.13	0.25	Trace	0.08
Epilabidocera amphitrites	Trace	—	—	—	Trace	0.01	Trace	—	—	—	Trace	Trace
Eucalanus bungii	0.01	0.18	0.08	0.06	1.68	2.46	0.23	0.61	0.78	0.15	0.76	1.12
Heterorhabdus sp. (juvenile)	—	—	Trace	—	—	—	—	—	Trace	—	—	—
Metridia pacifica	0.09	0.04	0.08	0.04	0.04	0.9	0.12	0.05	0.15	Trace	Trace	0.33
Neocalanus flemingeri	0.02	—	0.01	0.17	—	0.59	2.46	—	1.37	2.22	—	1.88
Neocalanus plumchrus	0.05	—	Trace	0.07	0.01	0.01	2.26	—	0.12	0.93	0.07	0.04
Neocalanus cristatus	Trace	Trace	Trace	0.03	Trace	0.1	1.89	0.46	0.84	3.95	0.17	4.19
Pseudocalanus male	0.2	0.09	0.25	0.9	0.01	0.01	0.37	0.18	0.26	0.11	Trace	Trace
Pseudocalanus spp.	16.69	6.63	9.31	10.41	0.17	0.14	7.23	4.45	3.3	1.19	Trace	0.01
Pseudocalanus minutus	0.23	0.01	0.15	0.96	0.02	1.01	0.58	0.04	0.33	0.43	Trace	0.14
Pseudocalanus acuspes	0.54	0.08	0.31	1.45	0.01	0.53	1.26	0.25	0.47	0.37	Trace	0.06
Pseudocalanus newmani	0.44	0.45	0.76	1.54	0.1	0.04	0.54	0.76	0.61	0.22	Trace	Trace
Pseudocalanus mimus	0.16	—	Trace	0.03	0.01	Trace	0.36	—	0.01	Trace	Trace	Trace
Tortanus discaudata	—	—	Trace	0.02	Trace	0.02	—	—	Trace	Trace	Trace	Trace
Oithona similis	6.7	16.55	9.29	—	—	—	1.67	6.54	1.72	—	—	—
Triconia (Oncaea) borealis	0.12	0.66	0.05	—	—	—	0.02	0.32	0.01	—	—	—
Harpacticoida	0.25	0.05	0.09	0.05	—	—	0.4	0.08	0.08	Trace	—	—
calanoid nauplius	8.86	4.35	6.81	0.03	—	—	Trace	1.26	0.84	Trace	—	—
cyclopoid nauplius	1.38	1.21	0.84	—	—	—	0.11	0.11	0.04	—	—	—
Larvaceans												
Oikopleura vanhoeffeni	4.18	0.03	1.19	5.44	0.03	2.66	2.92	Trace	4.95	3.7	Trace	0.78

Appendix 1.1 continued…

Fritillaria borealis	26.96	51	8.53	17.48
Pteropods				
Limacina helicina	0.15	7.03	2.55	0.13
Clione limacine	Trace	Trace	Trace	Trace
Cladocerans				
Evadne nordmanni	—	—	0.01	0.05
Podon leuckartii	0.01	0.01	0.41	0.03
Euphausiids[b]				
Euphausiid calyptopis	—	Trace	0.03	0.16
Euphausiid furcillia\juvenile	0.08	Trace	0.01	0.22
Thysanoessa inermis	—	—	—	0.07
Thysanoessa raschii	—	—	0.03	0.01
Thysanoessa spinifera	—	—	0.01	—
Shrimps and mysids[c]				
Hippollytidae (juveniles)	—	—	0.05	0.07
Eualus gaimardii	—	—	Trace	0.03
Pandalidae	—	—	—	—
Amphipods[d]				
Themisto abyssorum/pacifica	—	—	—	0.01
Themisto libellula	Trace	—	0.01	Trace
Hyperoche medusarum	—	—	—	—
Gammaridae	Trace	—	—	—
Hyperidae	—	Trace	—	0.01
Amphipod (misc.)	—	—	—	0.01
Ctenophores				
Beroe cucumis	0.01	—	Trace	0.02
Mertensia ovum	—	0.01	0.01	—
Cnidarians[e]				
Aeginopsis laurentii	—	—	0.08	—
A. digitale	1.05	0.17	0.31	2.82
Catablema vesicarium	—	Trace	0.01	—
Obelia spp.	0.06	0.02	0.01	0.22
Rathkea octopunctata	0.03	0.01	0.01	0.29
Miscellaneous hydrozoans	0.23	—	—	0.01
Aurelia aurita	—	—	—	—

84.58	8	0.12	0.2	0.04	0.15	0.42	Trace
0.09	0.61	0.08	4.03	1.88	0.02	0.74	0.42
0.01	0.03	0.03	0.04	0.05	0.22	0.21	0.07
—	0.53	—	—	0.02	Trace	—	0.11
—	0.09	Trace	Trace	0.54	1.31	—	Trace
0.01	0.26	—	0.45	0.01	0.07	Trace	0.03
0.49	0.62	1.19	0.16	0.11	2.41	1.47	0.4
Trace	Trace	—	—	—	4.15	Trace	0.02
0.12	0.15	—	—	0.01	0.49	10.33	3.02
Trace	0	—	—	0.11	—	Trace	Trace
0.02	0.08	—	—	7.91	1.98	0.13	0.44
—	0.01	—	—	1.08	0.45	—	0.1
Trace	—	—	—	—	—	0.27	—
Trace	Trace	—	—	—	0.89	Trace	0.03
0.01	0.01	0.17	—	4.98	0.28	7.68	0.67
Trace	0.01	—	—	0.01	—	Trace	0.03
Trace	—	Trace	—	—	—	Trace	—
0.01	—	—	0.06	—	Trace	0.07	—
0.02	—	—	—	—	0.08	Trace	—
—	—	0.04	—	0.04	1.45	—	—
0.07	0.1	—	2.59	3.32	—	7.86	2.6
Trace	0.03	—	—	0.25	—	Trace	Trace
0.48	7.85	3.44	0.99	5.27	8.82	9.53	12.43
0.02	0.01	—	0.08	7.57	—	0.14	0.09
0.01	0.01	1.93	0.07	0.12	3.72	Trace	Trace
0.02	0.02	0.07	Trace	Trace	1.22	0.11	Trace
—	Trace	2.72	—	—	0.61	—	0.31
0.01	Trace	—	—	—	—	9.53	0.17

Appendix 1.1 continued…

Cyanea capillata	—	Trace	Trace	0.02	0.02	Trace	—	0.13	0.04	—	7.33	1.18
Chaetognaths												
Parasagitta elegans	0.62	0.72	0.48	3.26	1.65	5.26	9.86	17.61	25.29	28.84	4.59	35.47
Ostracoda	—	—	—	0.01	Trace	—	—	—	—	Trace	Trace	—
Cumacea	—	—	—	Trace	Trace	—	—	—	—	Trace	Trace	—
Total Holozooplankton	**71.53**	**91.63**	**44.26**	**55.82**	**96.42**	**89.79**	**57.5**	**72.97**	**89.49**	**91.1**	**97.82**	**99.49**
Bivalve larvae	7.07	2.05	47.94	2.92	0.02	—	4.09	0.19	2.18	Trace	Trace	—
Barnacle cyprius	8.75	3.68	2.03	18.15	2.61	0.46	28.58	23.53	4.67	7.37	1.66	0.06
Barnacle nauplius	5.58	0.3	0.84	19.09	0.29	8.83	4.27	0.08	0.24	0.45	Trace	0.22
Decapod zoea	0.02	0.02	0.01	0.17	0.53	0.53	0.56	0.61	0.01	Trace	0.11	0.1
Megalops	—	Trace	Trace	—	0.12	0.04	—	0.14	0.01	—	0.36	0.04
Polychaete larvae	5.93	1.77	3.97	3.8	0.01	0.35	4.82	2.46	3.36	1.04	Trace	0.09
Ophiuroid larvae	0.19	0.46	0.57	—	—	—	0.03	Trace	0.01	—	—	—
Asteroid bipinnaria	0.18	Trace	0.02	0.02	—	—	0.08	Trace	0.01	Trace	—	—
Echinoid larvae	0.75	0.08	0.36	0.03	—	—	0.07	Trace	0.03	Trace	—	—
Total Meroplankton	**28.47**	**8.37**	**55.74**	**44.18**	**3.58**	**10.21**	**42.5**	**27.03**	**10.51**	**8.9**	**2.18**	**0.51**

[a] Trace amounts of the copepods *Acartia tumida*, *Calanus hyperboreus*, *Clausocalanus* spp., *Microcalanus* spp., *Scaphocalanus* spp., and *Scolecithricella minor* were found but not reported in the table.

[b] Trace amounts of the euphausiids specie *Thysanoessa longipes* was found but not reported in the table.

[c] Trace amount of the mysid *Neomysis awatschens* was found nut not reported in the table.

[d] Trace amounts of the amphipod specie *Hyperia galba/medusarum* was found but not reported in the table.

[e] Trace amounts of the cnidarian species *Bougainvillia supercilliaris, Euphysa flammea, Sarsia tubulosa, Melicertum octocostatum, Chrysaora melanaster, Halitholus cirratus,* and Ptychogena spp. were found but not reported in the table.

Appendix 1.2 Permission from co-author Cheryl Clarke to include manuscript in the dissertation.

Jennifer Questel <jmquestel@alaska.edu>

Permission to use manuscript in my dissertation

2 messages

Jennifer Questel <jmquestel@alaska.edu> Tue, Apr 26, 2016 at 6:21 PM
To: Cheryl Clarke-Hopcroft <cclarkehopcroft@alaska.edu>

Hi Cheryl,

You are co-authored on the manuscript "Seasonal and interannual variation in the planktonic communities of the northeastern Chukchi Sea during the summer and early fall" that I will be including as a chapter in my dissertation to fulfill the requirements of a PhD in Oceanography from the University of Alaska Fairbanks.

Please respond to this email indicating whether you grant permission to include this paper.

Thanks,
Jenn

--
Jennifer Questel
Doctoral Candidate
Biological Oceanography
University of Alaska Fairbanks

Cheryl Clarke Hopcroft <cclarkehopcroft@alaska.edu> Tue, Apr 26, 2016 at 8:48 PM
To: Jennifer Questel <jmquestel@alaska.edu>

Absolutely!
[Quoted text hidden]
--
Cheryl Clarke-Hopcroft
Institute of Marine Science
University of Alaska Fairbanks

CHAPTER 2: PHYLOGEOGRAPHY AND CONNECTIVITY OF THE *PSEUDOCALANUS* (COPEPODA: CALANOIDA) SPECIES COMPLEX IN THE EASTERN NORTH PACIFIC OCEAN AND THE PACIFIC ARCTIC REGIO[1]

2.1 Abstract

The genus *Pseudocalanus* (Copepoda, Calanoida) is among the most numerically dominant copepods in eastern North Pacific and Pacific-Arctic waters. We compared population connectivity and phylogeography based on DNA sequence variation for a portion of the mitochondrial cytochrome oxidase I gene for four *Pseudocalanus* species with differing biogeographical ranges within these ocean regions. Genetic analyses were linked to characterization of biological and physical environmental variables for each sampled region. Haplotype diversity was higher for the temperate species *(Pseudocalanus mimus* and *Pseudocalanus newmani*) than for the Arctic species (*Pseudocalanus acuspes* and *Pseudocalanus minutus*). Genetic differentiation among populations at regional scales was observed for all species, except *P. minutus*. The program Migrate-N tested the likelihood of alternative models of directional gene flow between sampled populations in relation to oceanographic features. Model results estimated predominantly northward gene flow from the Gulf of Alaska to the Beaufort Sea for *P. newmani*. Model scenarios that allowed bidirectional gene flow between sampled populations gave the best Bayesian predictions for *P. acuspes*, *P. mimus* and *P. minutus*. Under current warming trends, biogeographical boundaries and barriers for *Pseudocalanus* species may shift, allowing habitat range expansion or contraction and resulting in altered population connectivity between Arctic and sub-Arctic populations.

[1] Published as Questel, J.M., Blanco-Bercial, L., Hopcroft, R.R., and Bucklin, A., 2016. Phylogeography and connectivity of four sibling species of *Pseudocalanus* (Copepoda: Calanoida) in the North Pacific Ocean and Pacific–Arctic region. Journal of Plankton Research doi:10.1093/plankt/fbw025

2.2 Introduction

Phylogeography studies the patterns of genetic variation within and among species on a geographical scale. Specifically, it incorporates a species' biogeographical past and how underlying forces, such as evolutionary and ecological processes, have structured contemporary geographical distributions (Avise, 2000, Knowles & Maddison, 2002). Portions of mitochondrial genes have frequently been used as genetic markers in phylogeographic studies due to high concentrations of mitochondrial DNA in eukaryotic organisms, its clonal maternal inheritance pattern and the detectable patterns of haplotype diversity within and between populations (Avise, 2000). The mitochondrial cytochrome oxidase I (COI) gene has proven to be a useful genetic marker for studies of marine planktonic copepods to discriminate and identify cryptic species (Bucklin *et al.*, 1998, 2001, Goetze, 2003, Goetze & Ohman, 2010, Viñas *et al.*, 2015), to understand the degree of population connectivity of cosmopolitan species (Goetze, 2005, Blanco-Bercial *et al.*, 2011) and to measure gene flow between distinct geographic populations (Costa *et al.*, 2014). Among other genetic markers used for population genetic and phylogeographic studies of marine copepods are the mitochondrial genes cytochrome B (Provan *et al.*, 2009, Milligan *et al.*, 2011) and 16S rRNA (Goetze, 2003, Nelson *et al.*, 2009), nuclear microsatellites (Provan *et al.*, 2009) and genomic single nucleotide polymorphisms (Brito & Edwards, 2009, Unal & Bucklin, 2010).

In general, holozooplankton are regarded as having very large population sizes and high rates of dispersal, and therefore high evolutionary potential (Peijnenburg & Goetze, 2013). The phylogeographic patterns expressed within holozooplankton populations can be affected by a number of physical mechanisms that create obstructions to gene flow. In addition to physical barriers (Blanco-Bercial *et al.*, 2011), gene flow patterns may be determined by oceanographic features, such as gyre systems (Goetze, 2005) and physical characteristics of the water column including temperature and salinity (Yebra *et al.*, 2011). Temperature and salinity may be the most important structuring factors for the North Pacific Ocean and the Pacific Arctic Region (PAR), which would strongly influence how species' distributions will be altered with continued warming trends. Many zooplankton species are adapted to particular salinity and/or temperature ranges and may see either a range expansion or contraction with projected climate change scenarios. Therefore, it becomes necessary to understand the hydrographic controls of the study

region in order to accurately model and interpret patterns of gene flow within and between zooplankton populations.

Over the past decade, there have been several studies that focused on the population genetics, connectivity and phylogeography of planktonic copepods of the North Pacific and PAR. The sibling species *Calanus glacialis* and *Calanus marshallae*, which present continuing difficulties in identification using morphological characters (Frost, 1974), have been examined using mt16S rRNA, which revealed genetic differences between populations of *C. glacialis* in the North Pacific and Arctic Ocean (Nelson *et al.*, 2009). Studies have provided insights into identification of *Calanus pacificus* sub-species (Nuwer *et al.*, 2008), and evolutionary processes shaping the contemporary phylogeny of the *Neocalanus* genus (Machida *et al.*, 2006).

The copepod genus *Pseudocalanus* is comprised of seven species that co-occur as differing assemblages within their geographic ranges, which span the Arctic and temperate-boreal marine ecosystems of the Northern Hemisphere. They are herbivorous epipelagic filter-feeders that target a wide size range of food particles, such as diatoms, flagellates and coccolithophores (Poulet, 1973, Corkett & McLaren, 1979, Cleary *et al.*, 2015), and opportunistically feed on sea-ice algae in Arctic regions (Conover *et al.*, 1986). *Pseudocalanus* are small-bodied neritic copepods with *P. newmani* at the smaller end and *P. major* at the larger end of the size spectrum (Frost, 1989). Nonetheless, prosome length alone is not a reliable taxonomic tool for species identification, due to overlapping size ranges and temperature-dependent size shifts. *Pseudocalanus* species display only very subtle morphological differences in the adult stage, with diagnostic features dependent upon the shape of the urosomal segment containing the genital pore as well as the shape of the seminal receptacle itself (Frost, 1989). However, species of *Pseudocalanus* show typical levels of interspecific genetic divergence for COI sequences of copepods (10 – 23 %) (Bucklin *et al.*, 2003). These extremely subtle morphological differences have created immense difficulties in accurate species identification and have resulted in a general lack of detailed species-specific distribution data, with co-occurring species typically treated as a species complex and reported simply as *Pseudocalanus* spp.

Pseudocalanus newmani and *Pseudocalanus mimus* are considered as temperate species while *Pseudocalanus acuspes* and *Pseudocalanus minutus* are Arctic species (Frost, 1989).

Within the northern Gulf of Alaska (GoA), the predominant species are *P. mimus* and *P. newmani* with *P. minutus* present in low numbers in both the shelf region and within Prince William Sound (PWS) (Napp *et al.*, 2005). *Pseudocalanus mimus* is the most abundant *Pseudocalanus* species in the eastern North Pacific (Napp *et al.*, 2005), and is also found to numerically dominate the outer domains of the Bering Sea (Bailey *et al.*, 2015). *Pseudocalanus acuspes, P. minutus* and *P. newmani* numerically dominate the species complex in the shallow Chukchi (Lane *et al.*, 2008, Hopcroft & Kosobokova, 2010, Hopcroft *et al.*, 2010, Questel *et al.*, 2013) and Beaufort Seas (Horner & Murphy, 1985, Darnis *et al.*, 2008, Smoot, 2015). In the Pacific, the geographical distribution of *P. acuspes* is primarily restricted to the PAR and extends south into the Bering Sea (Bailey *et al.*, 2015), an ecosystem heavily influenced by seasonal ice cover.

Molecular protocols have been developed to discriminate *Pseudocalanus* species based on DNA sequence variation of the COI gene (Bucklin *et al.*, 1995, 2001, 2003), which allows reliable species discrimination and identification. Subsequent studies using this and other genetic markers have allowed researchers to gain better insights into species distribution and abundance (Bucklin *et al.*, 2001, 2015; Mcgillicuddy & Bucklin, 2002, Grabbert *et al.*, 2010, Bailey *et al.*, 2015, 2015, Erikson, 2015), confirmation of presence/absence within a region (Aarbakke *et al.*, 2011, Holmborn *et al.*, 2011), demographic inferences (Aarbakke *et al.*, 2014) and population genetic differentiation (Unal *et al.*, 2006).

This study undertakes a comparative phylogeographic analyses of temperate and Arctic *Pseudocalanus* species and characterizes patterns and pathways of connectivity among populations of four species that are broadly sympatric and numerically dominant in the copepod assemblages of the eastern North Pacific and the PAR (Coyle & Pinchuk, 2003, Llinás *et al.*, 2009, Questel *et al.*, 2013, Ershova *et al.*, 2015). Using COI sequence variation, we infer barriers to gene flow and provide a basis for predicting how the species' geographic distributions and ranges may respond to climate change.

2.3 Method

2.3.1 Sample collection

Zooplankton samples were collected in 2013 as part of various oceanographic programs conducted in the northern GoA and the PAR (Fig. 2.1). Samples from the GoA and two fjord systems within PWS (Icy Bay and Columbia Glacier) were collected as part of the Seward Line Research Program (https://www.sfos.uaf.edu/sewardline). Samples from the PAR were collected in the Beaufort Sea during the Transboundary program (Smoot, 2015), and in the Chukchi Sea by the Chukchi Sea Environmental Studies Program (CSESP) (Day *et al.*, 2013). All samples were collected down to a maximum of 100 m using 150-µm mesh nets and preserved in 95% nondenatured ethanol following the protocols in Bucklin (2000).

2.3.2 Pathways of transport

The GoA is a semi-enclosed sub-Arctic basin in the North Pacific Ocean that is heavily influenced by the Alaska Coastal Current (ACC), a nutrient-poor, buoyancy-driven current bound to the coastal regions of Alaska (Stabeno *et al.*, 1995, 2004, Weingartner *et al.*, 2005). Prince William Sound (PWS), a sub-Arctic embayment, is connected to the GoA through two main pathways: Hinchinbrook Entrance on the easternmost side and Montague Strait on the western side, through which the ACC enters and exits. The ACC then continues westward through the Aleutian Islands and into the Bering Sea, where it flows along the continental shelf break region (Stabeno *et al.*, 1995). From there, currents flow in a strong northward direction through Bering Strait and across the Chukchi Sea, a shallow shelf ecosystem, in a complicated mixture of water masses (Coachman & Aagard, 1988, Weingartner *et al.*, 1998, 2013). The majority of water flowing over the northeastern Chukchi Sea shelf exits through Barrow Canyon or turns eastward at Point Barrow and flows into the Beaufort Sea (Pickart, 2004). The anticyclonic Beaufort Gyre persists over the Canadian Basin and sets up a countercurrent to the water masses entering the region from the Chukchi Sea. Additionally, water masses situated below the upper 50 m of the water column over the Beaufort Sea's continental slope reverses flow and aids in the transport of Pacific water, and zooplankton, eastward within the Beaufort Undercurrent (Aagaard, 1984, Pickart, 2004). Hence, the dominant northward-flowing currents

play an important role in determining the degree of connectivity and the extent of penetration of Pacific copepods into the PAR.

2.3.3 Molecular analysis

Adult female *Pseudocalanus* were picked from preserved zooplankton samples using a Leica MZ16 or M205C dissecting microscope. Key morphological characteristics for species identification, as detailed by Frost (1989), were examined using a compound microscope. Disproportional effort was expended looking for the rarer species within each habitat. Copepods were then washed in sterile MilliQ water to remove traces of ethanol prior to DNA extraction. Total genomic DNA was extracted using a DNeasy Blood and Tissue Kit (QIAGEN), with a final elution volume of 200 µL in AE Buffer.

PCR amplification of a 710-base pair (bp) fragment of the COI gene was achieved using 5 µL of 5× Green GoTaq® Flexi Buffer, 2.5 µL of 25 mM $MgCl_2$, 0.7 µL of 10 mM dNTPs, 1 µL of each forward and reverse primer (10 µM), 0.15 units of GoTaq® Flexi DNA Polymerase (Promega), 11.8 µL MilliQ water and 3 µL of DNA template, for a total reaction volume of 25 µL. The PCR protocol used was as follows: 94 °C for 3 min, 35 cycles of 94 °C for 40 s 60 °C for 40 s, and 69 °C for 50 s, and 1 cycle of 69 °C for 7 min. The two primers used were PseudoF: 5′-TTCGAATAGAGYTAGGHMVAGY-3′ (forward) and the Folmer *et al.* (1994) primer HCO-2198: 5′-TAAACTTCAGGGTGACCAAAAAATCA-3′ (reverse). The forward primer, PseudoF, was designed from COI sequences obtained using the primer set LCO-1490 (5′-GGTCAACAAATCATAAAGATATTGG-3′) and HCO-2198 (Folmer *et al.*, 1994).

PCR products were checked by electrophoresis at 100 V for 50 min on a 1% agarose/TBE gel stained with Gel Red (Biotium). Cytochrome oxidase I bands were visualized under a UV light using a UVP ChemiDoc-It^2 imager. PCR products from successful amplifications were purified using 2 µL ExoSAP-IT for every 5 µL PCR product and incubated at 95 °C for 15 min.

DNA sequencing used the same primers as for PCR amplification and the Big Dye Terminator Ver. 3.1 kit (Applied Biosystems Inc., ABI). The cycle sequencing protocol used was modified from Glenn and Schable (2005) and was as follows: 95 °C for 1 min, 50 cycles of 96 °C for 10 s, 50 °C for 5 s and 60 °C for 4 min, and 1 cycle of 72 °C for 2 min. Sequence

reactions were cleaned using the CCDB Sephadex clean-up protocol (www.dnabarcoding.org) and run on an ABI 3130 Genetic Analyzer capillary DNA sequencer. Sequences were manually checked for accurate base calling and contigs generated using the DNA sequence assembly program Sequencher Ver. 5.2.4 (Gene Codes Corp.).

The COI sequences were aligned by CLUSTAL-W (Thompson *et al.*, 1994) using the Molecular Evolutionary Genetics Analysis (MEGA Ver. 6) software package (Tamura *et al.*, 2013). Primers were trimmed from the ends of sequences for an initial aligned length of ~535 bp. Species' identities for COI sequences were verified based on BLAST searches through the NCBI GenBank database (Altschul *et al.*, 1997).

2.3.4 Statistical analysis

Nucleotide diversity (π) and haplotype diversity (H_d) for the COI gene were calculated using the software DnaSP Ver. 5 (Librado & Rozas, 2009). Maximum Parsimony gene trees were analyzed using the best-fit nucleotide substitution model (Tamura model) (Tamura, 1992) as determined by MEGA Ver. 6. The significance of the substitution model was estimated through 10,000 coalescence simulations under a bootstrap test of 1000 replicates. Haplotype networks were determined using Haploviewer (Center for Integrative Bioinformatics; available at http://www.cibiv.at/~%20greg/haploviewer).

A hierarchical Analysis of MOlecular VAriance (AMOVA) was used to examine population genetic structure of each species using the software Arelquin 3.5 (Excoffier & Lischer, 2010). Samples were grouped according to their respective region (i.e. ocean basin; Table 2.1). The significance of the variance partitions, among-regions (Φ_{CT}), among-samples, within-regions (Φ_{SC}) and within-samples (Φ_{ST}), was determined based on 10 100 permutations. F_{ST} distances, reported as Φ_{ST} (Tamura substitution model), were calculated for all pairs of each *Pseudocalanus* species and tested for significance under 10 100 permutations and with $\alpha = 0.05$, after sequential Bonferroni correction (Holm, 1979). Samples with four or fewer individuals were removed from the analysis while all negative Φ_{ST} values obtained were assumed to be zero.

Gene flow between populations of each *Pseudocalanus* species from the GoA, PWS and PAR was modeled using the coalescent-based program Migrate-N Ver. 3.6.11 (Beerli, 2012). Migrate-N uses ratios of maximum likelihood or Bayesian inference to estimate migration rates

and effective population size (N_E) under the assumption of asymmetrical migration rates at different subpopulation sizes (Beerli & Felsenstein, 2001, Beerli, 2004, 2006). Custom migration models were constructed for each species of *Pseudocalanus* and structured based on the number of sequences obtained per area, as well as regional geography and hydrography.

For *P. acuspes*, Migrate-N model scenarios tested were as follows: South-to-North, North-to-South and Full (Fig. 2.2). The South-to-North model tested gene flow from the Chukchi Sea into the Beaufort Sea; the North-to-South scenario tested the reverse flow. The Full model scenario allowed for bidirectional gene flow between both the Chukchi and Beaufort Seas. Model scenarios tested for *P. minutus* and *P. newmani* were: All-North, Part-North, South and Full (Fig. 2.2). The All-North scenario tested gene flow in a northward flow pattern, with restrictions placed on exchange from more northern populations to southern ones (e.g. Chukchi Sea flowing into the GoA). The Part-North scenario modeled gene flow with unidirectional flow from the GoA into the Chukchi Sea, with bidirectional flow between the Chukchi and Beaufort Seas, as well as between the GoA and PWS populations. The South model was set up to test gene flow from the Beaufort Sea, into the Chukchi Sea and subsequently into the GoA, with bidirectional gene flow between the GoA and PWS populations. The Full model scenario allowed gene flow between all populations, but with restrictions due to geographical constraints. Those restrictions isolated the Beaufort Sea from the GoA and PWS populations, and the Chukchi Sea from the PWS population. Lastly, model scenarios tested for *P. mimus* were: Out-PWS, In-PWS and Full (Fig. 2.2). The Out-PWS model tested gene flow between Icy Bay and Columbia Glacier and subsequently out of PWS and into the GoA whereas the In-PWS model tested gene flow from the GoA into Icy Bay and Columbia Glacier and between the two fjord systems.

Parameters for each Migrate-N model run were kept at the default settings with the following exceptions: (i) parameter start settings for theta (θ) and migration rates (M) used the Mode values from the posterior distributions of an initial run's F_{ST}-based θ and M; (ii) the SLICE sampler method was used for Bayes-proposals for both θ and M; and (iii) long-chain values (1–3) were tested for optimal posterior distributions. We report the Bayes factor predictions for custom model scenarios for each species.

2.4 Results

A total of 822 COI sequences were obtained for the four species of *Pseudocalanus* collected from the GoA, PWS and the Chukchi and Beaufort Seas (Table 2.1; GenBank accession nos KU141424 – KU142246). The aligned sequence length used for the analyses ranged from 518 to 536 bp (Table 2.2). *Pseudocalanus minutus* and *P. newmani* were found throughout the entire study region, whereas *P. acuspes* was restricted to the PAR and *P. mimus* was confined to the eastern North Pacific sampling location. Few individuals of *P. acuspes* and *P. mimus* were sequenced from the eastern North Pacific and the PAR, respectively (Table 2.1), despite considerable effort to find them within our collections. The presence of *P. mimus* in the Arctic Ocean has also been confirmed through sequencing the 28S ribosomal RNA gene (GenBank accession no: EF460783).

In all, 178 unique haplotypes were identified among the four species of *Pseudocalanus* over the five sampling regions (Table 2.2). Nucleotide diversity (π) and haplotype diversity (H_d) were lower for the Arctic species *P. acuspes* and *P. minutus* (3.6×10^{-4} and 1.3×10^{-4}; 0.66 and 0.61, respectively), and higher for the temperate species *P. mimus* and *P. newmani* (7.8×10^{-4} and 6.9×10^{-4}; 0.91 and 0.81, respectively; Table 2.2). There were numerous haplotypes for all species, with a range of frequencies for *P. mimus*, and one (in the case of *P. acuspes*) or two (*P. minutus* and *P. newmani*) major haplotypes, with several less frequent or unique haplotypes (Fig. 2.3). Of the 188 *P. minutus* sequenced, only 13 haplotypes were detected; however, haplotype diversity was almost equal to that expressed for *P. acuspes*. Fifty-two unique haplotypes were identified for *P. mimus* with only one observed at all five sampling locations, which occurred most frequently (50%) in the Columbia Glacier sample. The two dominant haplotypes for each of *P. minutus* and *P. newmani* were found to be relatively abundant in all five sampling locations, with fairly equal representation exhibited by each haplotype.

Pairwise Φ_{ST} values for samples collected across the four regions showed comparisons between the Chukchi and Beaufort Seas to be significant for *P. acuspes* (Table 2.3). Significant values were also observed for *P. newmani* when Beaufort Sea samples were compared against samples from the GoA and PWS (Table 2.4). No significant values were observed between samples of *P. minutus* (Table 2.5), while *P. mimus* showed only one significant comparison between one GoA sample and Columbia Glacier (Table 2.6). Analyses of molecular variance

showed significant differentiation of regional populations for *P. acuspes*, *P. mimus* and *P. newmani* (Table 2.7); no significant differentiation at this scale was found for *P. minutus*. Overall, the greatest amount of variance was explained by individuals within samples for all four species, yet none of the variance components (i.e. variance among regions, among samples within a region or individuals within samples) were statistically significant for *P. minutus*.

Low numbers of *P. acuspes* were found in the GoA and PWS, which constrained the Migrate-N models of gene flow to the PAR. Similarly, low numbers of *P. mimus* were found in the PAR, which constrained the model scenarios of gene flow to the eastern North Pacific. Marginal likelihood outputs predicted the Full model to be the best pathway for gene flow between sampled populations of *P. acuspes* and *P. mimus* (Table 2.8). These results indicated strong bidirectional gene flow between the Chukchi and Beaufort Seas for *P. acuspes* and between the GoA and PWS for *P. mimus*. Marginal likelihood outputs predicted the Part-North model, simulating gene flow from the GoA north through the Chukchi Sea and into the Beaufort Sea, to be the best fit for sampled populations of *P. newmani* (Table 2.8). All model results for *P. acuspes, P. mimus* and *P. newmani* gave good Bayesian unimodal posterior distributions. Marginal likelihood outputs predicted the Full model, which allowed bidirectional gene flow between sampled populations with geographical restrictions, to be the best fit for *P. minutus* (Table 2.8). However, Bayesian posterior distributions were not unimodal, but instead showed noisy distributions for all migration rates tested. Models were further tested using Metropolis-Hastings as the Bayes-proposals and longer-running models, with long-chain increments set to 10,000. These parameter changes did not result in cleaner or more unimodal posterior distributions.

2.5 Discussion

An important component of forecasting how marine ecosystems will respond to climate change is understanding how individual species' distributions and abundances will change with warming trends. Multiyear studies of the mesozooplankton communities from the Chukchi Sea have revealed differing responses on a species level in warm years versus cold years (Matsuno *et al.*, 2011, Questel *et al.*, 2013, Ershova *et al.*, 2015). Specifically, *Pseudocalanus* spp., which numerically dominate the copepod assemblages, are least abundant in colder years (Questel *et*

al., 2013, Ershova *et al.*, 2015). Overall, the temperate *P. newmani* is the most prevalent of the four *Pseudocalanus* species across the Chukchi Sea (Matsuno *et al.*, 2011, Questel *et al.*, 2013, Ershova *et al.*, 2015) exhibiting broader spatial distributions in warmer years and, consequently, pushing faunal barriers for Arctic species northward (Ershova *et al.*, 2015). Interestingly, this exemplifies how even very closely related species, with similar niches and geographical distributions, elicit very different responses to changing environmental conditions.

Results from this study suggest *P. newmani* will likely exhibit greater resilience to climate change, as it was found in high abundances throughout the entire study region and displayed a dominant northward gene flow pattern, concurrent with local hydrography. Conversely, it is plausible that *P. acuspes* will experience – and perhaps already has done so – range contraction, where it would be restricted to the colder Arctic environment. *Pseudocalanus acuspes* was very rare in the GoA and PWS regions, being restricted to cold glacial fjords, and thus showed very low levels of population connectivity between the eastern North Pacific and PAR. Overall, results from our Migrate-N model simulations indicate high levels of connectivity between established populations of each *Pseudocalanus* species in the Arctic and eastern North Pacific. Shifting species boundaries will increase the need to understand how climate effects will cascade through marine ecosystems. In particular, northward movement of boreal generalist species has great potential to alter Arctic food webs (Kortsch *et al.*, 2015).

Results from the Migrate-N model scenarios indicated that there is a strong degree of population connectivity between North Pacific and Arctic populations of each of the four species, with bidirectional gene flow occurring between geographically adjacent populations. However, posterior distributions were quite noisy and resolution could not be improved by changing model parameters for *P. minutus*. These results could indicate that either this species has extremely high rates of contemporary gene flow or that it recently went through a population bottleneck, for which single locus mitochondrial data would not be informative enough on their own to definitively model gene flow. In the North Atlantic, *P. minutus* had the lowest level of genetic structuring of the studied *Pseudocalanus* species, with most of the variance explained by within-population comparisons (Aarbakke *et al.*, 2014). Bayesian skyline tests indicated that these populations of *P. minutus* underwent population expansion during the current interglacial 25,000 – 10,000 YBP (Aarbakke *et al.*, 2014). *Pseudocalanus minutus* was found to be evenly

distributed across the Bering Sea, with highest abundances occurring over the shelf region (Bailey *et al.*, 2015). Nucleotide and haplotype diversities expressed within that region were comparable to those found in our study $2.01x10^{-3}$ and 0.670 (Bailey *et al.*, 2015) versus $1.6x10^{-3}$ and 0.606, respectively.

Pseudocalanus acuspes appeared to be the most abundant of the four species in the Arctic populations. Despite sharing one highly frequent haplotype, populations of this species showed significant differentiation between the two regions in this study. Our results differed from a prior study, which showed no significant differences among populations (Sevigny *et al.*, 1989). This discrepancy is most likely the result of the reduced ability of allozymes to resolve population structure, as well as analyzing individual *P. acuspes* from a relict population (Bedford Basin) in the North Atlantic that has been genetically isolated since the last glacial maximum. The prospect of a relict population was also observed in the Gulf of Finland, where mitochondrial sequence data revealed a high degree of variance among samples of *P. acuspes*, yet populations exhibited extremely low mitochondrial diversity (H_d= 0.024) (Aarbakke *et al.*, 2014), suggesting that these populations started to diverge 200,000-50,000 YBP.

Pseudocalanus mimus and *P. newmani* were found throughout the samples collected from the eastern North Pacific. However, the lack of *P. mimus* within the Chukchi and Beaufort Seas was most likely a result of the abnormally cold temperatures experienced in the PAR for the 2013 open water season (Weingartner *et al.*, 2014), which may have impeded the survival and reproduction of *P. mimus* on the Bering Sea shelf. Nucleotide and haplotype diversities were high for all populations of *P. mimus* and *P. newmani*, complementing the patterns observed for the Bering Sea populations (Bailey *et al.*, 2015). Aarbakke *et al.* (2014) and Sevigny *et al.* (1989) both observed high levels of sequence diversity for *P. newmani* with approximations that populations in the North Atlantic have remained stable in size for over 250,000 years (Aarbakke *et al.*, 2014).

Estimates of gene flow for the Full model scenarios for both *P. minutus* and *P. mimus* indicated that population connectivity is bidirectional between the two sampled fjord systems of PWS, as well as within the northern GoA. This flow scenario was also incorporated into the accepted Part-North model for *P. newmani*. These patterns complement the regional hydrographic flow, where the ACC from the GoA enters PWS through Hinchinbrook Entrance

and exits through Montague Strait. During the summer months, hydrographic flow decreases in intensity, causing flow to reverse direction (Halverson *et al.*, 2013).

The portion of the Part-North model scenario for *P. newmani* simulating northward gene flow from the GoA through the Chukchi Sea and into to the Beaufort Sea is also consistent with the dominant northward flow of Pacific water through the Bering Sea and across the Chukchi Sea. However, this same model scenario was not the best choice for *P. minutus*. Instead, the model scenario that allowed for southward gene flow from the Chukchi Sea to the GoA gave the best Bayesian predictions. Explanations for these results could be attributed to the episodic southward flow of water through the Bering Strait during the winter months (Woodgate *et al.*, 2005), as well as the low diversity within *P. minutus* populations, which seemingly resulted in multimodal posterior distributions in the Migrate-N model simulations. Therefore, these results should be considered with caution for *P. minutus*. Model scenarios for *P. acuspes*, *P. minutus* and *P. newmani* supported bidirectional gene flow between the Beaufort and Chukchi Seas, which can be accredited to the juxtaposition of the anticyclonic Beaufort Gyre and the eastward flowing Chukchi Sea water masses setting up a countercurrent flow system in the region.

The moderate levels of haplotype diversity among Arctic species observed in this study may be a direct reflection of population size, where Arctic species have smaller population sizes and ranges than temperate species, thus resulting in lower haplotype diversities. This phenomenon has been observed in other marine copepods (e.g. *Calanus finmarchicus* and *Nannocalanus minor*), which display low mitochondrial diversity and small effective population sizes, most likely resulting from a population contraction during the last glacial maximum (Bucklin & Wiebe, 1998). The low nucleotide diversity, low numbers of alleles over a large number of individuals and moderate H_d recorded for *P. minutus* in this study are likely indications that the evolutionary history of this species entailed genetic isolation or a population bottleneck associated with the closing of the Bering Strait during the Pleistocene Ice Ages (1.6 MYA to 10,000 YBP) due to lower sea level exposing the Bering Land Bridge (Sancetta, 1983).

The phylogeographic analyses presented here confirm the biogeographic distribution of four sibling species of *Pseudocalanus*, which live sympatrically in the eastern North Pacific and PAR (Frost, 1989). Estimates of population connectivity based on COI sequence variation indicated that *Pseudocalanus* species inhabiting the eastern North Pacific and PAR show high

levels of gene flow. Similarly, Aarabakke *et al.* (2011) observed a high degree of connectivity among populations of *P. moultoni* in the North Atlantic/Arctic sector. Strong gene flow despite large geographic distances has been observed among the cosmopolitan copepod *Clausocalanus* spp. (Blanco-Bercial *et al.*, 2011) and *Calanus sinicus* (Huang *et al.*, 2014).

Our analyses also revealed gene flow patterns for *P. acuspes*, *P. newmani* and *P. mimus* that were in agreement with local hydrographic flow. For instance, gene flow models indicate a northward flow for populations of *P. newmani* in the GoA through the Chukchi Sea and into the Beaufort Sea, reflecting the dominant northward flow of water masses through the Bering Strait and into the PAR. The temperate species *P. newmani* and the Arctic species *P. minutus* were abundant in all sampling regions, yet genetic structuring was stronger for *P. newmani* compared to *P. minutus*. *Pseudocalanus mimus* (temperate species) and *P. acuspes* (Arctic species) were found in extremely low abundances in Arctic and temperate samples, respectively. These patterns indicate that physical environmental conditions in the eastern North Pacific and PAR, including hydrography and ocean currents, serve as both pathways of exchange and barriers to gene flow for planktonic marine copepods.

2.6 Funding

This work was primarily supported by the Chukchi Sea Environmental Studies Program (CSESP) funded by ConocoPhillips, Anchorage, AK; Shell Exploration and Production Company, Anchorage, AK and Statoil USA E+P, Inc., Anchorage, AK, with added contributions from the University of Alaska Fairbanks through the Northern Gulf of Alaska Applied Research Award. We would also like to thank the Bureau of Ocean Energy Management for supporting the Transboundary Program as well as the North Pacific Research Board, Exxon Valdez Oil Spill and Alaska Ocean Observing System for supporting the Seward Line cruises, both of which provided samples for this study. Research reported in this publication was supported by an Institutional Development Award (IDeA) from the National Institute of General Medical Sciences of the National Institutes of Health to JMQ (grant number P20GM103395).

2.7 Acknowledgements

We would like to thank the captains and crews of the *M/V Tiglax*, *R/V Westward Wind* and the *R/V Norseman II* for their help during the various research cruises. In particular, we would like to thank the lead biologists Caryn Rea (ConocoPhilips), Michael Macrander (Shell) and Steinar Eldøy (Statoil) for their contributions to the CSESP project. Sequencing was conducted at the University of Alaska Fairbanks' DNA Core lab facility. We would like to thank the Core Lab director, Ian Herriott, for his continued guidance with laboratory techniques.

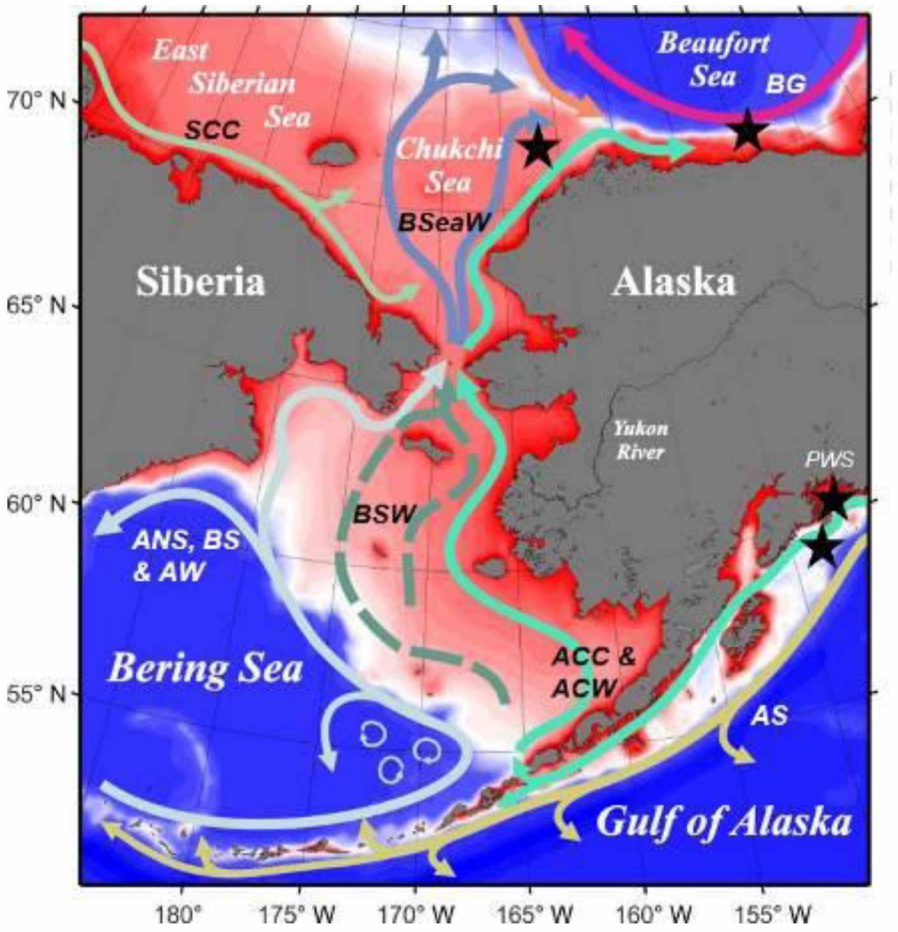

Figure 2.1 Averaged current flow fields for the eastern North Pacific Ocean and the PAR. Modified, with consent, from Danielson *et al.* (2011). Stars represent sampling locations. BG, Beaufort Gyre; SCC, Siberian Coastal Current; BSeaW, Bering Sea Water; BSW, Bering Shelf Water; ANS, Aleutian North Slope; BS, Bering Slope; AW, Anadyr Water; ACC, Alaska Coastal Current; ACW, Alaska Coastal Water; AS, Alaskan Stream; PWS, Prince William Sound.

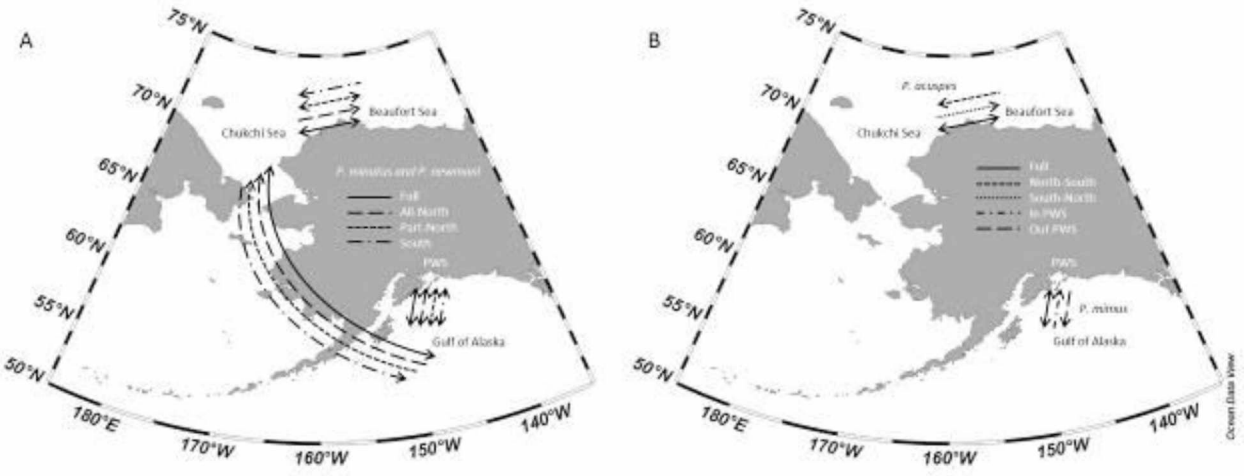

Figure 2.2 Conceptual representation of each Migrate-N model scenario tested for *P. minutus* and *P. newmani* (A), and *P. acuspes* and *P. mimus* (B) in the eastern North Pacific and PAR.

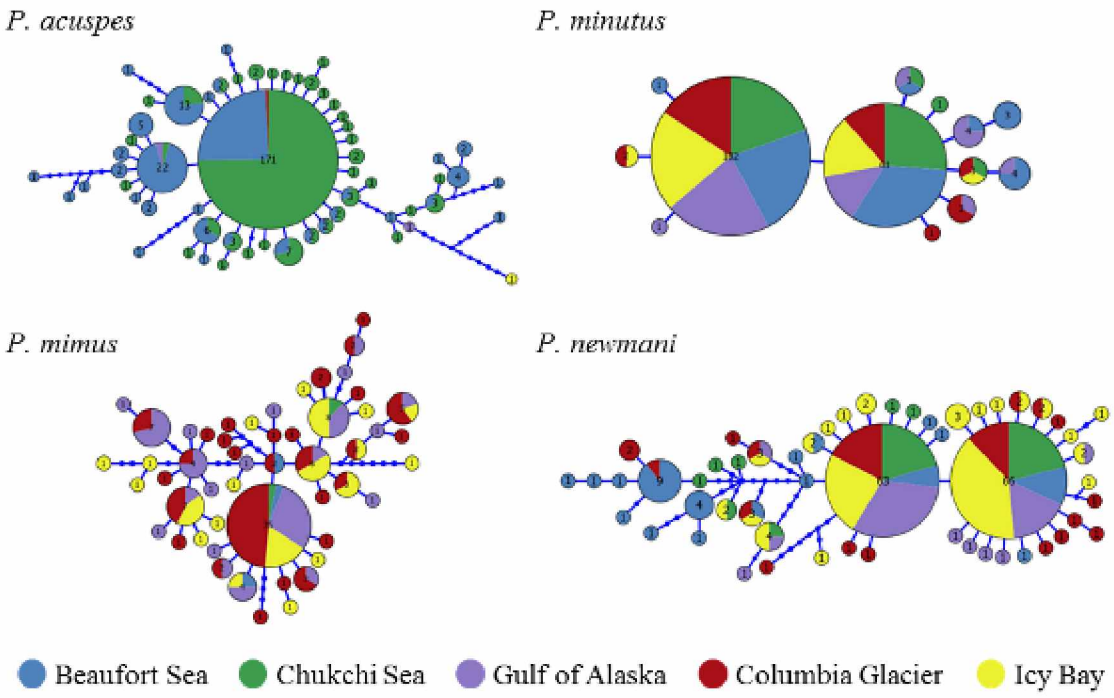

Figure 2.3 Cytochrome oxidase I haplotype networks for *P. acuspes*, *P. minutus*, *P. mimus* and *P. newmani*. Each circle represents a unique haplotype; sizes are scaled to the number of individuals expressing that particular haplotype. Each node represents a single bp mutation.

Table 2.1 Sampling locations and numbers of individuals sequenced for *Pseudocalanus* spp. collected during 2013 from the eastern North Pacific and PAR.

Basin	Cruise ID	Station	Bottom Depth (m)	Date	Lat (°N)	Long (°W)	*P. acuspes*	*P. minutus*	*P. mimus*	*P. newmani*
Beaufort	TB13	A1-50	50	21 August 2013	70.043	–141.1363	12	—	—	—
		A2-200	207	19 August 2013	70.512	–142.1004	42	13	1	13
		A2-1000	997	18 August 2013	70.628	–142.2088	—	2	1	10
		A6-50	50	14 August 2013	70.672	–146.1369	6	3	—	2
		A6-200	200	14 August 2013	70.889	–146.0859	18	21	—	8
		A6-1000	1004	17 August 2013	71.014	–146.1102	38	13	1	3
Chukchi	WWW1304	BF007	43	25 September 2013	71.241	–163.4092	39	9	2	9
		KF007	40	21 September 2013	70.772	–165.6299	62	14	—	9
		KF011	40	23 September 2013	70.895	–166.0141	11	5	—	4
		KF017	41	22 September 2013	71.021	–165.6390	48	10	—	8
		SF020	38	30 September 2013	71.994	–164.1493	11	—	—	—
		TF004	42	3 October 2013	71.247	–164.1828	6	—	—	4
PWS	TXF13	CG	193	7 May 2013	60.984	–147.0793	1	28	52	36
		Icy Bay	123	8 May 2013	60.241	–148.3303	1	33	33	63
GoA	TXF13	GAK1	271	5 May 2013	59.841	–149.4697	1	37	17	13
		GAK4	201	5 May 2013	59.402	–149.0572	1	—	12	13
		GAK8	289	4 May 2013	58.787	–148.4752	—	—	10	13
Total							297	188	129	208

Table 2.2 Summary of intraspecific variation for COI sequences for *Pseudocalanus* from the eastern North Pacific and PAR during 2013. *N*, number of individuals sequenced; BP, base pair sequence length; *H*, number of haplotypes; H_d, haplotype diversity; SD, standard deviation; π, nucleotide diversity.

Affinity	Species	*N*	BP	*H*	π	SD	H_d	SD
Arctic	*P. acuspes*	297	518	59	$3.3\text{x}10^{-3}$	$3.6\text{x}10^{-4}$	0.661	0.032
	P. minutus	188	535	13	$1.6\text{x}10^{-3}$	$1.3\text{x}10^{-4}$	0.606	0.027
Temperate	*P. mimus*	129	536	52	$7.8\text{x}10^{-3}$	$4.3\text{x}10^{-4}$	0.914	0.020
	P. newmani	208	529	54	$6.9\text{x}10^{-3}$	$6.6\text{x}10^{-4}$	0.807	0.020

Table 2.3 Pairwise Φ_{ST} distances between samples of *P. acuspes* from the eastern North Pacific and PAR during 2013. Φ_{ST} values are below and *P*-values are above the diagonal. Bold numbers indicate significant values after sequential Bonferroni correction ($\alpha = 0.05$).

P. acuspes	Beaufort Sea					Chukchi Sea					
Station	A1-50	A2-200	A6-50	A6-200	A6-1000	BF007	KF007	KF011	KF017	SF020	TF004
A1-50		0.215	0.902	0.001	**0.001**	**0.000**	**0.000**	**0.000**	**0.000**	**0.000**	0.061
A2-200	0.016		0.242	0.130	0.008	**0.000**	**0.000**	0.051	**0.000**	0.047	0.264
A6-50	0.000	0.024		0.004	0.017	**0.000**	**0.000**	**0.000**	**0.000**	**0.001**	0.034
A6-200	0.113	0.023	0.199		0.907	0.282	**-0.003**	0.464	0.139	0.336	0.057
A6-1000	**0.168**	0.051	0.247	0.000		0.410	**-0.002**	0.507	0.271	0.323	0.062
BF007	**0.247**	**0.092**	**0.375**	0.004	0.000		0.657	0.580	0.253	0.412	0.007
KF007	**0.310**	**0.127**	**0.414**	**0.024**	**0.013**	0.000		0.377	0.118	0.436	0.007
KF011	**0.142**	0.049	**0.294**	0.000	0.000	0.000	0.005		0.457	1.000	0.096
KF017	**0.249**	**0.105**	**0.343**	0.014	0.005	0.005	0.007	0.000		0.582	0.018
SF020	**0.137**	0.054	**0.305**	0.006	0.000	0.000	0.000	0.000	0.000		0.088
TF004	0.103	0.019	0.220	0.138	0.161	0.290	0.320	0.170	0.236	0.216	

Table 2.4 Pairwise Φ_{ST} distances between samples of *P. minutus* from the eastern North Pacific and PAR during 2013. Φ_{ST} values are below and *P*-values are above the diagonal. Bold numbers indicate significant values after sequential Bonferroni correction ($\alpha = 0.05$).

P. minutus	Beaufort Sea			Chukchi Sea				PWS		GoA
Station	A2-200	A6-200	A6-1000	BF007	KF007	KF011	KF017	CG	IB	GAK1
A2-200		0.418	0.694	0.614	0.604	0.243	0.747	0.317	0.218	0.736
A6-200	0.000		0.375	0.698	0.292	0.716	0.214	0.101	0.032	0.092
A6-1000	0.000	0.000		0.610	0.833	0.335	0.908	0.801	0.732	0.801
BF007	0.000	0.010	0.000		0.524	0.494	0.614	0.432	0.221	0.435
KF007	0.000	0.000	0.000	0.000		0.212	0.822	0.845	0.740	0.744
KF011	0.041	0.000	0.090	0.000	0.142		0.156	0.146	0.054	0.133
KF017	0.000	0.033	0.000	0.000	0.000	0.156		0.738	0.893	0.733
CG	0.000	0.041	0.000	0.000	0.000	0.111	0.000		0.694	0.506
IB	0.020	0.085	0.000	0.031	0.000	0.228	0.000	0.000		0.449
GAK1	0.000	0.039	0.000	0.000	0.000	0.120	0.000	0.000	0.000	

Table 2.5 Pairwise Φ_{ST} distances between samples of *P. newmani* from the eastern North Pacific and PAR during 2013. Φ_{ST} values are below and *P*-values are above the diagonal. Bold numbers indicate significant values after sequential Bonferroni correction ($\alpha = 0.05$).

P. newmani	Beaufort Sea			Chukchi Sea			PWS		GoA		
Station	A2-200	A2-1000	A6-200	BF007	KF007	KF017	CG	IB	GAK1	GAK4	GAK8
A2-200		0.721	0.079	0.011	**0.001**	0.006	**0.000**	**0.000**	**0.000**	**0.000**	**0.000**
A2-1000	0.000		0.056	0.005	**0.000**	0.004	**0.000**	**0.000**	**0.000**	**0.000**	**0.000**
A6-200	0.140	0.171		0.544	0.287	0.512	0.558	0.013	0.112	0.129	0.116
BF007	0.239	0.296	0.000		0.201	0.574	0.429	0.056	0.345	0.132	0.051
KF007	**0.423**	**0.480**	0.087	0.066		0.900	0.742	0.476	0.668	0.991	0.786
KF017	0.314	0.370	0.000	0.000	0.000		0.926	0.394	0.607	0.761	0.484
CG	**0.347**	**0.393**	0.000	0.000	0.000	0.000		0.061	0.563	0.447	0.436
IB	**0.553**	**0.605**	0.153	0.071	0.000	0.000	0.020		0.970	0.225	0.447
GAK1	**0.449**	**0.508**	0.105	0.028	0.000	0.000	0.000	0.000		0.695	0.698
GAK4	**0.433**	**0.486**	0.097	0.052	0.000	0.000	0.000	0.013	0.000		1.000
GAK8	**0.488**	**0.552**	0.154	0.119	0.000	0.000	0.000	0.000	0.000	0.000	

Table 2.6 Pairwise Φ_{ST} distances between samples of *P. mimus* from the eastern North Pacific and PAR during 2013. Φ_{ST} values are below and *P*-values are above the diagonal. Bold numbers indicate significant values after sequential Bonferroni correction ($\alpha = 0.05$).

P. mimus	PWS		GoA		
Station	CG	IB	GAK1	GAK4	GAK8
CG		0.067	**0.001**	0.844	0.856
IB	0.022		0.006	0.553	0.409
GAK1	**0.140**	0.105		0.027	0.017
GAK4	0.000	0.000	0.141		0.978
GAK8	0.000	0.000	0.178	0.000	

Table 2.7 Analysis of MOlecular VAriance (AMOVA) for *Pseudocalanus* species from the eastern North Pacific and PAR during 2013. Samples are grouped by region (Chukchi Sea, Beaufort Sea, Gulf of Alaska, Icy Bay and Columbia Glacier). Bold numbers indicate significant values (P = 0.05). DF, degrees of freedom.

	Source of Variation	DF	Sum of squares	Variance components	Percent of variation	Fixation indices	*P*-value
Arctic	*P. acuspes*						
	Among regions	1	8.672	**0.0460**	5.45	Φ_{CT} = 0.0545	0.0306 ± 0.0018
	Among samples, within regions	9	15.363	**0.0395**	4.68	Φ_{SC} = 0.0495	0.0008 ± 0.0003
	Within samples	282	213.791	**0.7581**	89.86	Φ_{ST} = 0.1014	0.0000 ±0.0000
	P. minutus						
	Among regions	3	1.619	0.0048	1.17	Φ_{CT} = 0.0117	0.2354 ± 0.0038
	Among samples, within regions	6	2.125	-0.0035	-0.85	Φ_{SC} = -0.0086	0.4866 ± 0.0054
	Within samples	174	70.555	0.4055	99.68	Φ_{ST} = 0.0032	0.4172 ± 0.0047
Temperate	*P. mimus*						
	Among regions	1	3.074	-0.0355	-1.65	Φ_{CT} = -0.0165	0.6045 ± 0.0049
	Among samples, within regions	3	14.349	**0.1245**	5.80	Φ_{SC} = 0.0571	0.0063 ± 0.0008
	Within samples	119	244.690	**2.0562**	95.85	Φ_{ST} = 0.0415	0.0046 ± 0.0006
	P. newmani						
	Among regions	3	65.476	**0.446**	21.9	Φ_{CT} = 0.2190	0.0210 ± 0.0014
	Among samples, within regions	7	18.015	0.0672	3.30	Φ_{SC} = 0.0423	0.1536 ± 0.0036
	Within samples	187	280.231	**1.5230**	74.79	Φ_{ST} = 0.2521	0.0000 ± 0.0000

Table 2.8 Bayesian predictions for custom migration models using Migrate-N for *Pseudocalanus* from the eastern North Pacific and PAR during 2013. Bold values indicate best model choice.

	P. acuspes	FULL	South-to-North	North-to-South	
Arctic	Bezier lmL	**-1841.328**	-1979.752	-1965.854	
	LBF (Besier)	**0.000**	-138.423	-124.526	
	Model Probability	**1.000**	0.000	0.000	
	Choice	**1 (best)**	3	2	
	P. minutus	FULL	All-North	Part-North	South
	Bezier lmL	**-972.779**	-983.676	-978.970	-1145.543
	LBF (Besier)	**0.000**	-10.897	-6.190	-172.764
	Model Probability	**0.998**	0.000	0.002	0.000
	Choice	**1 (best)**	3	2	4
	P. mimus	FULL	OUT-PWS	IN-PWS	
Temperate	Bezier lmL	**-1491.687**	-1565.433	-1589.876	
	LBF (Besier)	**0.000**	-73.746	-98.189	
	Model Probability	**1.000**	0.000	0.000	
	Choice	**1 (best)**	2	3	
	P. newmani	FULL	All-North	Part-North	South
	Bezier lmL	-1679.050	-1674.089	**-1669.113**	-1806.162
	LBF (Besier)	-9.936	-4.976	**0.000**	-137.048
	Model Probability	0.000	0.007	**0.993**	0.000
	Choice	3	2	**1 (best)**	4

2.8 References

Aagaard, K. (1984) The Beaufort Undercurrent. In P. W. Barnes, D. M. Schell and E. Reimnitz (eds.), *The Alaska Beaufort Sea: Ecosystems and Environments*. Academic Press, New York, pp. 47–71.

Aarbakke, O. N. S., Bucklin, A., Halsband, C. and Norrbin, F. (2011) Discovery of *Pseudocalanus moultoni* (Frost, 1989) in Northeast Atlantic waters based on mitochondrial COI sequence variation. *J. Plankton Res.*, **33**, 1487–1495.

Aarbakke, O. N. S., Bucklin, A., Halsband, C. and Norrbin, F. (2014) Comparative phylogeography and demographic history of five sibling species of *Pseudocalanus* (Copepoda: Calanoida) in the North Atlantic Ocean. *J. Exp. Mar. Bio. Ecol.*, **461**, 479–488.

Altschul, S. F., Madden, T. L., Schäffer, A. A., Zhang, J., Zhang, Z., Miller, W. and Lipman, D. J. (1997) Gapped BLAST and PSI-BLAST: A new generation of protein database search programs. *Nucleic Acids Res.*, **25**, 3389–3402.

Avise, J. C. (2000) *Phylogeography: The History and Formation of Species*. Harvard University Press, Cambridge, MA.

Bailey, J., Rynearson, T. and Durbin, E. G. (2015) Species composition and abundance of copepods in the morphologically cryptic genus *Pseudocalanus* in the Bering Sea. *Deep Sea Res. Part II Top. Stud. Oceanogr.*, doi:10.1016/j.dsr2.2015.01.017.

Beerli, P. (2004) Effect of unsampled populations on the estimation of population sizes and migration rates between sampled populations. *Mol. Ecol.*, **13**, 827–836.

Beerli, P. (2006) Comparison of Bayesian and maximum-likelihood inference of population genetic parameters. *Bioinformatics*, **22**, 341–345.

Beerli, P. (2012) *Migrate Documentation Version 3.2.1*. Florida State University, Tallahasee. FL, p. 119.

Beerli, P. and Felsenstein, J. (2001) Maximum likelihood estimation of a migration matrix and effective population sizes in n subpopulations by using a coalescent approach. *Proc. Natl. Acad. Sci. USA*, **98**, 4563–4568.

Blanco-Bercial, L., Álvarez-Marqués, F. and Bucklin, A. (2011) Comparative phylogeography and connectivity of sibling species of the marine copepod *Clausocalanus* (Calanoida). *J. Exp. Mar. Bio. Ecol.*, **404**, 108–115.

Brito, P. H. and Edwards, S. V. (2009) Multilocus phylogeography and phylogenetics using sequence-based markers. *Genetica*, **135**, 439–455.

Bucklin, A. (2000) Methods for population genetic analysis of zooplankton. In Harris, R., Wiebe, P., Lenz, J., Skjodal, H. R. and Huntley M. (eds.), *ICES Zooplankton Methodology Manual*. Academic Press, London, pp. 533–570.

Bucklin, A., Bentley, A. M. and Franzen, S. P. (1998) Distribution and relative abundance of *Pseudocalanus moultoni* and *P. newmani* (Copepoda: Calanoida) on Georges Bank using molecular identification of sibling species. *Mar. Biol.*, **132**, 97–106.

Bucklin, A., Frost, B. W., Bradford-Grieve, J., Allen, L. D. and Copley, N. J. (2003) Molecular systematic and phylogenetic assessment of 34 calanoid copepod species of the Calanidae and Clausocalanidae. *Mar. Biol.*, **142**, 333–343.

Bucklin, A., Frost, B. W. and Kocher, T. D. (1995) Molecular systematics of six *Calanus* and three *Metridia* species (Calanoida: Copepoda). *Mar. Biol.*, **121**, 655–664.

Bucklin, A., Guarnieri, M., McGillicuddy, D. J. and Sean Hill, R. (2001) Spring evolution of *Pseudocalanus* spp. abundance on Georges Bank based on molecular discrimination of *P. moultoni* and *P. newmani*. *Deep. Res. Part II Top. Stud. Oceanogr.*, **48**, 589–608.

Bucklin, A., McGillicuddy, D. J., Jr., Wiebe, P. H. and Davis, C. S. (2015) Habitat usage by the cryptic copepods *Pseudocalanus moultoni* and *P. newmani* on Georges Bank (Northwest Atlantic). *Cont. Shelf Res.*, **111**, 83–94.

Bucklin, A. and Wiebe, P. H. (1998) Low mitochondrial diversity and small effective population sizes of the copepods *Calanus finmarchicus* and *Nannocalanus minor*: Possible impact of climatic variation during recent glaciation. *J. Hered.*, **89**, 383–392.

Cleary, A. C., Durbin, E. G., Rynearson, T. A. and Bailey, J. (2015) Feeding by *Pseudocalanus* copepods in the Bering Sea: trophic linkages and a potential mechanism of niche partitioning. *Deep Sea Res. Part II Top. Stud. Oceanogr.*, doi:10.1016/j.dsr2.2015.04.001.

Coachman, L. K. and Aagard, K. (1988) Transports through Bering Strait: Annual and interannual variability. *J. Geophys. Res.*, **93**, 15515–15539.

Conover, R. J., Herman, A. W., Prinsenberg, S. J. and Harris, L. R. (1986) Distribution of and feeding by the copepod *Pseudocalanus* under fast ice during the arctic spring. *Science*, **232**, 1245–1247.

Corkett, C. J. and McLaren, I. A. (1979) The biology of *Pseudocalanus*. *Adv. Mar. Biol.*, **15**, 1–231.

Costa, K. G., Filho, L. F. S. R., Costa, R. M., Vallinoto, M., Schneider, H. and Sampaio, I. (2014) Genetic variability of *Acartia tonsa* (Crustacea: Copepoda) on the Brazilian coast. *J. Plankton Res.*, **36**, 1419–1422.

Coyle, K. O. and Pinchuk, A. I. (2003) Annual cycle of zooplankton abundance, biomass and production on the northern Gulf of Alaska shelf, October 1997 through October 2000. *Fish. Oceanogr.*, **12**, 327–338.

Danielson, S., Curchitser, E., Hedstrom, K., Weingartner, T. and Stabeno, P. (2011) On ocean and sea ice modes of variability in the Bering Sea. *J. Geophys. Res.*, **116**, 1–24.

Darnis, G., Barber, D. G. and Fortier, L. (2008) Sea ice and the onshore-offshore gradient in pre-winter zooplankton assemblages in southeastern Beaufort Sea. *J. Mar. Syst.*, **74**, 994–1011.

Day, R. H., Weingartner, T. J., Hopcroft, R. R., Aerts, L. A. M., Blanchard, A. L., Gall, A. E., Gallaway, B. J., Hannay, D. E., *et al.* (2013) The offshore northeastern Chukchi Sea, Alaska: a complex high-latitude ecosystem. *Cont. Shelf Res.*, **67**, 147–165.

Erikson, K. (2015) A time series investigation of the cryptic copepods *Pseudocalanus* spp. on the NW Atlantic continental self. Master's Thesis. University of Connecticut, 48 pp.

Ershova, E. A., Hopcroft, R. R. and Kosobokova, K. N. (2015) Inter-annual variability of summer mesozooplankton communities of the western Chukchi Sea: 2004–2012. Polar Biol., 38, 1461–1481.

Excoffier, L. and Lischer, H. E. L. (2010) Arlequin suite ver 3.5: a new series of programs to perform population genetics analyses under Linux and Windows. *Mol. Ecol. Resour.*, **10**, 564–567.

Folmer, O., Black, M., Hoeh, W., Lutz, R. and Vrijenhoek, R. (1994) DNA primers for amplification of mitochondrial cytochrome c oxidase subunit I from diverse metazoan invertebrates. *Mol. Mar. Biol. Biotechnol.*, **3**, 294–299.

Frost, B. W. (1974) *Calanus marshallae*, a new species of Calanoid copepod closely allied to the sibling species *C. finmarchicus* and *C. glacialis*. *Mar. Biol.*, **26**, 77–79.

Frost, B. W. (1989) A taxonomy of the marine calanoid copepod genus *Pseudocalanus*. *Can. J. Zool.*, **67**, 525–551.

Glenn, T. and Schable, N. A. (2005) Isolating microsatellite DNA loci. *Methods Enzymol.*, **395**, 202–222.

Goetze, E. (2003) Cryptic speciation on the high seas; global phylogenetics of the copepod family Eucalanidae. *Proc. R. Soc. Lond. B Biol. Sci.*, **270**, 2321–2331.

Goetze, E. (2005) Global population genetic structure and biogeography of the oceanic copepods *Eucalanus hyalinus* and *E. spinifer*. *Evolution*, **59**, 2378–2398.

Goetze, E. and Ohman, M. D. (2010) Integrated molecular and morphological biogeography of the calanoid copepod family Eucalanidae. *Deep. Res. Part II Top. Stud. Oceanogr.*, **57**, 2110–2129.

Grabbert, S., Renz, J., Hirche, H. J. and Bucklin, A. (2010) Species-specific PCR discrimination of species of the calanoid copepod *Pseudocalanus*, *P. acuspes* and *P. elongatus*, in the Baltic and North Seas. *Hydrobiologia*, **652**, 289–297.

Halverson, M. J., Bélanger, C. and Gay, S. M. (2013) Seasonal transport variations in the straits connecting Prince William Sound to the Gulf of Alaska. *Cont. Shelf Res.*, **63**, 63–78.

Holm, S. (1979) A simple sequentially rejective multiple test procedure. *Scand. J. Stat.*, **6**, 65–70.

Holmborn, T., Goetze, E., Põllupüü, M. and Põllumäe, A. (2011) Genetic species identification and low genetic diversity in *Pseudocalanus acuspes* of the Baltic Sea. *J. Plankton Res.*, **33**, 507–515.

Hopcroft, R. R. and Kosobokova, K. N. (2010) Distribution and egg production of *Pseudocalanus* species in the Chukchi Sea. *Deep. Res. Part II Top. Stud. Oceanogr.*, **57**, 49–56.

Hopcroft, R. R.., Kosobokova, K. N. and Pinchuk, A. I. (2010) Zooplankton community patterns in the Chukchi Sea during summer 2004. *Deep Sea Res. Part II Top. Stud. Oceanogr.*, **57**, 27–39.

Horner, R. and Murphy, D. (1985) Species composition and abundance of zooplankton in the nearshore Beaufort Sea in winter-spring. *Arctic*, **38**, 201–209.

Huang, Y., Liu, G. and Chen, X. (2014) Molecular phylogeography and population genetic structure of the planktonic copepod *Calanus sinicus* Brodsky in the coastal waters of China. *Acta Oceanol. Sin.*, **33**, 74–84.

Knowles, L. and Maddison, W. (2002) Statistical phylogeography. *Mol. Ecol.*, **11**, 2623–2635.

Kortsch, S., Primicerio, R., Fossheim, M., Dolgov, A. V, Aschan, M. and Kortsch, S. (2015) Climate change alters the structure of arctic marine food webs due to poleward shifts of boreal generalists. *Proc. R. Soc. Lond. B Biol. Sci.*, **282**, 1–9.

Lane, P. V. Z., Llinás, L., Smith, S. L. and Pilz, D. (2008) Zooplankton distribution in the western Arctic during summer 2002: hydrographic habitats and implications for food chain dynamics. *J. Mar. Syst.*, **70**, 97–133.

Librado, P. and Rozas, J. (2009) DnaSP v5: a software for comprehensive analysis of DNA polymorphism data. *Bioinformatics*, **25**, 1451–1452.

Llinás, L., Pickart, R. S., Mathis, J. T. and Smith, S. L. (2009) Zooplankton inside an Arctic Ocean cold-core eddy: probable origin and fate. *Deep. Res. Part II Top. Stud. Oceanogr.*, **56**, 1290–1304.

Machida, R. J., Miya, M. U., Nishida, M. and Nishida, S. (2006) Molecular phylogeny and evolution of the pelagic copepod genus *Neocalanus* (Crustacea: Copepoda). *Mar. Biol.*, **148**, 1071–1079.

Matsuno, K., Yamaguchi, A., Hirawake, T. and Imai, I. (2011) Year- to-year changes of the mesozooplankton community in the Chukchi Sea during summers of 1991, 1992 and 2007, 2008. *Polar. Biol.*, **34**, 1349–1360.

McGillicuddy, D. J. and Bucklin, A. (2002) Intermingling of two *Pseudocalanus* species on Georges Bank. *J. Mar. Res.*, **60**, 583–604.

Milligan, P. J., Stahl, E. A., Schizas, N. V. and Turner, J. T. (2011) Phylogeography of the copepod *Acartia hudsonica* in estuaries of the northeastern United States. *Hydrobiologia*, **666**, 155–165.

Napp, J. M., Hopcroft, R. R., Baier, C. T. and Clarke, C. (2005) Distribution and species-specific egg production of *Pseudocalanus* in the Gulf of Alaska. *J. Plankton Res.*, **27**, 415–426.

Nelson, R. J., Carmack, E. C., Mclaughlin, F. A. and Cooper, G. A. (2009) Penetration of Pacific zooplankton into the western Arctic Ocean tracked with molecular population genetics. *Mar. Ecol. Prog. Ser.*, **381**, 129–138.

Nuwer, M. L., Frost, B. W. and Armburst, E. V. (2008) Population structure of the planktonic copepod *Calanus pacificus* in the North Pacific Ocean. *Mar. Biol.*, **156**, 107–115.

Peijnenburg, K. T. C. A. and Goetze, E. (2013) High evolutionary potential of marine zooplankton. *Ecol. Evol.*, **3**, 2765–2783.

Pickart, R. S. (2004) Shelfbreak circulation in the Alaskan Beaufort Sea: mean structure and variability. *J. Geophys. Res.*, **109**, C04024.

Poulet, S. A. (1973) Grazing of *Pseudocalanus minutus* on naturally occurring particulate matter. *Limnol. Oceanogr.*, **18**, 564–573.

Provan, J., Beatty, G. E., Keating, S. L., Maggs, C. A. and Savidge, G. (2009) High dispersal potential has maintained long-term population stability in the North Atlantic copepod *Calanus finmarchicus*. *Proc. R. Soc. Lond. B Biol. Sci.*, **276**, 301–307.

Questel, J. M., Clarke, C. and Hopcroft, R. R. (2013) Seasonal and interannual variation in the planktonic communities of the northeastern Chukchi Sea during the summer and early fall. *Cont. Shelf Res.*, **67**, 23–41.

Sancetta, C. (1983) Effect of Pleistocene glaciation upon oceanographic characteristics of the North Pacific Ocean and Bering Sea. *Deep Sea Res.*, **30**, 851–869.

Sevigny, J., Mclaren, I. and Frost, B. (1989) Discrimination among and variation within species of *Pseudocalanus* based on the GPI locus. *Mar. Biol.*, **327**, 321–327.

Smoot, C. A. (2015) Contemporary mesozooplankton communities of the Beaufort Sea. Master's Thesis. University of Alaska Fairbanks, 96 pp.

Stabeno, P. J., Bond, N. A., Hermann, A. J., Kachel, N. B., Mordy, C. W. and Overland, J. E. (2004) Meteorology and oceanography of the Northern Gulf of Alaska. *Cont. Shelf Res.*, **24**, 859–897.

Stabeno, P. J., Reed, R. K. and Schumacher, J. D. (1995) The Alaska Coastal Current: continuity of transport and forcing. *J. Geophys. Res.*, **100**, 2477.

Tamura, K. (1992) Estimation of the number of nucleotide substitutions when there are strong transition-transversion and G+C-content biases. *Mol. Biol. Evol.*, **9**, 678–687.

Tamura, K., Stecher, G., Peterson, D., Filipski, A. and Kumar, S. (2013) MEGA6: molecular evolutionary genetics analysis version 6.0. *Mol. Biol. Evol.*, **30**, 2725–2729.

Thompson, J. D., Higgins, D. G. and Gibson, T. J. (1994) CLUSTAL W: improving the sensitivity of progressive multiple sequence alignment through sequence weighting, position-specific gap penalties and weight matrix choice. *Nucleic Acids Res.*, **22**, 4673–4680.

Unal, E. and Bucklin, A. (2010) Basin-scale population genetic structure of the planktonic copepod *Calanus finmarchicus* in the North Atlantic Ocean. *Prog. Oceanogr.*, **87**, 175–185.

Unal, E., Frost, B. W., Armbrust, V. and Kideys, A. E. (2006) Phylogeography of *Calanus helgolandicus* and the Black Sea copepod Calanus euxinus, with notes on *Pseudocalanus elongatus* (Copepoda, Calanoida). *Deep Sea Res. Part II Top. Stud. Oceanogr.*, 53, 1961–1975.

Viñas, M. D., Blanco-Bercial, L., Bucklin, A., Verheye, H., Bersano, J. G. F. and Ceballos, S. (2015) Phylogeography of the copepod *Calanoides carinatus s.l.* (Krøyer) reveals cryptic species and delimits *C. carinatus s.s.* distribution in SW Atlantic Ocean. *J. Exp. Mar. Biol. Ecol.*, **468**, 97–104.

Weingartner, T. J., Cavalieri, D. J., Aagaard, K. and Sasaki, Y. (1998) Circulation, dense water formation, and outflow on the northeast Chukchi Shelf. *J. Geophys. Res.*, **103**, 7647.

Weingartner, T. J., Danielson, S. L. and Royer, T. C. (2005) Freshwater variability and predictability in the Alaska Coastal Current. *Deep Sea Res. Part II Top. Stud. Oceanogr.*, **52**, 169–191.

Weingartner, T. J., Dobbins, E., Danielson, S., Winsor, P., Potter, R. and Statscewich, H. (2013) Hydrographic variability over the northeastern Chukchi Sea shelf in summer-fall 2008–2010. *Cont. Shelf Res.*, **67**, 5–22.

Weingartner, T. J., Danielson, S., Dobbins, E. and Potter, R. (2014) *Physical Oceanographic Measurements in the Northeastern Chukchi Sea: 2013*. University of Alaska Fairbanks, Fairbanks, AK, p. 64.

Woodgate, R. A., Aagaard, K. and Weingartner, T. J. (2005) A year in the physical oceanography of the Chukchi Sea: moored measurements from autumn 1990–1991. *Deep Sea Res. Part II Top. Stud. Oceanogr.*, **52**, 3116–3149.

Yebra, L., Bonnet, D., Harris, R. P., Lindeque, P. K. and Peijnenburg, K. T. C. A. (2011) Barriers in the pelagic: population structuring of *Calanus helgolandicus* and *C. euxinus* in European waters. *Mar. Ecol. Prog. Ser.*, **428**, 135–149.

Appendix 2.1 Permission from co-author Leocadio-Blanco Bercial to include manuscript in the dissertation.

Jennifer Questel <jmquestel@alaska.edu>

Permission to use manuscript in my disseration

2 messages

Jennifer Questel <jmquestel@alaska.edu> Tue, Apr 26, 2016 at 6:19 PM
To: Leocadio Blanco-Bercial <leocadio@bios.edu>

Hi Leo,

You are co-authored on the manuscript "Phylogeography and population connectivity of the Pseudocalanus (Copepoda: Calanoida) species complex in the eastern North Pacific Ocean and the Pacific Arctic Region" that I will be including as a chapter in my dissertation to fulfill the requirements of a PhD in Oceanography from the University of Alaska Fairbanks.

Please respond to this email indicating whether you grant permission to include this paper.

Thanks,
Jenn

--
Jennifer Questel
Doctoral Candidate
Biological Oceanography
University of Alaska Fairbanks

Leocadio Blanco-Bercial <Leocadio@bios.edu> Wed, Apr 27, 2016 at 3:49 AM
To: Jennifer Questel <jmquestel@alaska.edu>

Hi Jen,

I am delighted to grant you permission to include this paper in your dissertation.

Best,

Leo

CHAPTER 3: COMMUNITY PRODUCTION IN THE NORTHEASTERN CHUKCHI SEA AND ITS RELATIONSHIP TO PHYTOPLANKTON AND MESOZOOPLANKTON BIOMASS, 2010-2011

3.1 Abstract

The Chukchi Sea is one of the most productive continental shelves in the ocean and plays a vital role in the transport of nutrients and plankton from the North Pacific into the western Arctic Ocean and subsequently the global carbon cycle. The traditional understanding of the Chukchi Sea has been based around the assumption that the retreat of sea-ice in early June allows for the rapid utilization of inorganic nutrients and commensurately high rates of primary production, of which roughly 25% is consumed by pelagic grazers, with the remaining 75% being exported to the benthos or advected off the shelf into the deep Canada Basin. However, there has never been a comprehensive assessment of the biogeochemistry of the region later in the open water season when inorganic nutrients are presumed to be exhausted and rates of productivity at or near zero. To address this gap in our understanding, we sampled the northeastern Chukchi Sea during the 2010 and 2011 open-water seasons where the data provided a unique opportunity to relate seasonal production to concurrent changes in plankton biomass as the two years were distinctly different in both physical and biogeochemical characteristics. Late summer (August to September) net community production (NCP) rates were much lower on average in 2010 (5 mmol C m^{-2} d^{-1}) compared to 2011 (21 mmol C m^{-2} d^{-1}). However, the planktonic system remained net autotrophic for both years even after the initial high-magnitude phytoplankton bloom that occurred earlier in the growing season. NCP rates in Burger during autumn (September to October) of 2010 were negative (–2 mmol C m^{-2} d^{-1}), suggesting the system had shifted to being net heterotrophic. However, concentrations of DIC had decreased while nDIC concentrations simultaneously increased, indicating productivity was occurring faster than inorganic carbon could be added back into the system. Correlations of NCP to concurrent changes in biological parameters (chlorophyll-a and mesozooplankton biomass) showed no statistically significant relationships, insinuating that NCP was uncoupled or poorly coupled to planktonic processes. However, for both years, station-based estimates of NCP appeared to be highly variable and showed strong evidence of late season primary production at

some locations. This suggests that physical factors such as advection, shifting water mass boundaries, the uptake of atmospheric CO_2, and biological processes (i.e., benthic respiration and remineralization), are all highly influential within the northeastern Chukchi Sea during the late summer and early autumn months. As the biogeochemical character of the Chukchi region responds to changes in climate and sea-ice coverage, it will be critical to understand the relative importance of these multiple factors in altering the timing, extent, and fate of carbon production.

3.2 Introduction

The Chukchi Sea is a broad and shallow (<50 m) marginal sea of the western Arctic Ocean that lies between the Bering Sea and the deeper Amerasian Basin. It is a gateway or inflow shelf that provides the only connection between the Pacific and Arctic Oceans. On a seasonal basis, a complex mixture of Pacific-derived water masses enter the Chukchi Sea through the Bering Strait with an estimated 1–1.2 Sv average transport (e.g., Danielson et al., 2014), with most of the mass transport occurring during the open-water season (Coachman and Aagard, 1988; Woodgate et al., 2012; Danielson et al., 2014). Large quantities of Pacific-derived carbon, nutrients, phytoplankton, and zooplankton are transported into the region within three distinct water masses (i.e., Alaska Coastal Water, Bering Shelf Water, and Anadyr Water), each with distinct assemblages and qualities of zooplankton (Springer et al., 1989; Hopcroft et al., 2010; Ershova et al., 2015a). It has been estimated that 1.8×10^{12} g C of Bering Sea zooplankton (Springer et al., 1989), and more recently that $\sim 0.8 - 1.0 \times 10^{15}$ g of inorganic carbon (Bates and Mathis, 2009), are advected into the region annually, making it a significant component of the regional and global carbon cycles.

The Chukchi Sea is heavily influenced by sea-ice that covers more than 90% of the region for most of the year. Patterns of sea-ice melt and retreat vary greatly on a yearly basis, but typically melt-pools and leads begin to open up by early-mid May (Weingartner et al., 2013) followed by a rapid bloom of phytoplankton. The combination of the inflow of nutrient-rich Pacific waters (Codispoti et al., 2005) and sea-ice retreat, exposing surface waters to solar radiation, drive the high rates of pelagic primary productivity compared to the surrounding seas that are more nutrient limited (Cota et al., 1996; Hill and Cota, 2005). Rates of primary production in the Chukchi Sea shelf average > 300 g C m^{-2} y^{-1} (Hansell et al., 1993; Bates et al., 2005a; Hill and Cota, 2005), with an initial bloom followed by lower production for the remainder of the summer (Cota et al., 1996; Bates et al., 2005a; Hill and Cota, 2005; Mathis et al., 2009). Much of the organic matter produced during the initial phytoplankton bloom is exported to the sea floor where it sustains large quantities of macro- and megafaunal biomass (Grebmeier et al., 1988; Blanchard et al., 2013a, 2013b; Schonberg et al., 2014). However, the high rates of primary production also support large quantities of zooplankton biomass that fuel

higher trophic levels such as planktivorous fishes, seabirds (Piatt and Springer, 2003; Gall et al., 2013), and whales. Additionally, some of the organic carbon from the Bering Sea is entrained in Pacific winter water flowing along the bottom of the Chukchi Sea and is advected northward into the deep Arctic basin (Grebmeier et al., 2006; Mathis et al., 2007).

The inorganic carbon cycle in the Arctic Ocean is influenced by a multitude of abiotic and biotic factors that vary throughout the year due to regional and large-scale climate conditions. Physical processes such as the influx of atmospheric CO_2 to surface waters through the semi-permeable sea-ice or during sea-ice melt can add carbon to surface waters. The biological pump, specifically phytoplankton primary production, draws down carbon accumulating it as planktonic biomass. Some portion of this production is exported to the sea floor (or deeper parts of the ocean) via sedimentation, or becomes remineralized into CO_2 through heterotrophic processes, returning inorganic carbon back into the system (Bates et al., 2005a, 2005b; Mathis et al., 2007; Bates and Mathis, 2009; Dunton et al., 2014). The rate of phytoplankton production is regulated by the availability of both light (radiation) and nutrients in the euphotic zone. Phytoplankton biomass is also controlled by zooplankton, both quantitatively and qualitatively, through grazing and the subsequent regeneration of nutrients (Sterner, 1990), which occurs via sloppy feeding, excretion, and fecal pellet production (Ikeda, 1977; Banse, 1995; Saba et al., 2009).

In polar regions, the flow of production through pelagic food webs is seasonally pulsed and is highly governed by patterns in ice retreat and circulation, in addition to the nutrient and light availability. In particular, increasing light availability during spring promotes the uptake of CO_2 by phytoplankton and ice algae (Reigstad et al., 2002; Matrai et al., 2007). The high rate of primary productivity in the Chukchi Sea consequently leads to a significant drawdown of inorganic carbon in surface waters, reducing the partial pressure of carbon dioxide (pCO_2) to as low as 100 μatm. With atmospheric pCO_2 now well over 400 μatm the uptake of CO_2 from the atmosphere is extremely high, causing the entire Chukchi Sea to become a net sink for CO_2 during the open water period (Bates and Mathis, 2009; Evans et al., 2015). As rates of seasonal ice loss in the Chukchi continue to increase, understanding how zooplankton will respond to both physical and biological constrains will become essential in accurately predicting how energy flow will be altered through Arctic food webs.

Examining the rate of net community production (NCP) is one means of tracking change in overall ecosystem processes. Net changes in inorganic carbon inventories, as a result of air-sea interactions removing carbon from the atmosphere or biological processes drawing down carbon in surface layers of the ocean, can be quantified by estimating NCP. NCP can reach as high as 1500 mg C^{-2} d^{-1} along the Chukchi Sea shelf break (Mathis et al., 2009). Variability in sea-ice retreat not only influences rates of NCP by determining the magnitude of air-sea gas exchange, but it also greatly impacts the dynamics of primary production (Hill and Cota, 2005) and structuring of zooplankton communities on the Chukchi Sea shelf (Questel et al., 2013). Despite the conceptual relationship between NCP and an ecosystem's biological communities, no attempts have been made to specifically look for correlations between them.

This study seeks to better elucidate the biogeochemical controls on herbivorous mesozooplankton at high spatial resolution during the open water season in the northeastern Chukchi Sea. Repeat measurements of carbon chemistry, nutrients, chlorophyll-a, and mesozooplankton biomass from a fixed-station sampling design during 2010 and 2011 provides the unique opportunity to relate a portion of the seasonal production to concurrent changes in plankton biomass. Specifically, we seek to understand the role mesozooplankton play as part of the carbon system for the northeastern Chukchi Sea during the latter half of the open-water season, and whether the zooplankton biomass observed at that time can be sustained by local production.

3.3 Methods

3.3.1 Sample collection

Physical, chemical, and biological measurements were made as part of the seven-year Chukchi Sea Environmental Studies Program (CSESP) (Day et al., 2013). This study focused on a sub-set of the larger program with measurements collected during the 2010 and 2011 field seasons when repeat carbon measurements were made. Multiple cruises per year occurred during the open water season in three 900-square nautical mile (nm) grids designated as Burger, Klondike, and Statoil (Fig. 3.1). Physical, nutrient, and biological measurements were collected at 25 fixed stations within Burger and Klondike, and at 22 fixed stations within Statoil, with

mesozooplankton samples processed at every other station. Carbon samples were collected at stations to coincide with the mesozooplankton analysis. All three study areas were sampled twice per season with the first cruise occurring in late summer (hereafter "August"), the second cruise occurring in early autumn for 2010 (hereafter "September") and 2011 (hereafter "Sept/Oct"). A third cruise during 2010 occurring in late autumn (hereafter "October") in which only the Burger study site was reoccupied. Average bottom depth over the three grids was ~40 m.

Water column profiles were recorded with a CTD rosette consisting of a Seabird SBE25/SBE55 CTD (Weingartner et al., 2013) and fluorometer (Wetlabs) deployed at fixed oceanographic stations within Burger, Klondike, and Statoil. Dissolved inorganic carbon and total alkalinity (DIC/TA) samples were collected at the surface, 5 m, 10 m, 20 m, 30 m, and near bottom during the 2010 season while surface, 20 m, 30 m, and near bottom samples were collected during the 2011 field season. DIC/TA seawater samples were drawn from 4-L Niskin bottles into pre-cleaned 300 mL borosilicate bottles treated with mercuric chloride ($HgCl_2$) to halt biological activity (Mathis, 2012; Mathis and Questel, 2013). Nutrient and chlorophyll-a samples were taken from the same Niskin bottles as DIC/TA, filtered, and frozen immediately for post-cruise analysis (Hopcroft et al., 2013; Questel et al., 2013). Smaller mesozooplankton samples were collected by paired 150-μm-mesh ring nets of 60-cm diameter hauled vertically from within 3 m of the bottom to the surface at 0.5 m s^{-1} while the ship remained stationary. To target larger, more mobile mesozooplankton, a set of 60-cm-diameter 505-μm mesh Bongo nets were deployed in a double oblique tow while the ship moved at an average speed of 2 kt (~1 m sec^{-1}). The volume of water filtered was measured by Sea-Gear one-way flowmeters for the 150-μm-mesh nets and by General Oceanics flowmeters for the 505-μm-mesh nets. Samples were preserved in 10% formalin buffered with sodium hexamethaphosphate.

3.3.2 Analytical methods

Seawater samples were analyzed for DIC and TA using a highly precise and accurate gas extraction/coulometric detection system (Bates, 2001). The analytical system consists of a VINDTA 3C (Versatile Instrument for the Detection of Total Alkalinity; http://www.marianda.com) coupled to a CO_2 coulometer (model 5012; UIC Coulometrics). Total Alkalinity samples were also determined by potentiometric titration using VINDTA 3C. Routine

analysis of Certified Reference Materials (CRMs, provided by A.G. Dickson, Scripps Institute of Oceanography) ensured that the accuracy of the DIC and TA measurements were within 0.05% (~1.5 μmol kg^{-1}) and stable over time.

Direct rates of NCP were calculated at each fixed station in Klondike, Burger, and Statoil through measurements of the net seasonal consumption of DIC (Williams, 1993) integrated from the surface to 30 m. DIC measurements were normalized (nDIC) to a deep-water reference salinity (S = 35) (Mathis et al., 2009; Cross et al., 2012) to eliminate changes due to sea-ice melt, precipitation, and riverine inputs. Adjustments for the formation and dissolution of calcium carbonate ($CaCO_3$) on DIC concentrations (Mathis et al., 2010) are accounted for by measuring seasonal changes in TA (Codispoti et al., 1986; Lee, 2001), where relatively half of the seasonal changes in TA and nitrate affect DIC concentrations, such that:

$$\Delta nDIC_{Alk} = \left(\Delta Alk_{(0-30)} + \Delta NO_{3(0-30)}\right) * 0.5 \quad (1)$$

Thus, estimates of NCP are calculated where spatial and temporal distributions of nDIC reflects changes due to NCP (Cross et al., 2012):

$$NCP_{nDIC} = \Delta nDIC_{(0-30)} - \Delta nDIC_{Alk} \quad (2)$$

The rate of NCP is expressed as mg C m^{-2} d^{-1}, with an error of ~24 – 40 mg C m^{-2} d^{-1} due to imprecision and inaccuracy of ~1 μmol kg^{-1} associated with DIC analyses (Bates et al., 2005a).

NCP calculations assume the same water is being measured over time, and do not account for the lateral transport of water masses. Unfortunately, currents over most of the CSESP study area are generally eastward in summer and fall at speeds of ~5 cm s^{-1} (Weingartner et al., 2013). Sampling between cruises within the 30 x 30 nm^2 study areas occurred on an average of 25 days, but regrettably, advection cannot be reconciled. It is also important to note that sampling occurred after the termination of the initial phytoplankton bloom that had exhausted nitrate in surface waters, creating additional errors in our NCP calculations. Despite these caveats, we still believe this analysis provides valuable insight because it considers a portion of the productivity of the system during the height of the open-water season.

In-situ fluorescence was converted to chlorophyll-a concentration by empirically calibrating against extracted chlorophyll-a from Niskin bottle collections. Zooplankton samples were processed microscopically to the highest taxonomic level possible. Biomass, as ash-free dry weight (DW), was calculated for each individual zooplankton based on species-specific length-weight relationships, or from relationships of a morphologically similar species to mero- or holozooplankton (Hopcroft et al., 2010, 2013; Questel et al., 2013).

Mesozooplankton biomass data were partitioned into categories characterizing the herbivorous plankton community, including small- and large-bodied copepods, meroplankton, larvaceans, euphausiids, and pteropods. The smaller-bodied copepods, meroplankton, and larvacean categories are best represented in the smaller 150-μm-mesh net due to their efficiency at capturing the smaller size spectrum within the zooplankton assemblages. Likewise, the large-bodied copepods and euphausiid categories are best presented in the 505-μm-mesh net, which capture the larger size spectrum of the zooplankton assemblages. The pteropod category is encompassed by both the 150- and 505-μm-mesh nets where individuals $\leq$ 600 μm in length were taken from the smaller mesh net and individuals $\geq$ 600 μm in length were taken from the larger mesh net. To eliminate overlap between the two net types, the copepod categories were size fractionated at 1400 μm prosome length (Hopcroft et al., 2001), where individuals < 1400 μm were included in the small-bodied copepod category and individuals >1400 μm were included in the large-bodied copepod category. These groups have significantly different rates of feeding and growth making simple pooling of their biomass inappropriate for the purposes of estimating NCP.

3.3.3 Estimates of seasonal changes

Monthly changes were determined for integrated *in-situ* fluorescence (converted to chlorophyll-a) and mesozooplankton biomass by analyzing the differences between the September (2010) or Sept/Oct (2011) cruise from the August cruise. In 2010 a third occupation of the Burger study site occurred in late autumn, enabling differences between the October and September cruises to be analyzed. Through this approach, positive values indicate a parameter increased between observations, while negative values indicate a net loss of that particular parameter.

3.3.4 Statistical analysis

To determine the significance of change, a two-tailed t-test was performed on the means of nDIC, chlorophyll-a, and herbivorous mesozooplankton biomass from the preceding cruise. An *a priori* three-way analysis of variance (ANOVA) test was conducted with the statistical package R (V3.2.3) where the data were transformed (4^{th} root) to test for significant interactions among site (Klondike, Burger, and Statoil), year (2010 and 2011), and cruise (August, September, and Sept/Oct). P-values ≤ 0.05 were considered significantly different. Finally, to measure the strength and direction of association between NCP and changes in chlorophyll-a and herbivorous meozooplankton biomass, a Spearman rank-order correlation coefficient nonparametric test was conducted in R (V3.2.3).

3.3.5 Estimates of carbon production

As a supplement and cross-check to the NCP approach, a simple carbon flow box-model for the Klondike, Burger, and Statoil grids was developed to understand the energetic demand exerted by the mesozooplankton communities. This approach determined whether adequate amounts of carbon were produced from primary production during the late summer and early autumn to support growth and reproduction. Mesozooplankton biomass was converted from mg DW m^{-3} to g C m^{-3} by assuming a carbon content 40% that of DW (Båmstedt et al., 1999). A growth efficiency of 33% (Båmstedt et al., 1999; Kiørboe et al., 1985; Peterson, 1988) was estimated for copepods, assuming an average growth rate of 10% per day at 5 °C (Liu and Hopcroft, 2006, 2007, 2008). Copepods were used as a proxy for growth in this model due to the more robust data sets on growth measurements at these colder Arctic temperatures than for the other taxonomic groups. To estimate the amount of carbon produced per day by phytoplankton, integrated standing stocks were converted to g C m^{-3} using a 40:1 carbon to chlorophyll-*a* ratio (the lowest rate possible) (Sathyendranath et al., 2009) and a growth rate of a one-third-doubling per day based on biomass-specific hourly production for the Chukchi Sea (Hill and Cota, 2005) that was assumed to occur over a 12-hour period.

3.4 Results

3.4.1 Water mass distribution

At the start of sampling in August of 2010 there were multiple water masses present over the CSESP study area. Cool (-1–3 ˚C) and moderately saline (30–32.8) Bering Summer Water (BSW) inundated much of the Klondike and Burger study areas with traces of warm and fresh (3–8 ˚C and ~30) Alaska Coastal Water (ACW), and remnants of late season melt water (LSWM; -1–8 ˚C and 27–30; Fig. 3.2). Differences in water masses between the two study areas came from the presence of a cold and saline (-1–2 ˚C and 32.5–33 PSU) pool of Winter Water (WW) in Burger. The Statoil study area also harbored this WW yet surface waters were characteristic of a fresh and moderately warm (-1–8 ˚C and 27–30 PSU) Late Season Melt Water (LSMW) water mass, indicative of the delayed ice melt over the region. During the September cruise ACW and BSW became more prominent throughout the CSESP study area, displacing the LSMW pools. Burger and Statoil continued to harbor pools of cold WW which remained in Burger throughout the October cruise. A depression in water mass temperatures of the ACW and LSMW was also observed within Burger from September to October.

By the time of sampling in August of 2011, the entire study region was devoid of the LSMW water mass that was present in August of 2010 (Fig. 3.2). The most prominent water masses over the CSESP study area were ACW and BSW, with ACW more prevalent in Klondike compared to Burger and Statoil. At the time of sampling during the Sept/Oct cruise, ACW had become more widespread and relatively fresher and cooler compared to the August occupation whereas BSW remained the more predominant water mass within the Burger and Statoil study areas. Overall, salinity and temperature were less variable from August to October during the 2011 field season when compared to 2010. There was also no indication of the cold pool of WW observed in the 2010 sampling season for Burger, Klondike, or Statoil.

3.4.2 Seasonality of DIC

Throughout the entirety of the 2010 season, there was a pronounced DIC concentration gradient at 20 m depth associated with the pycnocline, with DIC low in surface waters above the pycnocline and increasing with depth (Fig. 3.3). In August, DIC concentrations were still well

below the typical spring (pre-bloom) values (Bates et al., 2005a; Mathis et al., 2007), but concentrations were beginning to rebound from their annual minimums as surface waters absorbed CO_2 from the atmosphere. DIC averaged over the entire water column ranged from 1999–2017 μmol kg^{-1} in our 3 study sites (Table 3.1) compared to pre-bloom conditions of ~2236 μmol kg^{-1} (Bates et al., 2005a). From August to September, significant increases in DIC were observed for all study sites, with the largest gain of 71 μmol kg^{-1} within Statoil (Table 3.2). As the season progressed into October, Burger experienced a significant drawdown in DIC of 18 μmol kg^{-1} where average concentrations ranged from ~1900 μmol kg^{-1} in surface waters to ~2150 μmol kg^{-1} near bottom (Fig. 3.3).

During August and Sept/Oct of 2011, DIC concentrations remained fairly uniform over the entire water column, with no clear evidence of a two-layered system that was observed in 2010. Average DIC concentrations throughout the water column during the August cruise were essentially equal for all 3 study sites (2033–2034 μmol kg^{-1}, Table 3.1). Increases of DIC from the August to Sept/Oct cruise was observed for the entire study region throughout the water column, with statistically significant changes detected for Klondike (Table 3.2, Fig. 3.3).

Concentrations of DIC experienced statistically significant variance between the 2010 and 2011 study seasons as well as when compared between cruises (ANOVA, Table 3.3). However, variance in DIC between years was non-significant when DIC concentrations were compared among Burger, Klondike, and Statoil. This is in agreement with earlier statements where large differences in DIC were not observed within a season among each study site.

3.4.3 Estimates of late season NCP

Decreases in integrated nDIC values from August to September of 2010 averaged 195 μmol kg^{-1} over the entire study region. The largest drawdown of nDIC occurred within the Burger study area with a decrease of 246 μmol kg^{-1} (Table 3.4). Comparatively similar decreases were observed between Klondike and Statoil of 189 and 150 μmol kg^{-1}, respectively. These decreases in nDIC imply that there was greater net heterotrophy within the Burger study area. However, net autotrophy occurred within Burger by October with an increase in nDIC of 31 μmol kg^{-1}.

Decreases in nDIC resulted in extremely low, yet positive, average rates of NCP (2 mmol C m^{-2} d^{-1}) within Burger and Klondike, with greater average rates of NCP (12 mmol C m^{-2} d^{-1}) observed within Statoil (Table 3.4). Spatially, negative rates of NCP (i.e., heterotrophy) were observed in the mid-sector of the CSESP study area in early autumn, where positive NCP rates (i.e., autotrophy) were apparent in the more southern and northern regions (Fig. 3.4). Between September and October Burger experienced an average NCP rate of –2 mmol C m^{-2} d^{-1}.

Compared to the 2010 season, 2011 experienced greater rates of NCP over the CSESP region, in concert with substantial increases of integrated nDIC from August into late September and early October (Table 3.4, Fig. 3.4). This implied that the system, on a whole, was characteristically more autotrophic in 2011 than 2010. NCP rates were highest within Klondike (28 mmol C m^{-2} d^{-1}), moderate within Statoil (20 mmol C m^{-2} d^{-1}), and lowest within Burger (17 mmol C m^{-2} d^{-1}, Table 3.4).

3.4.4 In situ Chlorophyll-a

Low *in situ* chlorophyll-a concentrations were found throughout the CSESP study area in August for both the 2010 and 2011 field seasons, indicating that the initial phytoplankton bloom had already occurred prior to sampling. During August of 2010, chlorophyll-a concentrations over the study area in August averaged 0.61 mg m^{-3} and 0.54 mg m^{-3} in September (Table 3.1). Compared to 2010, 2011 had higher concentrations of chlorophyll-a, averaging 0.96 mg m^{-3} in August and 0.82 mg m^{-3} in late September/early October. This pattern explained most of the variance observed within chlorophyll-a, with significant interaction between cruises or between years (Table 3.3). Interaction between site and year also explained a lesser, but significant, portion of the observed variance. Overall, there were no significant changes in chlorophyll-a concentrations between cruises for either 2010 or 2011 (Table 3.2).

3.4.5 Herbivorous zooplankton biomass

The majority of herbivorous mesozooplankton biomass for the northeastern Chukchi Sea during the late summer and early autumn of 2010 and 2011 consisted primarily of large- and small-bodied copepods (Table 3.1, Fig. 3.5). The meroplankton, larvaceans, euphausiids, and pteropod categories contributed much lower amounts of biomass to the system than the

copepods, with the exception of meroplankton in Klondike and Burger during the 2010 September cruise. For the most part, copepod biomass was greater in 2011 than in 2010, with large-bodied copepods averaging 13 mg DW m^{-3} in August, 10 mg DW m^{-3} in September, and 11 mg DW m^{-3} in October over the study region in 2010 compared to 19 mg DW m^{-3} in August and 8 mg DW m^{-3} in Sept/Oct of 2011. For the small-bodied copepods the region had similar biomass in August of 2011 and 2010 (7 and 6 mg DW m^{-3}, respectively), yet by September small-bodied copepod biomass was higher in 2010 than in 2011 (11 versus 3 mg DW m^{-3}, respectively). However, 2011 experienced a greater percent loss of copepod biomass for both categories, where roughly 13% of the large-bodied copepod biomass was lost from the August to September cruise in 2010 compared to a ~41% loss in biomass during 2011. For small-bodied copepods a 40% loss in biomass was observed between the August and Sept/Oct cruise, whereas there was about a 30% increase in biomass from August to September in 2010.

For the non-copepod mesozooplankton groups, 2011 experienced a decrease in biomass over the study region between cruises for all groups with the exception of euphausiids which gained biomass from August to late September/early October. However, all increases within the euphausiid category for both years were non-significant (Table 3.2). Within the other groups, significant changes in biomass between the cruises were variable within Klondike, Burger, and Statoil. In comparison, 2010 mainly experienced increases in biomass, with some significant changes of mean biomass from August to September, for all non-copepod categories over the entire study region.

The factors influencing the amount of variance observed among herbivorous mesozooplankton biomass varied between categories. Overall, spatial variance was significant for all groups except the pteropods, indicating that sample site had an important influence on biomass (Table 3.3). When sampling year was combined with study site, this interaction then became significant for all zooplankton categories, including pteropods, denoting considerable differences in biomass for each group between years as well as spatially over the study region. The largest amount of variance was explained by the year and cruise interaction for small-bodied copepods and pteropods, where sampling within Klondike, Burger, and Statoil over each season was substantially different between years. Likewise, the year in which meroplankton and euphausiids were present gave rise to the greatest amount of variance. Finally, the greatest

amount of variance within the large-bodied copepod biomass was explained by relatively equal contributions from study site and cruise, as well as interactions between study site and year.

3.5 Discussion

Rates of NCP varied considerably between the two CSESP field seasons, with 2011 exhibiting higher rates of NCP than 2010. Nevertheless, we observed a substantial amount of production occurring during the late summer and early autumn months when the region was considered to operate under oligotrophic conditions. Surprisingly, NCP did not significantly correlate to the matching changes in mesozooplankton biomass, either because of differences in temporal scales or, as our box model suggests, because the energetic requirements of the mesozooplankton are not highly limited by late season production during both field seasons. The pattern and magnitude of production within and between years are a reflection of the characteristically complex physical and biological processes occurring within this highly dynamic shelf ecosystem. We expand upon these processes within the following sections.

3.5.1 Hydrographic controls on dissolved inorganic carbon

At the onset of each sampling year, sea-ice concentrations covered the entire CSESP study area followed by rapid changes in the pattern of sea-ice retreat and concentration, leading to markedly different structuring of the water column for 2010 and 2011 (Weingartner et al., 2013, 2012). Northeastern winds in early May of 2010 stimulated leads along the western Alaskan coast, creating a relatively ice-free region by mid-June (Weingartner et al., 2013). However, ice persisted over the northern region of the CSESP study area, completely covering Statoil until mid-August. The delayed ice retreat lead to a pool of cold and fresh melt water (LSMW) in surface waters that overlaid colder and saltier pools of winter-formed water (WW), creating a strongly stratified two-layer water column that persisted throughout the sampling period. Patterns in DIC concentrations mimicked this two-layered system, resulting in higher concentrations below the 20 m pycnocline and lower within surface waters. The low DIC concentration in surface waters is due to a combination of primary production that draws down DIC as well as a dilution signal from the remaining pool of LSMW that is characteristically low in DIC with respect to pre-bloom conditions (Bates et al., 2005a). Increased DIC concentrations

at depth are likely a product of biological processes (i.e., remineralization and benthic respiration) adding DIC back into the system. This two-layered water column DIC pattern persisted throughout the sampling timeframe as a result of strongly stratified waters inhibiting bottom water to mix with surface waters.

In comparison, ice retreated faster in 2011 than in 2010 (Weingartner et al., 2012), leaving the Chukchi Sea shelf completely ice-free by early July. The longer open-water conditions increased the amount of solar heating while strong winds created a well-mixed but weakly stratified water column that was driven by temperature compared to salinity-driven stratification in 2010. This well mixed water column aided in the fairly uniform DIC concentrations observed throughout the system from August to October of 2011. DIC concentrations in 2011 were, on average, higher than 2010 values (2040 μmol kg^{-1} versus 2024 μmol kg^{-1}, respectively), signifying the system had rebounded more from the initial drawdown of DIC during the spring phytoplankton bloom during 2011, either through sequestration of atmospheric CO_2, through the advection of water masses with higher DIC concentrations, or through remineralization processes. The sampling region was also devoid of any LSMW and WW water masses that were present during 2010. By the onset of sampling, these water masses had either been advected out of the region or were mixed with saltier water that then continued to warm (Weingartner et al., 2012). Additionally, little variation in temperature and salinity fields were recorded for the Klondike, Burger, and Statoil study areas (Fig. 3.2), suggesting hydrographic conditions were in a more continuous and steady state in 2011 than 2010.

Overall, the Chukchi Sea appeared to experience a limited range of DIC, where large differences in concentrations were not observed within Klondike, Burger, and Statoil, both within a season and between years (Table 3.1). The range of values observed during this study was similar to those reported in the North Pacific and Western Arctic (Bates et al., 2005a; Cross et al., 2012; Mathis and Questel, 2013; Mathis et al., 2010, 2009, 2005). Throughout the productive season DIC concentrations appeared to recover rather quickly from deviations from pre-bloom values, rates which were conceivably magnified in the Chukchi Sea compared to surrounding regions due to the Chukchi being the largest sink for atmospheric CO_2 globally (Evans et al., 2015).

3.5.2 Variability in NCP

Rates of NCP for the late summer-early autumn period were highly variable at small spatial scales, with 2011 having higher rates of NCP than 2010 (Table 3.4). These spatial patterns are consistent with previous NCP estimates from the Hanna Shoal and Chukchi Sea shelf break region (Bates et al., 2005a; Mathis et al., 2009). Additionally, our late season NCP rates correspond to those estimated between spring and summer observations for the Hanna Shoal region, with 2011 rates exceeding those from earlier in the productive season.

Considerable spatial variability in NCP rates was observed during the 2010 field season (Fig. 3.4), with negative NCP values most prominent in the middle portion of the study area. This "band" of negative NCP rates may reflect frontal zones present in the study area (Weingartner et al., 2013), with NCP being highest (~ 25 mmol C m^{-2} d^{-1}) at the convergence zones that are hot spots for production (Russell et al., 1999), and lower (~ –20 mmol C m^{-2} d^{-1}) outside of these zones. Comparatively, NCP rates during 2011 were more homogeneous with negative rates being recorded at only a few stations. Presumably, the well-mixed and weakly-stratified water column that characterized the 2011 season discouraged strong vertical fronts, aiding in the more uniform NCP rates.

The high rates of NCP late in the open-water season of 2011 can also be attributed to the higher availability of macronutrients, with nitrate concentrations still high (> 6 μmol m^{-3}) at or below the pycnocline during August (Hopcroft et al., 2013). Nitrate levels continued to persist over the study area into September and October, presumably stimulating production and giving rise to the high estimates of NCP. Comparatively, nitrate concentrations in 2010 had been completely exhausted throughout the entire water column by the time of sampling in August, and remained low for the remainder of the season (Questel et al., 2013). The absence of nitrate later in the open-water season contributed to the very low, yet positive, NCP rates calculated between August and September.

On average, negative NCP rates (–2 mmol C m^{-2} d^{-1}) were recorded in the Burger study area between the September and October 2010 occupations. Simultaneously, this region underwent a decrease in DIC but an increase in nDIC concentrations (Table 3.2 & 3.4).

Decreases in DIC concentrations are typically associated with primary production or with fresh water input, either through sea-ice melt, fluvial influences, or advection of a fresher water mass from the previously sampled water mass (i.e., initial sampling of saltier BSW, and subsequent sampling of fresher ACW) (Bates et al., 2005a, 2005b). Increases in nDIC concentrations arise from the input of CO_2 back into the system via air-sea gas exchange, remineralization, benthic respiration, or advection of water masses containing higher nDIC concentrations from the previously sampled water mass. It is plausible that there was a significant decrease in the pCO_2 of surface waters relative to atmospheric pCO_2 levels between the August and September cruise, and, because the rate of air-sea gas exchange occurs faster than biological processes (Mumane and Sarmiento, 2000), it is likely that NCP was still occurring but its signal was dampened due to the rapid uptake of atmospheric CO_2.

3.5.3 Relating NCP to changes in plankton biomass

Relationships between rates of NCP to concurrent changes in phytoplankton or herbivorous mesozooplankton biomass were only significant for chlorophyll-a and euphausiids (Table 3.5). For chlorophyll-a, there was a strong positive monotonic correlation in Burger during the transition of the ecosystem from September into October of 2010 ($r_s = 0.61$; $p < 0.05$). However, this relationship showed significantly strong negative monotonic correlations within Burger and Klondike in 2011 between August and late September/early October ($r_s = –0.661$ and $–0.730$, respectively; $p < 0.05$). The positive relationships between chlorophyll-a and NCP are not surprising as these two processes are tightly coupled to one another, but negative correlations are nonsensical. A significantly strong negative monotonic correlation of NCP to euphausiids biomass was observed in Burger from September into October 2010 ($r_s = –0.629$; $p < 0.05$), whereas this relationship showed significantly strong positive correlations ($r_s = 0.745$; $p < 0.05$) in Burger from August to late September/early October of 2011, also precluding a mechanistic justification.

The lack of correlation between NCP and changes in zooplankton is likely a consequence of stronger factors driving this system. The multiple water masses encountered in the Chukchi Sea each have characteristic assemblages of zooplankton (e.g., Eisner et al., 2013; Questel et al., 2013; Ershova et al., 2015a). Consequently, the seasonal variability and advection of those water

masses have been shown to be a primary determinant of zooplankton spatial patterns (Pisareva et al., 2015). For instance, southern water masses (i.e., Bering shelf water) containing larger lipid-rich zooplankton displace winter and melt water, along with their associated zooplankton communities, as the season progresses. The timing and extent to which Bering Sea water infiltrates the northeastern Chukchi Sea study area heavily dictates the observed composition, abundance, and biomass of zooplankton assemblages. Additionally, years with warmer temperatures contain a higher proportion of temperate taxa, while colder years exhibit taxa of greater Arctic affinity (Questel et al., 2013). Upwelling events in Barrow Canyon are even capable of introducing colder water masses from the Arctic Basin into the northeastern Chukchi Sea (Itoh et al., 2015) along with their own distinctive species. Inter-annual differences in primary productivity within these upwelled water masses likely influence zooplankton biomass, such that increases in overall primary productivity of the Chukchi Sea (e.g., Arrigo et al., 2008) are responsible for long-term increases in zooplankton biomass (Ershova et al., 2015b). However, at the spatial scales of the Chukchi Sea, productivity differences within a study-year are overwhelmed by the spatial patterning of the water masses themselves.

3.5.4 Energetic requirements of mesozooplankton

Calculated rates of NCP compared to those of modeled gross primary production ranged from -16–63% during 2010 and 2–4% during 2011 (Table 3.6). The lower values of NCP compared to gross primary production are not surprising because the former rate accounts for recycling of carbon, although it is somewhat surprising the differences are often so large. In fact, NCP is 1–3 orders of magnitude lower than the observed change in copepods carbon biomass during late summer of 2010. Such a comparison cannot be made in 2011 because zooplankton biomass declined between cruises even though NCP suggested enhanced primary productivity. The daily rate of grazing on the gross primary production by copepods ranged from 35–70% in 2010 and from 10–75% in 2011. Nonetheless, we found that both the 2010 and 2011 field seasons contained enough carbon in the system to support the energetic needs for growth and reproduction of the copepod assemblages from August to October.

Somewhat surprisingly, the simple box-model proved to be more capable of answering one of our most basic questions about the study area. The traditional view of the Bering and

Chukchi Seas is that zooplankton production is highly dependent upon the initial phytoplankton bloom (Hunt et al., 2011), and that their production is much reduced for the remainder of the season. Despite relatively low phytoplankton and high zooplankton biomass, this system does not appear to be vastly mismatched during the open-water season when the system is often characterized as oligotrophic (based on chlorophyll-a concentrations). This suggests that although zooplankton may exploit some portion of the initial bloom, their inability to exploit it fully (due to low biomass) is compensated by the persistence of an adequate food resource to sustain the observed zooplankton assemblage during summer and well into autumn. This is probably because the water column temperatures are so low that zooplankton metabolic rates are depressed relative to their biomass. This may help explain why the Chukchi Sea zooplankton communities differ in biomass by less than an order of magnitude from the Barents Sea that is viewed as "highly productive" (Hunt et al., 2013). It is also notable that in the case of the Barents Sea, zooplankton biomass is dominated by the advected copepod species *Calanus finmarchicus* that is not considered sustainable within that habitat (Wassmann et al., 2015).

A potential shortcoming of our simple model is that mesozooplankton in the Chukchi and Bering Sea often prey preferentially upon microzooplankton (Campbell et al., 2015, 2009), which can become abundant during the summer months. Although data are lacking for 2010 and 2011, microzooplankton observations during the 2012 season found that heterotrophic dinoflagellates dominated abundance whereas ciliates dominated biomass, together exceeding phytoplankton biomass over the entire study region (Hopcroft et al., 2013). Thus, it is likely that microzooplankton are tightly coupled in their grazing and growth rates to that of the phytoplankton (Sherr et al., 2013; Stoecker et al., 2014). Although there still needs to be enough phytoplankton production to sustain both the microzooplankton and the mesozooplankton, the mesozooplankton benefit by having the combined prey resources of both phytoplankton and microzooplankton, even though the food chain is lengthened by the microzooplankton pathway.

It has been considered energetically advantageous for mesozooplankton to consume more heterotrophic prey over autotrophic prey at higher latitudes (Boersma et al., 2016) where cold water temperatures allow mesozooplankton to decrease their respiration rates and efficiently channel ingested food into growth, thus reducing their energy demand for high concentrations of carbon-rich food while simultaneously supporting a high biomass of planktonic organisms

(Ikeda, 1985, Ikeda et al., 2001). Our carbon estimates imply that there is enough energy available in the system to support both holoplanktonic growth and reproduction and meroplanktonic growth with subsequent benthic reproduction. These resources may be further supplemented by bacterial production on resuspended materials energy as the system progresses towards winter conditions (Berge et al., 2015; Kosobokova and Hirche, 2016). Clearly the production dynamics of the bloom versus post-bloom period, and the relative importance of each for sustaining the pelagic ecosystem, are worthy of reassessment.

3.6 Conclusion

This study marks the first attempt to reconcile late-season production to mesozooplankton biomass in the Chukchi Sea. The repeat-measures sampling design of concurrent physical, chemical, and biological measurements at high spatial resolutions allowed us to estimate productivity through two different methods. First, NCP calculations showed a large degree of spatial variability over the CSESP study region during late summer and early autumn that were driven largely by physical processes. NCP rates also insinuated that moderate to high rates of production were still occurring late in the open-water season when the Chukchi Sea is traditionally considered to be operating under oligotrophic conditions. Secondly, despite a lack of correlation between NCP and mesozooplankton biomass, a less complicated conceptual model of estimating carbon production in the ecosystem suggests that the Chukchi Sea could support the energetic demands of the observed mesozooplankton communities during the open-water season, long after the high-magnitude phytoplankton bloom had generated the majority of the primary production.

The Chukchi Sea ecosystem is undergoing the most dramatic rate of change due to perturbations in climate of any region in the Arctic Ocean (Grebmeier and Maslowski, 2014). The most striking change has been the loss of sea-ice during summer months, with thick multi-year ice being completely replaced with first-year ice that is thin and more mobile (Wood et al., 2015). A consequence of longer ice-free season has led to an increase in solar heating due to a lower albedo, resulting in increases in both stratification and ocean heat storage (Jackson et al., 2010). Additionally, wind anomalies have created large variations in sea-ice distribution (Frey et al., 2015), ocean currents (Woodgate et al., 2012), and increased freshwater influx (Morison et

al., 2012; Wood et al., 2013) through Bering Strait. The longer open water season will undoubtably increase the flux of atmospheric CO_2 into the ocean, leading to an even greater regional and global carbon sink than presently estimated (Evans et al., 2015). As it will be hard to predict what the "new normal" climate will be for the Chukchi Sea, it is likely that the high rates of NCP observed during the late 2011 season will foreshadow future scenarios of a more productive Chukchi Sea that will sustain the high biomass of ecologically important zooplankton species.

3.7 Acknowledgments

This research was funded by ConocoPhillips Alaska, Anchorage, AK; Shell Exploration and Production, Anchorage, AK; and Statoil USA E & P, Anchorage, AK. We thank Jeff Hastings and Sheyna Wisdom from Olgoonik-Fairweather LLC for their logistical support, the captains and crew of the R/V *Westward Wind*, marine technicians, Aldrich Offshore Services, and chief scientists Robert H. Day and John. Burns Sr. Carbonate samples were processed by Natalie Monacci and Daniel Naber at the UAF Ocean Acidification Research Center. We also thank Cheryl Clarke, T. Chris Stark, and Katherine Trahanovsky for aiding in the processing of chlorophyll and mesozooplankton samples.

3.8 References

Arrigo, K.R., van Dijken, G., Pabi, S., 2008. Impact of a shrinking Arctic ice cover on marine primary production. Geophysical Research Letters 35, 1–6.

Båmstedt, U., Nejstgaard, J.C., Solberg, P.T., 1999. Utilisation of small-sized food algae by *Calanus finmarchicus* (Copepoda, Calanoida) and the significance of feeding history. Sarsia 84, 19–38.

Banse, K., 1995. Zooplankton: pivotal role in the control of oceanic production. ICES Journal of Marine Science 52, 265–277.

Bates, N.R. 2001. Interannual variability of oceanic CO_2 and biogeochemical properties in the Western North Atlantic subtropical gyre. Deep Sea Research Part II: Topical Studies in Oceanography 48, 1507–1528.

Bates, N.R., Best, M.H.P., Hansell, D.A., 2005a Spatio-temporal distribution of dissolved inorganic carbon and net community production in the Chukchi and Beaufort Seas. Deep Sea Research Part II: Topical Studies in Oceanography 52, 3303–3323.

Bates, N.R., Hansell, D.A., Moran, S.B., Codispoti, L.A., 2005b. Seasonal and spatial distribution of particulate organic matter (POM) in the Chukchi and Beaufort Seas. Deep Sea Research Part II: Topical Studies in Oceanography 52, 3324–3343.

Bates, N.R., Mathis, J.T., 2009. The Arctic Ocean marine carbon cycle: evaluation of air-sea CO_2 exchanges, ocean acidification impacts and potential feedbacks. Biogeosciences, 6, 6695–6747.

Berge, J., Daase, M., Renaud, P.E., Ambrose, W.G., Jr., Darnis, G., Last, K.S., Leu, E., Cohen, J.H., Johnsen, G., Moline, M.A., Cottier, F., Varpe, Ø., Shunatova, N., Balazy, P., Morata, N., Massabuau, J.C., Falk-Peterson, S., Kosobokova, K., Hoppe, C.J.M., Weslawski, J.M., Kukliński, P., Legeżyńska, J., Nikishina, D., Cusa, M., Kedra, M., Wlodarska-Kowalczuk, M., 2015. Unexpected levels of biological activity during the polar night offer new perspectives on a warming arctic. Current Biology 25, 2555–2561.

Blanchard, A.L., Parris, C.L., Knowlton, A.L., Wade, N.R., 2013a. Benthic ecology of the northeastern Chukchi Sea. Part I. Environmental characteristics and macrofaunal community structure, 2008-2010. Continental Shelf Research 67, 52–66.

Blanchard, A.L., Parris, C.L., Knowlton, A.L., Wade, N.R., 2013b. Benthic ecology of the northeastern Chukchi Sea. Part II. Spatial variation of megafaunal community structure, 2009-2010. Continental Shelf Research 67, 67–76.

Boersma, M., Mathew, K.A., Niehoff, B., Schoo, K.L., Franco-Santos, R.M., Meunier, C.L., 2016. Temperature driven changes in the diet preference of omnivorous copepods: no more meat when it's hot? Ecology Letters 19, 45–53.

Campbell, R.G., Ashjian, C.J., Sherr, E.B., Sherr, B.F., Lomas, M.W., Ross, C., Alatalo, P., Gelfman, C., Van Keuren, D., 2015. Mesozooplankton grazing during spring sea-ice conditions in the eastern Bering Sea. Deep Sea Research Part II: Topical Studies in Oceanography. doi:10.1016/j.dsr2.2015.11.003.

Campbell, R.G., Sherr, E.B., Ashjian, C.J., Plourde, S., Sherr, B.F., Hill, V., Stockwell, D.A., 2009. Mesozooplankton prey preference and grazing impact in the western Arctic Ocean. Deep Sea Research Part II: Topical Studies in Oceanography 56, 1274–1289.

Coachman, L.K., Aagard, K., 1988. Transports through Bering Strait: annual and interannual variability. Journal of Geophysical Research 93, 15515–15539.

Codispoti, L.A., Flagg, C.N., Swift, J.H., 2005. Hydrographic conditions during the 2002 SBI process experiments. Deep Sea Research Part II: Topical Studies in Oceanography 52, 3199–3226.

Codispoti, L.A., Friederich, G.E., Hood, D.W., 1986. Variability in the inorganic carbon system over the southeastern Bering Sea shelf during spring 1980 and spring-summer 1981. Continental Shelf Research 5, 133–160.

Cota, G.F., Pomeroy, L.R., Harrison, W.G., Jones, E.P., Peters, F., Sheldon, W.M., Weingartner, T.J., 1996. Nutrients, primary production and microbial heterotrophy in the southeastern Chukchi Sea: Arctic summer nutrient depletion and heterotrophy. Marine Ecology Progress Series 135, 247–258.

Cross, J.N., Mathis, J.T., Bates, N.R., 2012. Hydrographic controls on net community production and total organic carbon distributions in the eastern Bering Sea. Deep Sea Research Part II: Topical Studies in Oceanography 65-70, 98–109.

Danielson, S.L., Weingartner, T.J., Hedstrom, K.S., Aagaard, K., Woodgate, R., Curchitser, E., Stabeno, P.J., 2014. Coupled wind-forced controls of the Bering-Chukchi shelf circulation and the Bering Strait throughflow: ekman transport, continental shelf waves, and variations of the Pacific-Arctic sea surface height gradient. Progress in Oceanography 125, 40–61.

Day, R.H., Weingartner, T.J., Hopcroft, R.R., Aerts, L.A.M., Blanchard, A.L., Gall, A.E., Gallaway, B.J., Hannay, D.E., Holladay, B.A., Mathis, J.T., Norcross, B.L., Questel, J.M., Wisdom, S.S., 2013. The offshore northeastern Chukchi Sea, Alaska: a complex high-latitude ecosystem. Continental Shelf Research 67, 147–165.

Dunton, K.H., Grebmeier, J.M., Trefry, J.H., 2014 The benthic ecosystem of the northeastern Chukchi Sea: an overview of its unique biogeochemical and biological characteristics. Deep Sea Research Part II: Topical Studies in Oceanography 102, 1–8.

Eisner, L., Hillgruber, N., Martinson, E., Maselko, J., 2013. Pelagic fish and zooplankton species assemblages in relation to water mass characteristics in the northern Bering and southeast Chukchi seas. Polar Biology 36, 87–113.

Ershova, E.A., Hopcroft, R.R., Kosobokova, K.N., 2015a. Inter-annual variability of summer mesozooplankton communities of the western Chukchi Sea: 2004–2012. Polar Biology 38, 1461–1481.

Ershova, E.A., Hopcroft, R.R., Kosobokova, K.N., Matsuno, K., Nelson, R.J., Yamaguchi, A., Eisner, L.B., 2015b. Long-term changes in summer zooplankton communities of the western Chukchi Sea, 1945-2012. Oceanography 28, 100–115.

Evans, W., Mathis, J.T., Cross, J.C., Bates, N.R., Frey, K.E., Else, B.G.T., Papkyriakou, T.N., Degrandpre, M.D., Islam, F., Cai, W., Baoshan, C., Yamamoto-Kawai, M., Carmack, E.C., Williams, W.J., Takahashi, T., 2015. Sea-air CO_2 exchange in the western Arctic coastal ocean. Global Biogeochemical Cycles 29, 1190–1209.

Frey, K.E., Moore, G.W.K., Cooper, L.W., Grebmeier, J.M., 2015. Divergent patterns of recent sea ice cover across the Bering, Chukchi, and Beaufort seas of the Pacific Arctic Region. Progress in Oceanography 136, 32–49.

Gall, A.E., Day, R.H., Weingartner, T.J., 2013. Structure and variability of the marine-bird community in the northeastern Chukchi Sea. Continental Shelf Research 67, 96–115.

Grebmeier, J.M., Cooper, L.W., Feder, H.M., Sirenko, B.I., 2006. Ecosystem dynamics of the Pacific-influenced Northern Bering and Chukchi Seas in the Amerasian Arctic. Progress in Oceanography 71, 331–361.

Grebmeier, J.M., Maslowski, W. (Eds.). 2014. The Pacific Arctic Region: ecosystem status and trends in a rapidly changing environment. Springer Dordrecht Heidelberg, New York, pp. 450.

Grebmeier, J.M., McRoy, C.P., Feder, H.M., 1988. Pelagic-benthic coupling on the shelf of the northern Bering and Chukchi Seas. I. food supply source and benthic biomass. Marine Ecology Progress Series 53, 79–91.

Hansell, D.A., Whitledge, T.E., Goering, J.J., 1993. Patterns of nitrate utilization and new production over the Bering-Chukchi shelf. Continental Shelf Research 13, 601–328.

Hill, V., Cota, G., 2005. Spatial patterns of primary production on the shelf, slope and basin of the Western Arctic in 2002. Deep Sea Research Part II: Topical Studies in Oceanography 52, 3344–3354.

Hopcroft, R.R., Hariharan, P., Questel, J.M., Lamb, J., Lessard, E., Foy, M., Clarke, C., 2013. Oceanographic assessment of the planktonic communities in the northeastern Chukchi Sea: report for survey year 2011. Report prepared by Institute of Marine Science, University of Alaska Fairbanks, for ConocoPhillips Company, Shell Exploration and Production Company and Statoil USA E&P, Inc. pp. 1–80.

Hopcroft, R.R., Kosobokova, K.N., Pinchuk, A.I., 2010. Zooplankton community patterns in the Chukchi Sea during summer 2004. Deep Sea Research Part II: Topical Studies in Oceanography 57, 27–39.

Hopcroft, R.R., Roff, J.C., Chavez, F.P., 2001. Size paradigms in copepod communities: a re-examination. Hydrobiologia 453-454, 133–141.

Hunt, G.L., Blanchard, A.L., Boveng, P., Dalpadado, P., Drinkwater, K.F., Eisner, L., Hopcroft, R.R., Kovacs, K.M., Norcross, B.L., Renaud, P., Reigstad, M., Renner, M., Skjoldal, H.R., Whitehouse, A., Woodgate, R.A., 2013. The Barents and Chukchi Seas: comparison of two Arctic shelf ecosystems. Journal of Marine Systems 109-110, 43–68.

Hunt, G.L., Coyle, K.O., Eisner, L., Farley, E.V, Heintz, R., Mueter, F., Napp, J.M., Overland, J.E., Ressler, P.H., Sale, S., Stabeno, P.J., 2011. Climate impacts on eastern Bering Sea food webs: a synthesis of new data and an assessment of the Oscillating Control Hypothesis. ICES Journal of Marince Science 68, 1230–1243.

Ikeda, T., 1985. Metabolic rates of epipelagic marine zooplankton as a function of body mass and temperature. Marine Biology 85, 1–11.

Ikeda, T., 1977. The effect of laboratory conditions on the extrapolation of experimental measurements to the ecology of marine zooplankton. IV. Changes in respiration and excretion rates of boreal zooplankton species maintained under fed and starved conditions. Marine Biology 41, 241–252.

Ikeda, T., Kanno, Y., Ozaki, K., Shinada, A., 2001. Metabolic rates of epipelagic marine copepods as a function of body mass and temperature. Marine Biology 139, 1020–1020.

Itoh, M., Pickart, R.S., Kikuchi, T., Fukamachi, Y., Ohshima, K.I., Simizu, D., Arrigo, K.R., Vagle, S., He, J., Ashjian, C., Mathis, J.T., Nishino, S., Nobre, C., 2015. Water properties, heat and volume fluxes of Pacific water in Barrow Canyon during summer 2010. Deep Sea Research Part I: Oceanographic Research Papers 102, 43–54.

Jackson, J.M., Carmack, E.C., McLaughlin, F.A., Allen, S.E., Ingram, R.G., 2010. Identification, characterization, and change of the near-surface temperature maximum in the Canada Basin, 1993-2008. Journal of Geophysical Research: Oceans 115, 1–16.

Kiørboe, T., Møhlenberg, F., Hamburger, K., 1985. Bioenergetics of the planktonic copepod *Acartia tonsa*: relation between feeding, egg production and respiration, and composition of specific dynamic action. Marine Ecology Progress Series 26, 85–97.

Kosobokova, K.N.. Hirche, H.J., 2016. A seasonal comparison of zooplankton communities in the Kara Sea – with special emphasis on overwintering traits. Estuarine, Coastal and Shelf Science 175, 146–156.

Lee, K., 2001. Global net community production estimated from the annual cycle of surface water total dissolved inorganic carbon. Limnology and Oceanography 46, 1287–1297.

Liu, H., Hopcroft, R.R., 2008. Growth and development of *Pseudocalanus* spp. in the northern Gulf of Alaska. Journal of Plankton Research 30, 923–935.

Liu, H., Hopcroft, R.R., 2007. A comparison of seasonal growth and development of the copepods *Calanus marshallae* and *C. pacificus* in the northern Gulf of Alaska. Journal of Plankton Research 29, 569–581.

Liu, H., Hopcroft, R.R., 2006. Growth and development of *Metridia pacifica* (Copepoda: Calanoida) in the northern Gulf of Alaska. Journal of Plankton Research 28, 769–781.

Mathis, J.T., 2012. Seasonal observations of carbonate chemistry and ocean acidification in 2011. Report prepared by Institute of Marine Science, University of Alaska Fairbanks, for ConocoPhillips Company, Shell Exploration and Production Company and Statoil USA E&P, Inc. pp. 1–21.

Mathis, J.T., Bates, N.R., Hansell, D.A., Babila, T., 2009. Net community production in the northeastern Chukchi Sea. Deep Sea Research Part II: Topical Studies in Oceanography 56, 1213–1222.

Mathis, J.T., Cross, J.N., Bates, N.R., Moran, S.B, Lomas, M.W., Mordy, C.W., Stabeno, P.J., Lomas, M.W., Mordy, C.W., Stabeno, P.J., 2010. Seasonal distribution of dissolved inorganic carbon and net community production on the Bering Sea shelf. Biogeosciences 7, 1769–1787.

Mathis, J.T., Hansell, D.A., Bates, N.R., 2005. Strong hydrographic controls on spatial and seasonal variability of dissolved organic carbon in the Chukchi Sea. Deep Sea Research Part II: Topical Studies in Oceanography 52, 3245–3258.

Mathis, J.T., Pickart, R.S., Hansell, D.A., Kadko, D., Bates, N.R., 2007. Eddy transport of organic carbon and nutrients from the Chukchi Shelf: impact on the upper halocline of the western Arctic Ocean. Journal of Geophysical Research: Oceans 112, 1–14.

Mathis, J.T., Questel, J.M., 2013. Assessing seasonal changes in carbonate parameters across small spatial gradients in the Northeastern Chukchi Sea. Continental Shelf Research 67, 42–51.

Matrai, P., Vernet, M., Wassmann, P., 2007. Relating temporal and spatial patterns of DMSP in the Barents Sea to phytoplankton biomass and productivity. Journal of Marine Systems 67, 83–101.

Morison, J., Kwok, R., Peralta-Ferriz, C., Alkire, M., Rigor, I., Andersen, R., Steele, M., 2012. Changing Arctic Ocean freshwater pathways. Nature 481, 66–70.

Mumane, R.J., Sarmiento, J.L., 2000. Roles of biology and gas exchange in determining the $\delta^{13}C$ distribution in the ocean and the preindustrial gradient in atmospheric $\delta^{13}C$. Global Biogeochemical Cycles 14, 389–405.

Peterson, W.T., 1988. Rates of egg production by the copepod *Calanus marshallae* in the laboratory and in the sea off Oregon, USA. Marine Ecology Progress Series 47, 229–237.

Piatt, J.F., Springer, A.M., 2003. Advection, pelagic food webs and the biogeography of seabirds in Beringia. Marine Ornithology 31, 141–154.

Pisareva, M.N., Pickart, R.S., Spall, M.A., Nobre, C., Torres, D.J., Moore, G.W.K., Whitledge, T.E., 2015. Flow of Pacific water in the western Chukchi Sea: results from the 2009 RUSALCA expedition. Deep Sea Research Part I: Oceanographic Research Papers 105, 53–73.

Questel, J.M., Clarke, C., Hopcroft, R.R., 2013. Seasonal and interannual variation in the planktonic communities of the northeastern Chukchi Sea during the summer and early fall. Continental Shelf Research 67, 23–41.

Reigstad, M., Wassmann, P., Riser, C.W., Øygarden, S., Rey, F., 2002. Variations in hydrography, nutrients and chlorophyll a in the marginal ice-zone and the central Barents Sea. Journal of Marine Systems 38, 9–29.

Russell, R.W., Harrison, N.M., Hunt, G.L., 1999. Foraging at a front: hydrography, zooplankton, and avian planktivory in the northern Bering Sea. Marine Ecology Progress Series 182, 77–93.

Saba, G.K., Steinberg, D.K., Bronk, D.A., 2009. Effects of diet on release of dissolved organic and inorganic nutrients by the copepod *Acartia tonsa*. Marine Ecology Progress Series 386, 147–161.

Sathyendranath, S., Stuart, V., Nair, A., Oka, K., Nakane, T., Bouman, H., Forget, M.H., Maass, H., Platt, T., 2009. Carbon-to-chlorophyll ratio and growth rate of phytoplankton in the sea. Marine Ecology Progress Series 383, 73–84.

Schonberg, S.V., Clarke, J.T., Dunton, K.H., 2014. Distribution, abundance, biomass and diversity of benthic infauna in the Northeast Chukchi Sea, Alaska: relation to environmental variables and marine mammals. Deep Sea Research Part II: Topical Studies in Oceanography 102, 144–163.

Sherr, E.B., Sherr, B.F., Ross, C., 2013. Microzooplankton grazing impact in the Bering Sea during spring sea ice conditions. Deep Sea Research Part II: Topical Studies in Oceanography 94, 57–67.

Springer, A.M., McRoy, C.P., Turco, K.R., 1989. The paradox of pelagic food webs in the northern Bering Sea–II. Zooplankton communities. Continental Shelf Research 9, 359–386.

Sterner, R.W., 1990. The ratio of nitrogen to phosphorus resupplied by herbivores: zooplankton and the algal competitive arena. The American Naturalist 136, 209–229.

Stoecker, D.K., Weigel, A., Goes, J.I., 2014. Microzooplankton grazing in the Eastern Bering Sea in summer. Deep Sea Research Part II: Topical Studies in Oceanography 109, 145–156.

Wassmann, P., Kosobokova, K.N., Slagstad, D., Drinkwater, K.F., Hopcroft, R.R., Moore, S.E., Ellingsen, I., Nelson, R.J., Carmack, E., Popova, E., Berge, J., 2015. The contiguous domains of Arctic Ocean advection: trails of life and death. Progress in Oceanography 139, 42–65.

Weingartner, T.J., Danielson, S., Dobbins, E., Potter, R., 2012. Physical oceanographic measurements in the northeastern Chukchi Sea: 2011. Report prepared by Institute of Marine Science, University of Alaska Fairbanks, for ConocoPhillips Company, Shell Exploration and Production Company and Statoil USA E&P, Inc. pp. 1–89.

Weingartner, T.J., Dobbins, E., Danielson, S., Winsor, P., Potter, R., Statscewich, H., 2013. Hydrographic variability over the northeastern Chukchi Sea shelf in summer-fall 2008-2010. Continental Shelf Research 67, 5–22.

Williams, P.J., 1993. Measurements of primary production from the molecular and global scale, in: Li, W.K.W., Maestrini, S.Y. (Eds.), ICES Marine Sciemce Symposium, pp. 9–19.

Wood, K.R., Bond, N.A., Danielson, S.L., Overland, J.E., Salo, S.A., Stabeno, P.J., Whitefield, J., 2015. A decade of environmental change in the Pacific Arctic region. Progress in Oceanography 136, 12–31.

Wood, K.R., Overland, J.E., Salo, S.A., Bond, N.A., Williams, W.J., Dong, X., 2013. Is there a "new normal" climate in the Beaufort Sea? Polar Resrarch 32, 1–9.

Woodgate, R.A., Weingartner, T.J., Lindsay, R., 2012. Observed increases in Bering Strait oceanic fluxes from the Pacific to the Arctic from 2001 to 2011 and their impacts on the Arctic Ocean water column. Geophysical Research Letteres 39, 2–7.

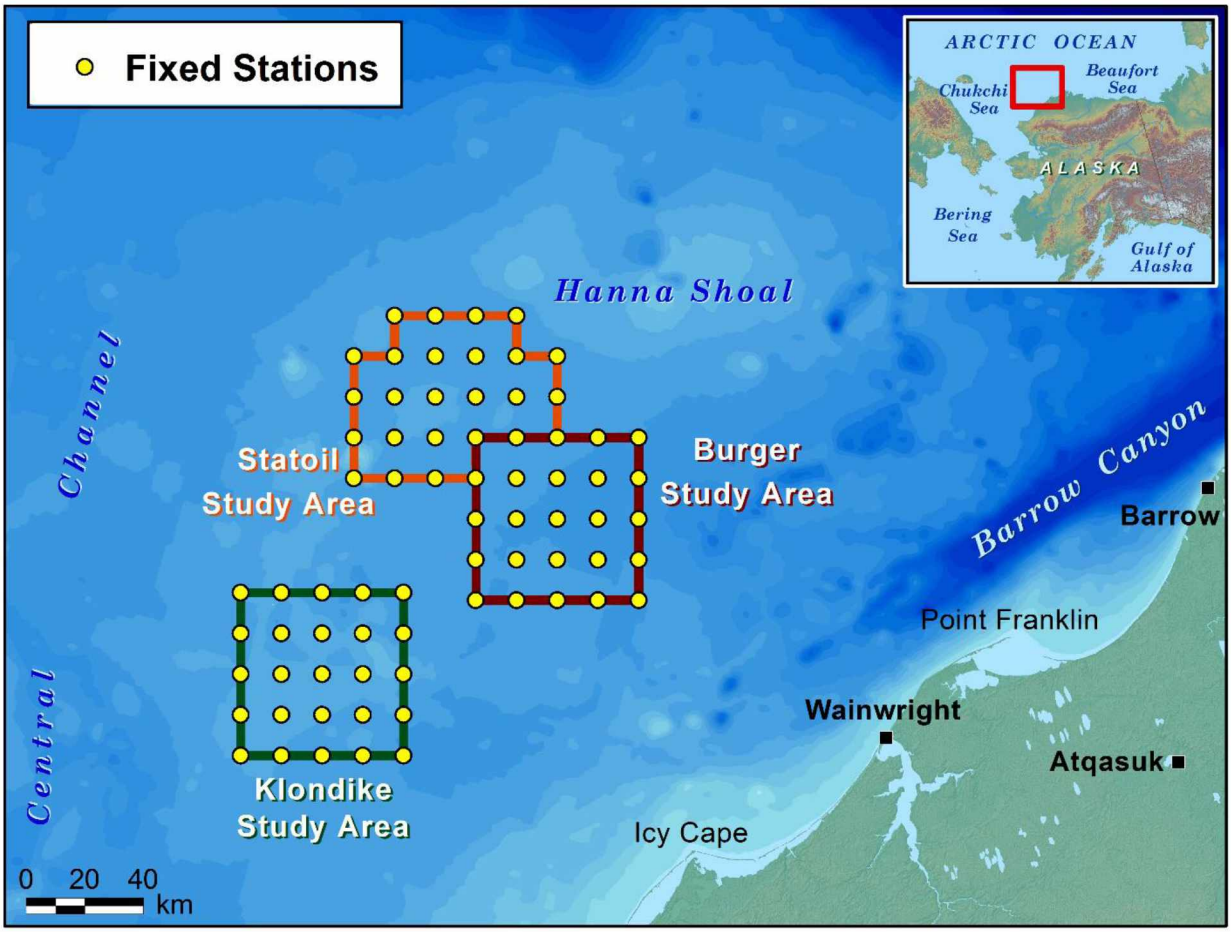

Figure 3.1 Map of the northeastern Chukchi Sea showing sampling locations of the Burger, Klondike, and Statoil survey grids where carbon, nutrient, and plankton measurements were concurrently made during 2010 and 2011.

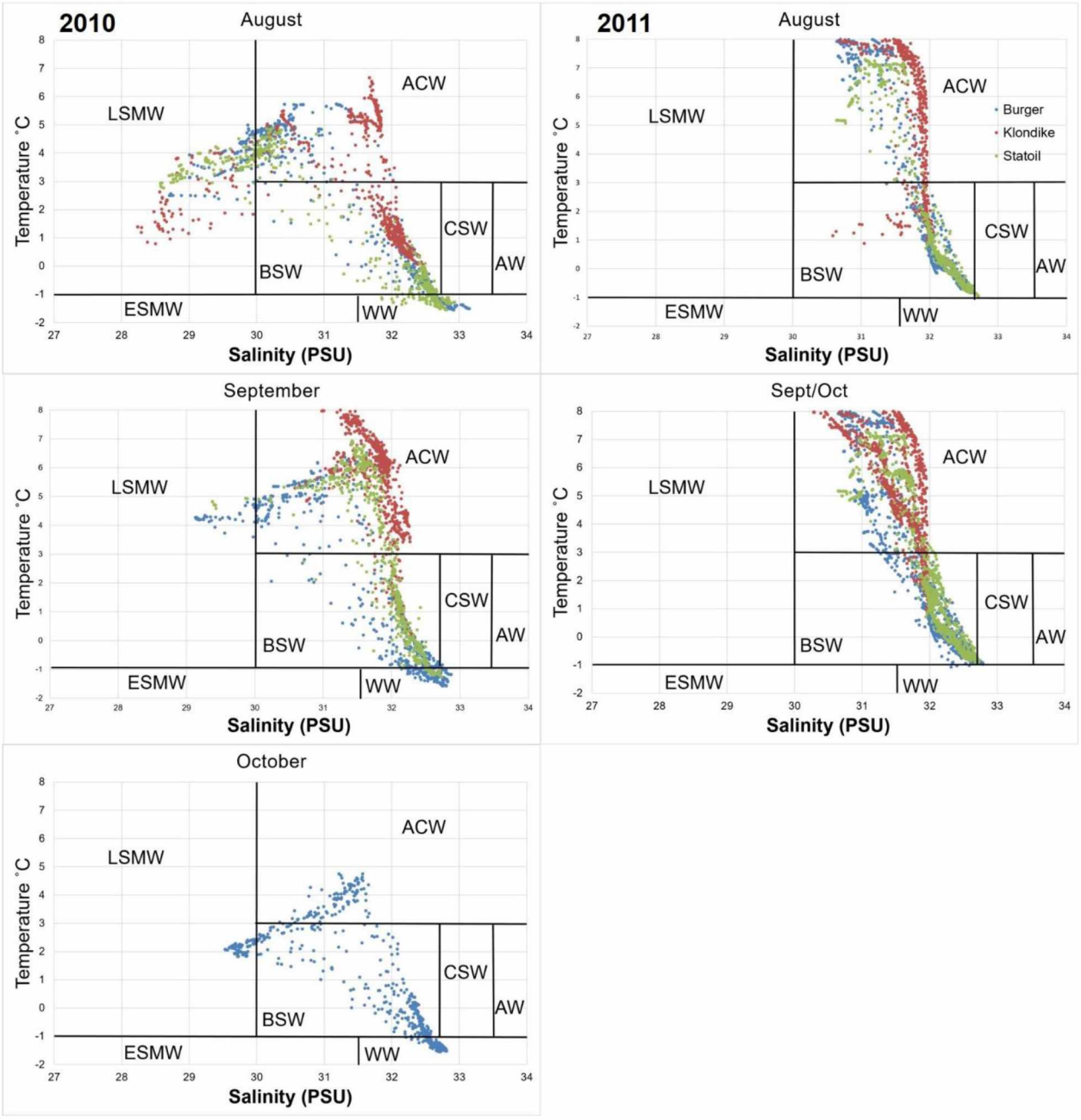

Figure 3.2 Temperature-salinity diagrams characterizing water masses present within the Burger, Klondike, and Statoil study areas in the northeastern Chukchi Sea during 2010 (left) and 2011 (right). LSMW, late season melt water; ESMW, early season melt water; ACW, Alaska coastal water; BSW, Bering summer water; CSW, Chukchi summer water; AW, Atlantic water; WW, winter water.

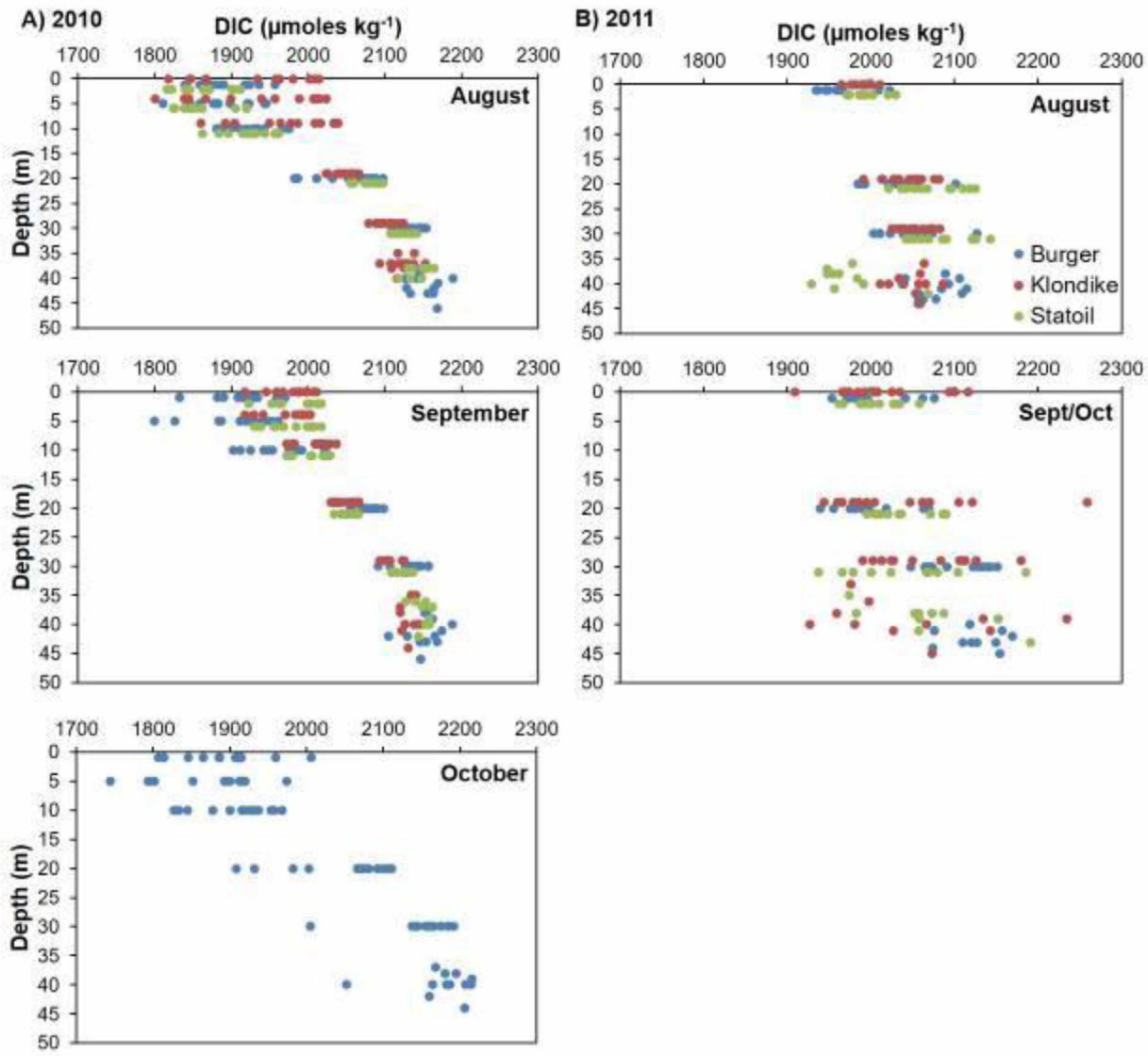

Figure 3.3 Seasonal and spatial distribution of DIC in the Burger, Klondike, and Statoil study areas in the northeastern Chukchi Sea during A) 2010 and B) 2011. Data points offset by ± 1 m for Klondike and Statoil, respectively.

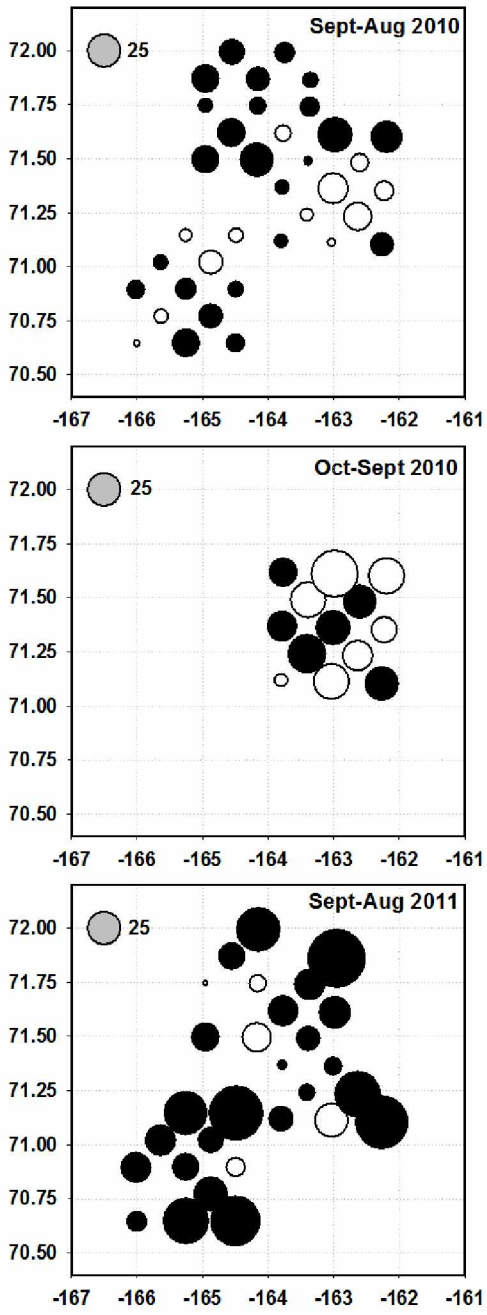

Figure 3.4 NCP rates (mmol C m^{-2} d^{-1}) for late-summer and autumn in 2010 and 2011 within the Burger, Klondike, and Statoil study areas in the northeastern Chukchi Sea. Filled circles indicate positive values, open circles indicate negative values.

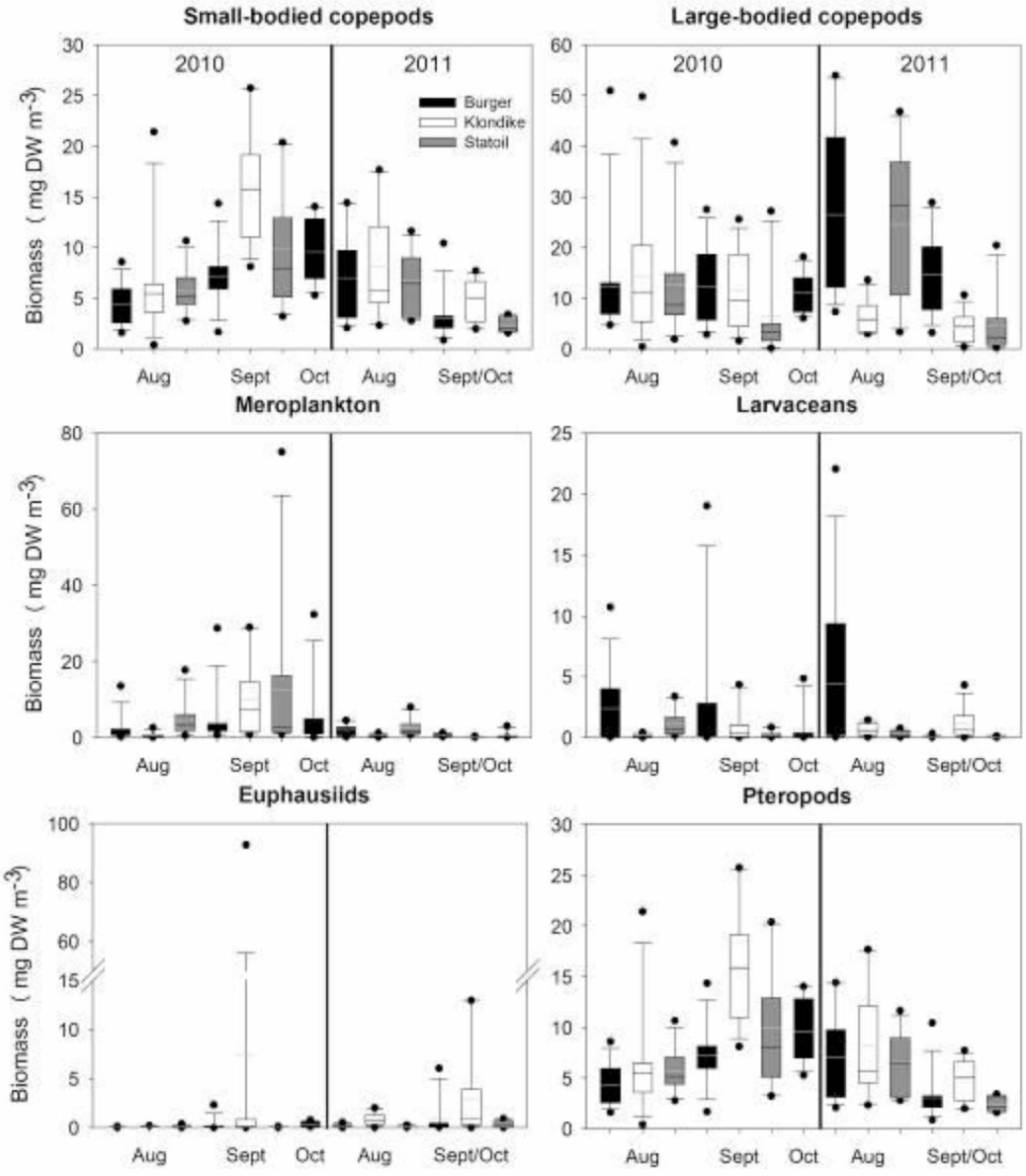

Figure 3.5 Biomass of small- and large-bodied copepods, meroplankton, larvaceans, euphausiids, and pteropods within the Burger, Klondike, and Statoil study areas in the northeastern Chukchi Sea during the 2010 and 2011 field seasons. The black or gray line through the box is the sample mean; limits of the box are the 25th and 75th percentile. Whiskers are the 10th and 90th percentiles and the single points are the 5th and 95th percentiles.

Table 3.1 Average DIC, chlorophyll-a, and herbivorous zooplankton biomass in the Burger, Klondike, and Statoil study areas for the northeastern Chukchi Sea during 2010 and 2011.

	DIC (μmol kg^{-1})	Chl-a (mg m^{-3})	Small Copepods (mg DW m^{-3})	Large Copepods (mg DW m^{-3})	Meroplankton (mg DW m^{-3})	Larvaceans (mg DW m^{-3})	Euphausiids (mg DW m^{-3})	Pteropods (mg DW m^{-3})
2010								
August								
Burger	2007	0.41	4.34	12.34	2.26	2.38	0.04	0.17
Klondike	2017	0.62	6.46	14.18	0.51	0.13	0.04	0.14
Statoil	1999	0.79	5.67	12.69	4.38	1.11	0.10	0.07
September								
Burger	2026	0.52	7.18	12.26	4.40	2.85	0.24	0.51
Klondike	2042	0.52	16.01	11.49	10.09	0.98	7.41	2.92
Statoil	2070	0.57	9.91	6.48	12.53	0.25	0.04	2.23
October								
Burger	2008	0.79	9.57	11.05	5.22	0.75	0.35	0.47
2011								
August								
Burger	2033	0.91	7.00	26.47	1.84	4.44	0.17	1.91
Klondike	2033	0.99	8.15	6.19	0.46	0.65	0.80	0.85
Statoil	2034	0.97	6.70	24.60	2.58	0.29	0.09	2.54
Sept/Oct								
Burger	2052	0.81	3.06	14.60	0.60	0.04	0.89	0.12
Klondike	2053	0.52	4.86	4.15	0.12	1.10	2.95	0.03
Statoil	2037	1.13	2.30	4.67	0.51	0.06	0.34	0.05

Table 3.2 Average changes in DIC, chlorophyll-a, and herbivorous zooplankton biomass, and associated paired t-tests, in the Burger, Klondike, and Statoil study areas for the northeastern Chukchi Sea during 2010 and 2011. Bold values are significantly different ($p \leq 0.05$).

	ΔDIC ($\mu mol\ kg^{-1}$)	ΔChl-a ($mg\ m^{-3}$)	ΔSmall Copepods ($mg\ DW\ m^{-3}$)	ΔLarge Copepods ($mg\ DW\ m^{-3}$)	ΔMeroplankton ($mg\ DW\ m^{-3}$)	ΔLarvaceans ($mg\ DW\ m^{-3}$)	ΔEuphausiids ($mg\ DW\ m^{-3}$)	ΔPteropods ($mg\ DW\ m^{-3}$)
2010								
Sept-Aug								
Burger	19.00	0.11	2.84	–0.08	2.14	0.47	0.20	0.35
p-value	***0.001***	*0.218*	***0.000***	*0.980*	*0.362*	*0.770*	*0.261*	*0.098*
Klondike	25.00	–0.10	9.97	–1.87	9.86	0.84	7.99	2.86
p-value	***0.027***	*0.404*	***0.001***	*0.630*	***0.006***	*0.089*	*0.322*	***0.001***
Statoil	71.00	–0.22	4.24	–6.21	8.15	–0.86	–0.06	2.16
p-value	***0.006***	*0.256*	***0.048***	***0.010***	*0.265*	***0.036***	*0.095*	***0.005***
Oct-Sept								
Burger	–18.00	0.27	2.28	–0.73	0.79	–2.21	0.09	–0.08
p-value	***0.014***	*0.095*	*0.094*	*0.729*	*0.294*	*0.142*	*0.680*	*0.566*
2011								
Sept/Oct -Aug								
Burger	19.00	–0.10	–3.94	–11.87	–1.24	–4.39	0.72	–1.79
p-value	*0.099*	*0.621*	***0.024***	***0.036***	***0.015***	***0.041***	*0.150*	*0.070*
Klondike	20.00	–0.47	–3.28	–2.04	–0.34	0.45	2.15	–0.82
p-value	***0.003***	*0.137*	*0.062*	*0.100*	***0.007***	*0.218*	*0.139*	*0.071*
Statoil	3.00	0.15	–4.40	–19.93	–2.08	–0.23	0.25	–2.49
p-value	*0.860*	*0.582*	***0.001***	***0.001***	***0.003***	***0.020***	*0.055*	***0.009***

Table 3.3 F-statistics and p-values from a three-way analysis of variance (ANOVA) of DIC, chlorophyll-a, and herbivorous zooplankton biomass by site (Burger, Klondike, and Statoil), year (2010 and 2011), and cruise (August, September, October and Sept/Oct) effects for the northeastern Chukchi Sea. Probabilities significantly different at $p \leq 0.05$ are boldface.

	SITE	YEAR	CRUISE	SITE:YEAR	SITE:CRUISE	YEAR:CRUISE	SITE:YEAR:CRUISE
DIC	1.2	10.2	7.2	0.6	0.2	1.2	2.7
p-value	0.292	**0.001**	**0.001**	0.524	0.843	0.278	0.101
Chlorophyll-a	1.4	25.4	3.3	8.7	1.8	0.4	0.8
p-value	0.250	**0.000**	**0.04**	**0.000**	0.163	0.544	0.369
Small copepods	7.0	35	3.9	1.7	4.3	68.3	0.4
p-value	**0.001**	**0.000**	**0.022**	0.180	**0.016**	**0.000**	0.650
Large copepods	11.8	0.1	11.9	10.1	7.5	6.7	0.6
p-value	**0.000**	0.716	**0.000**	**0.000**	**0.001**	**0.010**	0.552
Meroplankton	9.2	57.3	0.91	2.9	6.3	46	3.6
p-value	**0.000**	**0.000**	0.405	0.059	**0.002**	**0.000**	**0.029**
Larvaceans	2	0.7	6.2	6.8	9.2	4.6	3.7
p-value	**0.139**	0.395	**0.003**	**0.001**	**0.000**	**0.033**	**0.028**
Euphausiids	7.7	17	9.6	2.4	3.2	0.1	2.7
p-value	**0.001**	**0.000**	**0.000**	0.094	**0.043**	0.726	0.068
Pteropods	2.6	9.5	0	6.6	3.3	91.6	8
p-value	0.077	**0.002**	0.985	**0.002**	**0.040**	**0.000**	**0.001**

Table 3.4 Average changes in integrated nDIC, nTA, NO_3, and TIN between cruises to determine rates of NCP in the Burger, Klondike, and Statoil study areas in the northeastern Chukchi Sea during 2010 and 2011.

	ΔnDIC (mmol m^{-2})	ΔnTA (mmol m^{-2})	ΔNO_3 (mmol m^{-2})	ΔTIN (mmol m^{-2})	NCP (mmol C m^{-2} d^{-1})
2010					
Sept - Aug					
Burger	–246	–535	19	31	0.28
Klondike	–189	–483	–7	5	3.09
Statoil	–150	–222	–4	13	12.22
October - Sept					
Burger	31	227	–13	–33	–2.47
2011					
Sept/Oct - Aug					
Burger	775	222	–9	–10	16.62
Klondike	659	–147	–5	–4	27.73
Statoil	597	9	–9	–0.22	19.79

Table 3.5 Spearman rank correlation coefficients for NCP in relation to changes in chlorophyll-a and herbivorous zooplankton categories within the Klondike, Burger, and Statoil study areas in the northeastern Chukchi Sea during 2010 and 2011.

	Chl-a	Small copepods	Large copepods	Meroplankton	Larvaceans	Euphausiids	Pteropods
2010 September							
Burger	0.412	0.511	-0.407	-0.280	0.165	-0.313	0.066
Klondike	-0.364	0.455	-0.238	0.203	0.552	0.378	-0.070
Statoil	-0.464	-0.273	0.300	-0.091	-0.182	-0.036	-0.136
All stations	-0.130	0.123	-0.311	-0.138	-0.036	-0.367	0.092
2010 October							
Burger	**0.608**	0.294	0.056	0.182	0.091	**-0.629**	-0.112
2011							
Burger	**-0.661**	0.382	-0.479	-0.261	-0.079	**0.745**	0.030
Klondike	**-0.730**	-0.027	-0.091	0.018	-0.236	0.173	0.073
Statoil	-0.333	-0.024	0.309	-0.286	0.286	-0.262	-0.571
All stations	-0.622	0.079	-0.133	-0.136	0.010	0.158	-0.026

Table 3.6 Estimates of carbon production for the Burger, Klondike, and Statoil study areas during 2010 and 2011.

	Phytoplankton (mg C m^{-3})	Total copepods (mg C m^{-3})	NCP (mg C m^{-3} d^{-1})	% NCP of PP d^{-1}	Grazing % PP d^{-1}
2010 August					
Burger	10.36	6.67		3%	64%
Klondike	20.19	8.26		15%	41%
Statoil	20.92	7.34		58%	35%
2010 September					
Burger	14.70	7.78	0.084	2%	53%
Klondike	15.71	11.00	0.929	20%	70%
Statoil	18.07	6.55	3.670	68%	36%
2010 October					
Burger	19.20	8.25	-0.740	-13%	43%
2011 August					
Burger	19.65	6.85		85%	35%
Klondike	17.29	12.95		116%	75%
Statoil	19.18	11.88		94%	62%
2011 Sept/Oct					
Burger	23.44	3.61	5.000	71%	15%
Klondike	18.35	7.07	8.326	151%	38%
Statoil	28.17	2.93	4.401	64%	10%

General Conclusions

This dissertation explored a variety of factors that influence and control the biological patterns expressed by zooplankton assemblages within the Chukchi Sea. This high-latitude region has proven to be an immensely complex ecosystem that is experiencing large perturbations due to climate change. The implementation of long-term sampling programs, such as the CSESP, will be critical for understand how this ecosystem may change and how fluctuations within the zooplankton communities will inevitably influence higher trophic levels.

The first chapter described the seasonal and inter-annual variability of the zooplankton communities, where variations in sea-ice retreat, water temperature, and the timing of the phytoplankton bloom created large difference in spatio-temporal patterns of abundance and biomass. The high-intensity repeat-measure sampling design helped decipher ecological patterns driven by site-specific conditions from interannual climatological variations. Results from this chapter were integrated into a multi-disciplinary synthesis paper that I co-authored describing the ecology and function of the northeastern Chukchi Sea (Day et al., 2013). Additionally, macro-nutrient analysis from this chapter were analysed in combination with the marine carbonate system to assess the magnitude of ocean acidification over the CSESP study area (Mathis and Questel, 2013). I have also contributed to an analysis that encompasses the entirety of the CSESP (2008–2014), including the Greater Hanna Shoal Study area. That manuscript examines the variability within the pelagic and benthic ecosystems and considers the challenges of detecting ecological change in a highly variable Arctic ecosystem (Day et al., in prep).

Chapter two represents the first phylogeographic study of the *Pseudocalanus* species complex in the North Pacific and Pacific Arctic region. This analysis confirmed the biogeographic distribution of four sibling species of *Pseudocalanus* that live sympatrically within the region. Estimates of population connectivity based on COI sequence variation revealed high rates of gene flow between adjacent populations that were in agreement with local hydrographic flow. An indication of species-specific responses to climate change also became apparent within the Arctic species *P. acuspes* and the temperate species *P. mimus*, where abundances were low outside their desired habitat affinities. The species-specific responses observed in this chapter stress the need for zooplankton analyses to obtain positive identification

within the *Pseudocalanus* genus because important species-level information governing distribution, life history, habitat preference, and population dynamics are being lost. Subsequent efforts are now using COI sequences from this study to generate species-specific polymerase chain reaction (ssPCR) to positively identify copepodite and adult stages of *Pseudocalanus,* thereby establishing species-specific distributions, population structure, and production within the Chukchi Sea (Ershova et al., submitted), This work also lays the foundation for a phylogeographic study of the genus over its entire Arctic domain (Questel et al., in prep).

The third chapter marked the first attempt to relate summer production to mesozooplankton biomass in the Chukchi Sea. Standard approaches to calculating net community production (NCP) proved problematic due to several underlying oceanographic complexities of this shallow inflow shelf system. The highly advective nature of the Chukchi Sea and shifting water masses introduced a large degree of spatial variability in all biotic and abiotic factors that further complicated the NCP approach. Nonetheless, a simple box-model to estimate carbon production suggested that the Chukchi Sea is capable of supporting the zooplankton communities observed during the latter portion of the open-water season. This in turn suggested that the system is not unbalanced during the summer months when phytoplankton biomass is low and the region is presumed to be oligotrophic.

One of the greatest concerns for the Chukchi Sea ecosystem is how it will respond to the rapid changes occurring due to climate change. The work carried out in this dissertation has further increased our knowledge of how the zooplankton communities may respond to a warming Arctic and stresses how many species are sensitive to the underlying physical environment. For example, geographic distributions of ecologically important species are already starting to shift (Ershova et al., 2015b), as suggested here for the *Pseudocalanus* species complex. Even with the large degree of physical and ecological changes occurring, the most astounding aspect of the Chukchi Sea is that the pelagic communities are always in a state of flux, seemingly operating under different pressures within any given year. This makes it very difficult to predict future community state for such a dynamic and complex system where the pelagic system seems to reset itself after each open-water season.

There are still many unknowns as to the mechanisms behind the observed biological patterns and variability of the zooplankton communities of the Chukchi Sea. Increased

international collaborations along with standardizing sampling techniques will vastly improve our understanding in the broader context of ecosystem process of the Arctic Ocean. Seasonal ice cover has limited our access and timing of operations within the Chukchi Sea, where strategically timed sampling, both upstream and downstream, of the Chukchi Sea could become advance our understanding the influences of advection, primary, and secondary production of the Arctic ecosystem.

The research in this dissertation was part of the Chukchi Sea Environmental Program (CSESP) that was supported by ConocoPhillips, Shell, and Statoil to gain a better understanding for how the highly complex Chukchi Sea ecosystem functions. Although efforts associated with oil and gas exploration in the Chukchi have recently been abandoned for the foreseeable future, the tangible legacy of that process is the attention it drew to this poorly-studied region, and consequently, the vast increase in our knowledge of its ecosystem. The data acquired over the 7-year program is currently the longest-running and most robust time series within the region. Although CSESP has come to an end, efforts still continue through various multi-disciplinary programs to resample CSESP stations, gaining a better understanding of what controls the variability and how to detect change in an ever-evolving ecosystem.

References

Carroll, M.K., Carroll, J., 2003. The Arctic Seas. In: Black, K. D., Shimmield, G. B. (Eds.), Biogeochemistry of Marine Systems. Blackwell Sheffield, pp. 127–156.

Coachman, L.K., Aagard, K., 1988. Transports through Bering Strait: Annual and interannual variability. Journal of Geophysical Research 93, 15515–15539.

Codispoti, L.A., Flagg, C.N., Swift, J.H., 2009. Hydrographic conditions during the 2004 SBI process experiments. Deep Sea Research Part II: Topical Studies in Oceanography 56, 1144–1163.

Danielson, S.L., Weingartner, T.J., Hedstrom, K.S., Aagaard, K., Woodgate, R., Curchitser, E., Stabeno, P.J., 2014. Coupled wind-forced controls of the Bering-Chukchi shelf circulation and the Bering Strait throughflow: Ekman transport, continental shelf waves, and variations of the Pacific-Arctic sea surface height gradient. Progress in Oceanography 125, 40–61.

Day, R.H., Weingartner, T.J., Hopcroft, R.R., Aerts, L.A.M., Blanchard, A.L., Gall, A.E., Gallaway, B.J., Hannay, D.E., Holladay, B.A., Mathis, J.T., Norcross, B.L., Questel, J.M., Wisdom, S.S., 2013. The offshore northeastern Chukchi Sea, Alaska: A complex high-latitude ecosystem. Continental Shelf Research 67, 147–165.

Day, R.H., Blanchard, A.L., Gall, A.E., Weingartner, T.J., Aerts, L.A.M., Delarue, J., Dobbins, E.L., Hopcroft, R.R., Questel, J.M., Wisdom, S.S. Interannual variability and change in an arctic ecosystem: can we separate a signal from the noise?. In prep.

Dunton, K.H., Goodall, J.L., Schonberg, S.V., Grebmeier, J.M., Maidment, D.R., 2005. Multi-decadal synthesis of benthic-pelagic coupling in the western arctic: Role of cross-shelf advective processes. Deep Sea Research Part II: Topical Studies in Oceanography 52, 3462–3477.

Ershova, E.A., Hopcroft, R.R., Kosobokova, K.N., 2015a. Inter-annual variability of summer mesozooplankton communities of the western Chukchi Sea: 2004–2012. Polar Biology 38, 1461–1481.

Ershova, E.A., Hopcroft, R.R., Kosobokova, K.N., Matsuno, K., Nelson, R.J., Yamaguchi, A., Eisner, L.B., 2015b. Long-term changes in summer zooplankton communities of the western Chukchi Sea, 1945-2012. Oceanography 28, 100–115.

Ershova, E.A., Hopcroft, R.R., Questel, J.M., Kosobokova, K.N., Population structure and production of four sibling species of *Pseudocalanus* spp. in the Chukchi Sea. Submitted.

Gall, A.E., Morgan, T.C., Day, R.H., Kuletz, K.J., 2016. Ecological shift from piscivorous to planktivorous seabirds in the Chukchi Sea, 1975–2012. Polar Biology doi:10.1007/s00300–016–1924–z.

Grebmeier, J.M., Smith, W.O., Jr., Conover, R.J., 1995. Biological processes on Arctic continental shelves: ice-ocean-biotic interactions. In: Smith, W.O., Jr., Grebmeier, J.M. (Eds.), Arctic Oceanography: marginal ice zones and continental shelves. American Geophysical Union, Washington, pp. 231-261.

Grebmeier, J.M., Cooper, L.W., Feder, H.M., Sirenko, B.I., 2006. Ecosystem dynamics of the Pacific-influenced Northern Bering Seas in the Amerasian Arctic. Progress in Oceanography 71, 331–361.

Grebmeier, J.M., Harvey, R.H., Stockwell, D.A., 2009. The Western Arctic Shelf–Basin Interactions (SBI) project: An overview. Deep Sea Research Part II: Topical Studies in Oceanography 56, 1137–1143.

Grebmeier, J.M., Maslowski, W. (Eds.), 2014. The Pacific Arctic Region: ecosystem status and trends in a rapidly changing environment. Springer Dordrecht Heidelberg, New York, pp. 450.

Hopcroft, R.R., Kosobokova, K.N., 2010. Distribution and egg production of *Pseudocalanus* species in the Chukchi Sea. Deep Sea Research Part II: Topical Studies in Oceanography 57, 49–56.

Hopcroft, R.R., Kosobokova, K.N., Pinchuk, A.I., 2010. Zooplankton community patterns in the Chukchi Sea during summer 2004. Deep Sea Research Part II: Topical Studies in Oceanography 57, 27–39.

Lane, P.V.Z., Llinás, L., Smith, S. L., Pilz, D., 2008. Zooplankton distribution in the western Arctic during summer 2002: Hydrographic habitats and implications for food chain dynamics. Journal of Marine Systems 70, 97–133.

Mathis, J.T., Questel, J.M., 2013. Assessing seasonal changes in carbonate parameters across small spatial gradients in the Northeastern Chukchi Sea. Continental Shelf Research 67, 42–51.

Nelson, R.J., Ashjian, C.J., Bluhm, B.A., Conlan, K.E., Gradinger, R.R., Grebmeier, J.M., Hill, V.J., Hopcroft, R.R., Hunt, B.P.V., Joo, H.M., Kirchman, D.L., Kosobokova, K.N., Lee, S.H., Li, W.K.W., Lovejoy, C., Poulin, M., Sherr, E., Young, K.V., 2014. Biodiversity and biogeography of the lower trophic taxa of the Pacific Arctic Region: Sensitivities to climate change, in: Grebmeier, J.M., Maslowski, W. (Eds.), The Pacific Arctic Region: Ecosystem Status and Trends in a Rapidly Changing Environment. Springer Dordracht Heidelberg, New York, pp. 270–336.

Nelson, R.J., Carmack, E.C., McLaughlin, F.A., Cooper, G.A., 2009. Penetration of pacific zooplankton into the western arctic ocean tracked with molecular population genetics. Marine Ecology Progress Series 381, 129–138.

Plourde, S., Campbell, R.G., Ashjian, C.J., Stockwell, D.A., 2005. Seasonal and regional patterns in egg production of *Calanus glacialis/marshallae* in the Chukchi and Beaufort Seas during spring and summer, 2002. Deep Sea Research Part II: Topical Studies in Oceanography 52, 3411–3426.

Questel, J.M., Bucklin, A., Blanco-Bercial, L., Hopcroft, R.R., Aarbakke, O.N.S., Halsband, C., Norrbin, F. Pan-Arctic phylogeography and connectivity of the genus *Pseudocalanus*. In prep.

Springer, A.M., McRoy, C.P., Turco, K.R., 1989. The paradox of pelagic food webs in the northern Bering Sea—II. Zooplankton communities. Continental Shelf Research 9, 359–386.

Walsh, J.J., McRoy, C.P., Coachman, L.K., Goering, J.J., Nihoul, J.J., Whitledge, T.E., Blackburn, T.H., Parker, P.L., Wirick, C.D., Shuert, P.G., Grebmeier, J.M., Springer, A.M., Tripp, R.D., Hansell, D.A., Djenidi, S., Deleersnijder, E., Henriksen, K., Lund, B.A., Andersen, P., Müller-Karger, F.E., Dean, K., 1989. Carbon and nitrogen cycling within the Bering/Chukchi Seas: source regions for organic matter effecting AOU demands of the Arctic Ocean. Progress in Oceanography 22, 277–359.

Wang, J., Hu, H., Mizobata, K., Saitoh, S.I., 2009. Seasonal variations of sea ice and ocean circulation in the Bering Sea: a model-data fusion study. Journal of Geophysical Research: Oceans 114, 1–24.

Weingartner, T.J., Dobbins, E., Danielson, S., Winsor, P., Potter, R., Statscewich, H., 2013. Hydrographic variability over the northeastern Chukchi Sea shelf in summer-fall 2008-2010. Continental Shelf Research 67, 5–22.

Woodgate, R.A., Weingartner, T.J., Lindsay, R., 2012. Observed increases in Bering Strait oceanic fluxes from the Pacific to the Arctic from 2001 to 2011 and their impacts on the Arctic Ocean water column. Geophysical Research Letters 39, 2–7.